

**HYDROLOGICAL RESPONSE UNDER CLIMATE CHANGE OF  
HUNZA RIVER CATCHMENT– A COMPARATIVE  
HYDROLOGICAL MODELING**

By

**Kashif Jamal**

(NUST201362217MSCEE15313F)

A Thesis submitted in partial fulfillment  
of the requirements for the degree of

**Master of Science**

in

**Water Resources Engineering and Management**



**DEPARTMENT OF WATER RESOURCES ENGINEERING AND MANAGEMENT  
NUST INSTITUTE OF CIVIL ENGINEERING  
SCHOOL OF CIVIL AND ENVIRONMENTAL ENGINEERING  
NATIONAL UNIVERSITY OF SCIENCE AND TECHNOLOGY  
SECTOR H-12, ISLAMABAD, PAKISTAN**

(2016)

This is to certify that the

Thesis entitled

**HYDROLOGICAL RESPONSE UNDER CLIMATE CHANGE OF  
HUNZA RIVER CATCHMENT– A COMPARATIVE  
HYDROLOGICAL MODELING**

Submitted by

**Kashif Jamal**

**(NUST201362217MSCEE15313F)**

Has been accepted in partial fulfillment of the requirements

Towards the award of the degree of

**Master of Science in Water Resources Engineering and Management**

---

**Dr. Shakil Ahmad**

**Assistant Professor**

**NUST Institute of Civil Engineering (NICE)**

**School of Civil & Environmental Engineering (SCEE)**

**National University of Sciences & Technology, Islamabad**

***Disclaimer***

*The views expressed in this work are those of the creators and do not necessarily represent those of the UK Government's Department for International Development, the International Development Research Centre, Canada or its Board of Governors.*

***DEDICATED TO***

*My Beloved Parents and Family*

## **ACKNOWLEDGEMENTS**

*I am very excited to express my deepest gratitude to all those who contributed in making this study possible, valuable and successful. First of all, I like to thank Almighty God for the wisdom, knowledge and perseverance He has been bestowed on me during whole of my life.*

*Then, I would like to extend my appreciation for my supervisor Dr. Shakil Ahmad (NICE, NUST) for spending his enormous valuable time in teaching, guiding, being patient and providing moral and technical support to perform this research.*

*I would like to thanks Dr. Muhammad Azmat (IGIS, NUST) for their valuable and technical support and encouragement during all the course of research work. Their comments and valuable advises helped me to take this research in right direction.*

*I am very grateful to the rest of my thesis guidance committee members, Dr. Hamza Farooq Gabriel (NICE, NUST), Dr. Sajjad Haider (NICE, NUST) and Dr. Bashir Ahmed (NARC, Islamabad), for their willingness to serve as members of the thesis committee on a very short notice. Their participation in editing and their valuable suggestions for improving my thesis was quite valuable.*

*I also like to acknowledge the support of my class fellows, especially Mr. Muhammad Adnan Khan and Mr. Asad Abbas for their valuable support in thesis editing.*

*This work was carried out by the Himalayan Adaptation, Water and Resilience (HI-AWARE) consortium under the Collaborative Adaptation Research Initiative in Africa and Asia (CARIAA) with financial support from the UK Government's Department for International Development and the International Development Research Centre, Ottawa, Canada. The views expressed in this work do not necessarily represent those of the supporting organizations.*

*Last but not least, I like to thank my brothers and sisters especially, Asif Jamal, for providing me their support, love and lot of prayers throughout my studies. I am very grateful to all of you for your contribution and support.*

**(Kashif Jamal)**

## ABSTRACT

Investigation of streamflows in high–altitude cryosphere due to the changing climate is an immense challenge under inadequate climate records. The current study compares the efficiency of rainfall–runoff model (HEC–HMS) and the snowmelt–runoff model (SRM) for current climate in Hunza River catchment. Landsat–5 & 8 imagery was selected for land cover classification and change detection using Earth Resources Data Analysis System (ERDAS) Imagine tool. The Moderate Resolution Imaging Spectroradiometer (MODIS) Snow Cover Area (SCA) products were used for the generation of cloud free composite SCA by removing the clouds. The hydrological models were calibrated by using observed daily streamflows of 6 years (2001–2006), while validated for 3 years (2008–2010). Overall, the simulated streamflow results showed that the performance of SRM was significantly better than HEC–HMS, as depicted by Nash–Sutcliffe coefficient (NS) and coefficient of determination ( $R^2$ ) of 0.95 and 0.92 (0.97 and 0.89) for SRM, compared with values of 0.63 and 0.57 (0.61 and 0.54) for HEC–HMS, during calibration (validation) period on annual basis. Further, the potential streamflows during decades of 2030s, 2060s and 2090s were projected for RCPs scenarios (RCPs in combination of Unchanged SCA i.e. UCSCA), Hypothetical scenarios (RCPs in combination with Change in SCA i.e. CSCA) and Hypothetical scenarios (Baseline (observed) in combination with change in temperature and precipitation i.e. BL+T<sub>x</sub>P<sub>x</sub>) using SRM. Firstly, the bias corrected temperature showed basin–wide significant increase in mean annual temperature 0.7, 2.4 and 4.6 °C (0.6, 1.3 and 1.9 °C) for RCP8.5 (RCP4.5), during 2030s, 2060s and 2090s, respectively. While bias corrected precipitation inferred maximum precipitation increases in winter season 19.1–36.2 mm (19.4–27.8 mm) for RCP8.5 (RCP4.5) on decadal basis. Secondly, increasing trends of streamflows were found in consistent with the climatic dataset and overall mean annual streamflows are expected to increase by 16–113% (42–304 m<sup>3</sup>/s) for RCP8.5 in comparison with 13–43% (35–115 m<sup>3</sup>/s) for RCP4.5 on decadal basis. Similarly, for hypothetical scenarios (RCPs+%CSCA) i.e. with increase of SCA by 5% (2030s), 10% (2060s) and 15% (2090s), the potential increase in mean annual streamflows are expected to be 33–186% (87–501 m<sup>3</sup>/s) and 29–103% (79–276 m<sup>3</sup>/s) for RCP8.5 and RCP4.5, respectively, while with decrease in SCA by 5% (2030s), 10% (2060s) and 15% (2090s), the mean annual streamflows are expected to increase (decrease) by 42% (7%) for RCP8.5

(RCP4.5) during 2090s. Additionally, for hypothetical scenario (BL+T<sub>x</sub>P<sub>x</sub>) i.e. positive change in temperature (precipitation) by 1 °C (5%) by 2030s, 2 °C (10%) by 2060s, 3 °C (15%) and 4 °C (20%) by 2090s, the potential increase in mean annual streamflows are expected to be 29% (78 m<sup>3</sup>/s), 57% (153 m<sup>3</sup>/s), 87% (234 m<sup>3</sup>/s) and 118% (318 m<sup>3</sup>/s), respectively. Overall, the results of this study revealed that SRM has high efficiency for simulation streamflows of high–altitude cryosphere catchment under changing climate.

## TABLE OF CONTENTS

<b>ACKNOWLEDGEMENTS .....</b>	<b>v</b>
<b>ABSTRACT.....</b>	<b>vi</b>
<b>TABLE OF CONTENTS .....</b>	<b>viii</b>
<b>LIST OF FIGURES .....</b>	<b>xi</b>
<b>LIST OF TABLES .....</b>	<b>xiv</b>
<b>LIST OF ABRIVATIONS.....</b>	<b>xvi</b>
<b>INTRODUCTION.....</b>	<b>1</b>
1.1    GENERAL .....	1
1.2    PROBLEM STATEMENT .....	4
1.3    OBJECTIVES OF THE STUDY .....	5
1.4    RESEARCH HYPOTHESIS .....	5
1.5    SCOPE OF STUDY .....	5
1.6    ORGANIZATION OF THESIS.....	6
<b>LITERATURE REVIEW .....</b>	<b>7</b>
2.1    GENERAL .....	7
2.2    DESCRIPTION OF ERDAS IMAGINE TOOL.....	7
2.2.1    Methods for Land Cover Classification.....	7
2.2.1.1    Unsupervised classification .....	7
2.2.1.2    Supervised classification .....	8
2.3    DESCRIPTION OF HYDROLOGICAL MODELS.....	8
2.3.1    Rainfall–Runoff Model (HEC–HMS).....	8
2.3.2    Snowmelt Runoff Model (SRM) .....	9
2.4    TERMS USED FOR CLIMATE STUDIES .....	10
2.4.1    General Circulation Model (GCM).....	10
2.4.2    Coupled Model Inter–Comparison Project (CMIP).....	11
2.4.3    Representative Concentration Pathways (RCPs).....	11
2.4.4    Climate Data Downscaling .....	11
2.4.5    Bias Correction .....	12
2.4.5.1    Delta technique .....	12

2.5	PREVIOUS STUDIES .....	13
2.5.1	Land Cover Classification.....	13
2.5.2	Hydrological Modeling.....	14
2.5.3	Climate Change Impact Assessment.....	16
2.6	EFFICIENCY CRITERIA .....	18
2.6.1	Nash–Sutcliffe Coefficient (NS).....	18
2.6.2	Percent Volume Difference.....	18
2.6.3	Correlation Coefficient .....	19
2.6.4	Coefficient of Determination .....	19
2.6.5	Mean absolute error (MAE).....	19
2.6.6	Root mean squared error (RMSE) .....	19
	<b>METHODOLOGY .....</b>	<b>20</b>
3.1	STUDY AREA.....	20
3.2	DESCRIPTION OF DATASET.....	21
3.2.1	Hydro–Climatic Data .....	21
3.2.2	RCPs Climate Dataset.....	22
3.3	SATELLITE DATA.....	22
3.3.1	ASTER GDEM .....	22
3.3.2	MODIS Snow Cover Data .....	23
3.3.3	Landsat Data .....	24
3.4	PRELIMINARY DATA ANALYSIS.....	25
3.4.1	Time Series Analysis .....	25
3.4.1.1	Precipitation analysis.....	25
3.4.1.2	Temperature analysis.....	26
3.4.1.3	Stream flow data analysis .....	26
3.5	METHODOLOGY .....	27
3.5.1	Land Cover Classification.....	27
3.5.2	Snow Cover Variability .....	28
3.5.3	Application of Hydrological Models .....	28
3.5.3.1	Application of HEC–HMS .....	28
3.5.3.2	Application of SRM.....	31
3.5.3.3	Comparison of HEC–HMS and SRM .....	33

3.5.4	Bias Correction of Climatic Dataset .....	33
3.5.5	Climate Change Impact on Streamflows .....	34
3.5.5.1	Based on RCPs scenarios (RCPs+UCSCA).....	35
3.5.5.2	Hypothetical scenarios (RCPs±%CSCA).....	35
3.5.5.3	Hypothetical scenarios (BL+T <sub>x</sub> P <sub>x</sub> ) .....	35
3.5.5.4	Comparison of RCPs and hypothetical scenarios.....	36
<b>RESULTS AND DISCUSSIONS .....</b>		<b>37</b>
4.1	LAND COVER CHANGE IN HUNZA RIVER CATCHMENT .....	37
4.1.1	Land Cover Change from 1994–2014 in Hunza Catchment.....	37
4.2	SNOW COVER IN HUNZA RIVER CATCHMENT .....	39
4.3	COMPARISON OF HYDROLOGICAL MODELS .....	41
4.3.1	Calibration and Validation.....	41
4.3.2	Comparison of HEC–HMS and SRM.....	42
4.4	CLIMATE CHANGE IMPACT ASSESSMENT.....	45
4.4.1	Climate Dataset.....	45
4.4.1.1	Monthly dataset .....	45
4.4.1.2	Seasonal dataset.....	55
4.4.2	Projected Streamflows .....	57
4.4.2.1	RCPs scenarios (RCPs+UCSCA).....	57
4.4.2.2	Hypothetical scenarios (RCPs±%CSCA).....	59
4.4.2.3	Hypothetical Scenarios (BL+T <sub>x</sub> P <sub>x</sub> ).....	64
4.4.3	Comparison of GCMs and Hypothetical Results.....	65
<b>CONCLUSIONS AND RECOMMENDATIONS.....</b>		<b>67</b>
5.1	CONCLUSIONS .....	67
5.2	RECOMMENDATIONS .....	69
<b>REFERENCES.....</b>		<b>70</b>

## LIST OF FIGURES

Figure 1.1: A Map of Pakistan (Source: Tahir et al. (2011b) .....	2
<i>Figure 1.2: Indus Basin Irrigation System in Pakistan (Source: PCRWR, 2012).....</i>	<i>3</i>
Figure 1.3: Reason of Climate Change (Technical Report No. PMD–25/2012).....	4
Figure 1.4: Change in (a) Temperature and (b) Precipitation, Globally (IPCC 2014) ..	4
Figure 2.1: Climate Data Downscaling Scheme .....	11
Figure 2.2: Methodology Adopted for Selection of Climate Models by Lutz et al. (2016) .....	17
Figure 3.1: Hunza River Catchment alongwith Climate Stations and Stream Gauge Locations .....	20
Figure 3.2: Zone Wise Distribution of the Hunza Catchment along with Location of Climate Stations and Streamflow Gauging Station .....	23
Figure 3.3: MODIS Satellite Images Presenting the Mean Monthly SCA in the Hunza River Catchment (2001–2010). .....	24
Figure 3.4: Landsat–8 Image for Hunza River Catchment .....	25
Figure 3.5: Preliminary Time Series Data ( Precipitation, Temperature and Streamflow) Analysis (2001–2010) .....	26
Figure 3.6: Streamflow at Dainyor Bridge Station in Hunza River Catchment .....	27
Figure 3.7: Schematic Diagram Showing the Methodology, Hunza River Catchment.....	27
Figure 3.8: Five Subbasins of Hunza River Catchment used for HEC–HMS .....	29
Figure 3.9: Hypsometric Curve of the Hunza River Catchment is Showing the Area Distribution in six Different Elevation Zones (Zones–1, Zone–2, Zones–3, Zone–4, Zone–5 and Zone–6) .....	31
Figure 3.10: Zone Wise Distribution of (a) Temperature (°C), and (b) SCA (%), during 2001–2010, Hunza River Catchment .....	32
Figure 4.1: Land Cover Map of Hunza River Catchment in August, 1994. ....	37
Figure 4.2: Land Cover Map of Hunza River Catchment in August, 2014. ....	38

Figure 4.3: Attabad Lake in Hunza River Catchment (Ali et al., 2015).....	39
Figure 4.4: Percentage SCA form 2001–2010 in Hunza River Catchment. ....	40
Figure 4.5: Inter Annual Variability in SCA in Hunza River Catchment from 2001– 2010. ....	40
Figure 4.6: Simulations of Daily Streamflows ( $\text{m}^3/\text{s}$ ) during Calibration (2001–2006) and Validation (2008–2010) Periods using SRM and HEC–HMS Models, Hunza River Catchment .....	44
Figure 4.7: Scattered plot Showing the Performance of SRM and HEC–HMS Models during 9–year simulation Period (Calibration 2001–2006 and Validation 2008–2010), of Hunza River Catchment.....	45
Figure 4.8: IGB Precipitation Data before and after Bias Correction for Hunza Climate Station.....	46
Figure 4.9: IGB Precipitation Data before and after Bias Correction for Naltar Climate Station.....	47
Figure 4.10: IGB Precipitation Data before and after Bias Correction for Ziarat Climate Station.....	48
Figure 4.11: IGB Precipitation Data before and after Bias Correction for Khunjrab Climate Station .....	49
Figure 4.12: IGB Temperature Data before and after Bias Correction for Hunza Climate Station.....	50
Figure 4.13: IGB Temperature Data before and after Bias Correction for Naltar Climate Station.....	51
Figure 4.14: IGB Temperature Data before and after Bias Correction for Ziarat Climate Station.....	52
Figure 4.15: IGB Temperature Data before and after Bias Correction for Khunjrab Climate Station .....	53
Figure 4.16: Projected Monthly Streamflow ( $\text{m}^3/\text{s}$ ) for RCP4.5, RCP8.5, under RCPs Scenarios (RCPs+UCSCA)) during 2030s, 2060s and 2090s, Hunza River Catchment.....	59

Figure 4.17: Projected Monthly Streamflow ( $\text{m}^3/\text{s}$ ) for (a) RCP4.5, and (b) RCP8.5, under Hypothetical Scenarios (RCPs $\pm$ %CSCA) during 2030s, 2060s and 2090s, Hunza River Catchment.....	61
Figure 4.18: Projected Streamflows under Hypothetical Scenarios(BL+T <sub>x</sub> P <sub>x</sub> ) in Hunza River Catchment.....	65
Figure 4.19: Comparisan of Projected Water Avalability under RCPs(UCSCA) and Hypothetical Scenarios(BL+T <sub>x</sub> P <sub>x</sub> ) for Hunza River Catchment .....	66

## LIST OF TABLES

Table 2.1: Selected Climate Models by Lutz et al. (2016). .....	17
Table 3.1: Salient Feature Hunza River Catchment.....	21
Table 3.2: Zone Wise Characteristics of Hunza River Catchment .....	22
Table 3.3: Subbasin Wise Characteristics of Hunza River Catchment.....	29
Table 3.4: Methods used in HEC–HMS .....	29
Table 3.5: Gage Weights for Hunza River Catchment .....	30
Table 3.6: Range of Parameter Values for Application of HEC–HMS in Hunza River Catchment .....	30
Table 3.7: Range of Parameter Values for Application of SRM in Hunza River Catchment .....	33
Table 4.1: Percentage Change in Land Cover Area from 1994 to 2014 for Hunza Catchment .....	39
Table 4.2: Calibrated Zone Wise Parametric Values for SRM Model, Hunza River Catchment .....	42
Table 4.3: Calibrated Subbasin Wise Parametric Values forHEC–HMS Model, Hunza River Catchment .....	42
Table 4.4: Statistical Performance of SRM and HEC–HMS Models during Calibration (2001–2006) and Validation (2008–2010) Periods, Hunza River Catchment .....	43
Table 4.5: Efficiency Parameters after Bias Correction for Climate Station (Hunza Naltar, Ziarat and Khunjrab).....	54
Table 4.6: Station–wise and Basin–wide Projected Temperature (°C) and Precipitation (mm) Deviations from Baseline (Observed) Temperature and Precipitation for RCP8.5 and RCP4.5 during 2030s, 2060s and 2090s, Hunza River Catchment .....	56
Table 4.7: Projected Streamflow Deviations(%) from Baseline (Observed)Streamflow for RCP8.5 and RCP4.5under RCPs Scenarios(RCPs+UCSCA) and	

Hypothetical Scenarios (RCPs±%CSCA) during 2030s, 2060s and 2090s,  
 Hunza River Catchment..... 63

Table 4.8:Percent Increase in Projected Streamflows under Hypothetical  
 Scenarios((BL+T<sub>x</sub>P<sub>x</sub>) in Hunza River Catchment. .... 65

## LIST OF ABRIVATIONS

ASTER GDEM	Advance Space-borne Thermal Emission and Reflection Radiometer Global Digital Elevation Model
BW	Basin Wide
CAD	Computer Aided Drawing
CMIP5	Couple Models Inter Comparison Phase 5
CN	Curve Number
CSCA	Changed Snow Cover Area
DDF	Degree Day Factor
DV	Volume Difference
ERDAS	Earth Recourses Data Analysis System
GIS	Geographic information System
HEC-HMS	Hydrological Engineering Center- Hydrological Modeling System
HI-AWARE	Himalayan Adaptation, Water and Resilience
IRIS	Indus River Irrigation System
IGB	Indus, Ganges and Brahmaputra
IPCC	Intergovernmental Panel on Climate Change
IWT	Indus Waters Treaty
LULC	Land Use Land Cover
MA	Million Acre
MAE	Mean Absolute Error
MAF	Million Acre Feet
m a.s.l	Meter Above Sea Level
MODIS	Moderate Resolution Imaging Spectroradiometer
NAM	NedbØr-AfstrØmnings Rainfall-Runoff Model
NS	Nash Sutcliff coefficient

PCRWR	Pakistan Council of Research in Water Resources
PES	Pakistan Economic Survey
PIDE	Pakistan Institute of Development Economics
PMD	Pakistan Meteorological Department
RCPs	Representative Concentration Pathways
RMSE	Root Mean Square Error
RS	Remote Sensing
SCA	Snow Cover Area
SCS	Soil Conservation Service
SIHP	Snow and Ice Hydrology Project
SRES	Special Report Emissions Scenarios
SRM	Snowmelt Runoff Model
SWHP	Surface Water Hydrology Project
UCSCA	Unchanged Snow Cover Area
UIB	Upper Indus Basin
US	United States
UTM	Universal Transverse Mercator
WAPDA	Water and Power Development Authority
WGS	World Geographic Coordinate System
ZW	Zone Wise

## **INTRODUCTION**

### **1.1 GENERAL**

Human sustainability is entirely depends on the earth water. Globally, increasing population growth and unlimited consumption of water resources impends the spatiotemporal freshwater resources availability. This extortion is risky in emerging countries, as in Pakistan (Figure 1.1), where considerable population ( $\approx 40\%$ ) is associated with agriculture activities (PIDE, 2007). Pakistan is ranked as sixth largest populated (population  $\approx 190$  million) country in the world (PES, 2014) with increasing rate of 1.92% per annum and its economy is highly dependent upon agriculture and more than 90% of available water is being used by the agriculture sector (PIDE, 2007).

Pakistan is extremely reliant upon the Indus River Irrigation System (IRIS), which is one of the world biggest irrigation networks in the Pakistan (SIHP, 1990). IRIS is formed by the Indus River Jhelum and Chenab (eastern tributaries) (Figure 1.2). The origin of Indus River is Tibetan–Plateau, China, where it flow toward northern areas of Pakistan (Figure 1.2) where it changes its path to the south and falls into the Arabian Sea. Total catchment area is approximately 966,000 km<sup>2</sup> and situated in four countries: Pakistan, India, China and Afghanistan. More than 60% area is located in Pakistan (Yang et al., 2014). It has a storage reservoir at Tarbela dam and catchment area above Tarbela is known as Upper Indus Basin (UIB).

About 40 percent of average annual Indus River flow is contributed by glaciers– and snow–melt. About 70 percent of annual Indus River flow is generated during the month of July and August. Peak streamflows occurred during these months due to glacier– and snow–melt (Yu et al., 2013). Climate change is expected that will result in changes in seasonal streamflow pattern (likely to cause in severe flood) that will creates new water management challenges in the Indus basin.

Pakistan has five major rivers (Indus, Jhelum, Chenab, Ravi and Sutlej) that are being flow through its territory but unfortunately all these five rivers are transboundary and are originating/flowing through the rival state of India. In 1960, an agreement known as Indus Waters Treaty (IWT) was signed between Pakistan and India, through which

the water of three Eastern Rivers (Ravi, Sutlej & Beas) was allocated to India and water of three Western Rivers (Indus, Jhelum & Chenab) was allocated to Pakistan. After signing the IWT–1960, Pakistan constructed 02 mega dams, 08 link canals and 05 barrages in–order to overcome the deficiency of water caused from the non–availability of water from the Eastern Rivers (WAPDA, 2013).

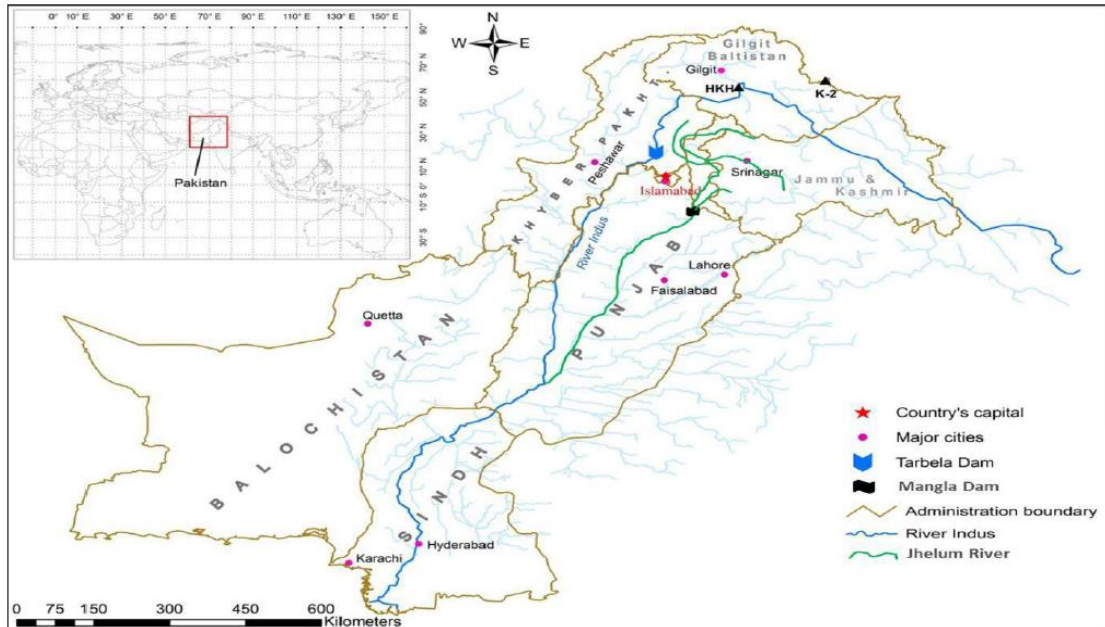


Figure 1.1: A Map of Pakistan (Source: Tahir et al. (2011b))

The basic water requirement of Pakistan is fulfilled by 3 major reservoirs that are namely Mangla Dam, Tarbela Dam, and Chashma Reservoir. Out of these three reservoirs, Mangla and Tarbela Dams are also serving as major source of hydel electricity of whole country. All these reservoir are rapidly losing their storage capacities due to sedimentation and will lose up to 37% of storage capacity (5.96 MAF) by 2025 (WAPDA, 2013).

Cultivable land of Pakistan is almost 77 MA (Million Acre), from which almost 27 MA is commanded by the canal system. The total land that is being cultivated (Barani & Irrigated) in Pakistan is almost 52.3 MA, but still about 20.3 MA of land is laying virgin that can be brought under irrigation, after having sufficient water storage capacity (Abid, 2012).

Pakistan's food–security and economy is highly reliant on these water resources and their managements. Any change in international policies, socio–economic factors and climate will affect the food–security and the environment of Pakistan (Azmat et al.,

2015). Consequently, it is essential to conduct a study on the hydro–meteorological, snow cover and the hydrologic regime of the Indus River Basin (Hunza River catchment– major tributary of Indus River) under climate change for better water management.

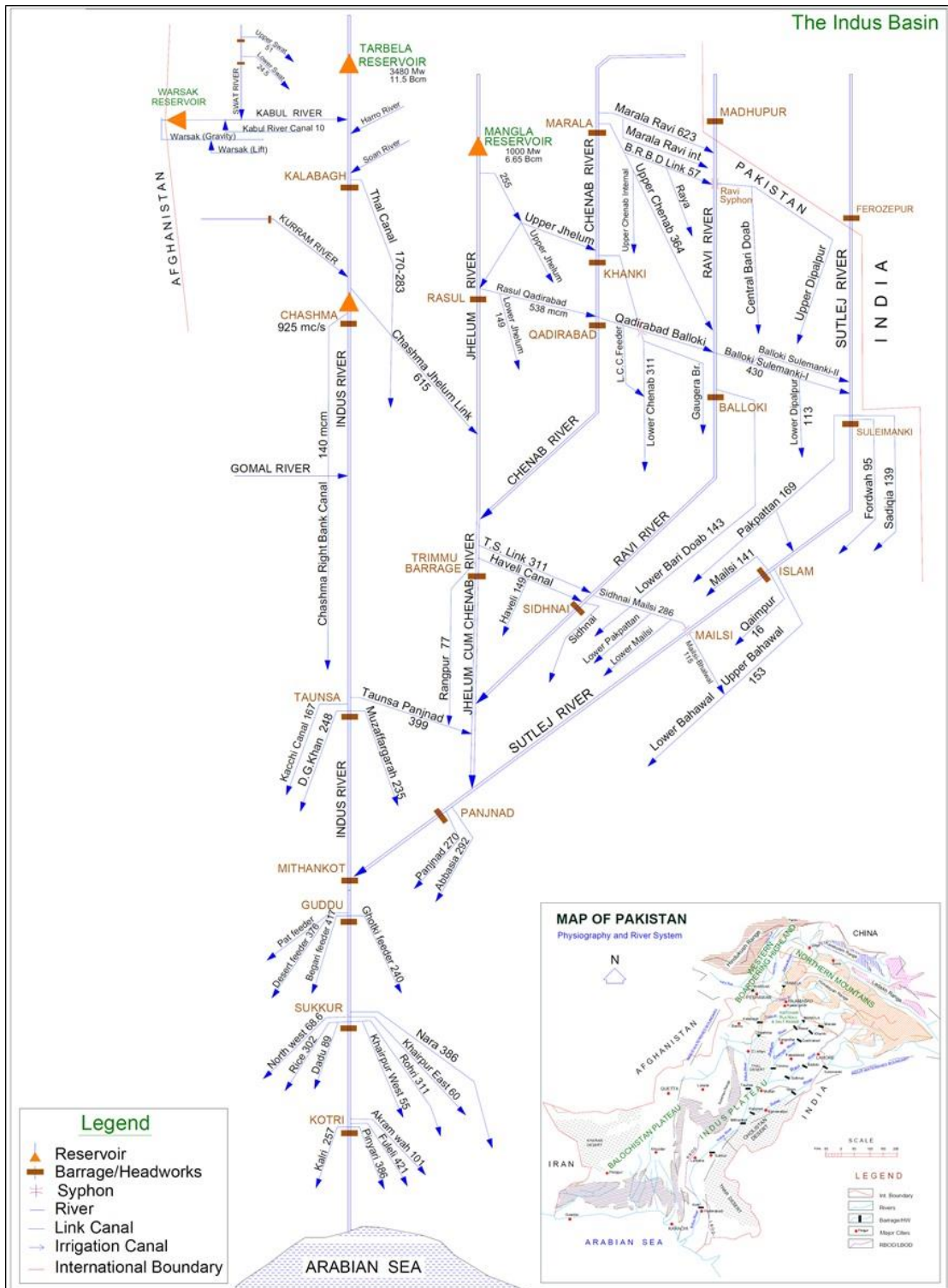


Figure 1.2: Indus Basin Irrigation System in Pakistan (Source: PCRWR, 2012)

## 1.2 PROBLEM STATEMENT

Above one-sixth of the global population is dependent upon water resources that were produced by snow-melt and glacier-melt for their water supply. Due to anthropogenic activities, change in precipitation and temperature (Figure 1.3 and 1.4) is to be likely that will considerably affect the melting (snow and glaciers) processes and the hydrology of catchments in the high altitude region (IPCC, 2014). Accurate hydrological modeling and climate change impact study in these catchments is complicated due to large heterogeneity climate, the resolution and accuracy of General Circulation Model's (GCM) outputs and uncertain response of snow and glacier dynamics. This study was carried out to define a baseline by developing a hydrological model for snow and glacier based Hunza River catchment under climate change, for better water resources management in future regard.

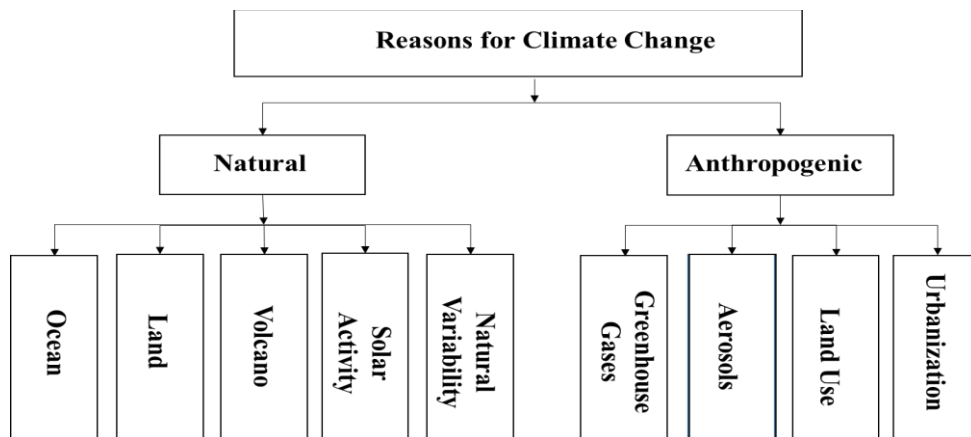


Figure 1.3: Reason of Climate Change (Technical Report No. PMD-25/2012)

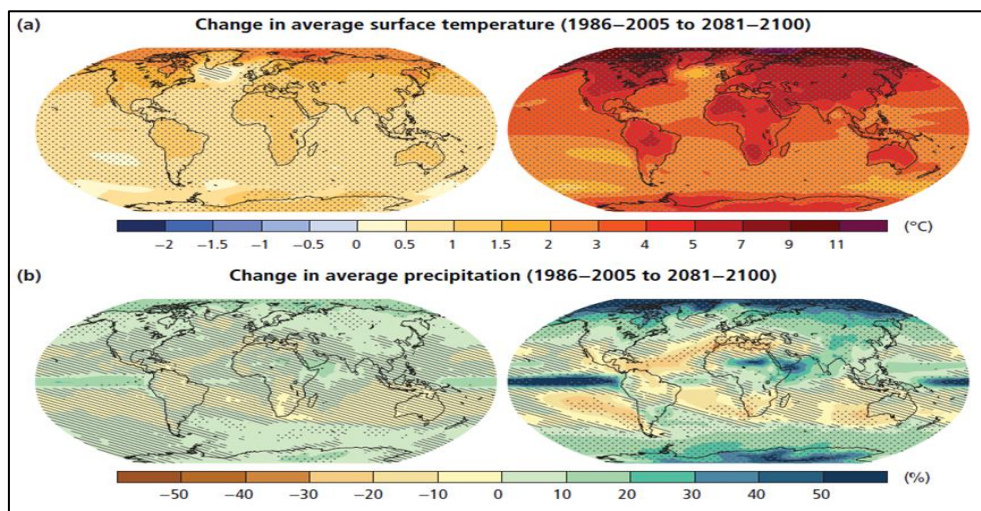


Figure 1.4: Change in (a) Temperature and (b) Precipitation, Globally (IPCC 2014)

### **1.3 OBJECTIVES OF THE STUDY**

- i. Assessment of land cover change and temporal snow cover variability in Hunza River catchment.
- ii. Application of Rainfall runoff model and snowmelt runoff model to simulate the streamflow of Hunza River catchment.
- iii. Assessment of future water availability in the context of changing climate.

### **1.4 RESEARCH HYPOTHESIS**

To accomplish the abovementioned objectives, we started with extraction of land cover information from Landsat-5 & 8 imagery with the help of ERDAS Imagine tool and snow cover variation from the Moderate Resolution Imaging Spectroradiometer (MODIS) Snow Cover Area (SCA) products MYD10A2 and MOD10A2 of Aqua and Terra satellite with the help of ArcGIS tool. Streamflow simulation was carried out with the help of two different hydrological models (Hydrological Engineering Center–Hydrological Modeling System (HEC–HMS) and snowmelt runoff (SRM) by utilizing observed climate data (Precipitation and Temperature) and snow cover data. Further selection of the appropriate hydrological model was made by comparing simulation efficiency of both hydrological model. Future water availability was assessed by incorporating bias corrected Indus, Ganges and Brahmaputra (IGB) future climate RCPs dataset in addition with hypothetical scenarios i.e. change in SCA (CSCA) as well as change in baseline (obs) temperature and precipitation data (BL+T<sub>x</sub>P<sub>x</sub>).

### **1.5 SCOPE OF STUDY**

This study was primarily conducted to investigate the land and snow cover change in cryosphere based Hunza River catchment. This study analyses the quantification of spatiotemporal land– and snow–cover change for the specific period of time in that area. The study mainly focused on the comparison of two hydrological models such as snow melt runoff model (SRM) and rainfall runoff model (HEC–HMS) for high altitude cryosphere catchment.

This study was also considered the future hydrological modeling using IGB climate dataset to evaluate the future water availability by using different climate models present in Couple Model Inter Comparison Phase 5 (CMIP5) as well as hypothetical climate scenarios.

## **1.6 ORGANIZATION OF THESIS**

Thesis contain total 5 chapters, outline of which is given below.

Chapter 1 presents the introduction of the study area that includes, problem statement, objectives of study, research hypothesis and scope of the study.

Chapter 2 has mainly focused on the literature review. In this chapter basic terminologies and data type is explained. This chapter has also comprises some previous studies carried out for the determination of land cover change and their impact on stream flows. Some methodologies that previous studies used to simulate stream flow were also described of different hydrological models. Studies related to selection of different climate models were also discussed in this chapter.

Chapter 3 is composed of detail study area and some salient characteristics were described. In this chapter meteorological station, data acquisition and sources of data was described. Preprocessing of DEM, land cover classification, application of hydrological models and efficiency parameter were described in detail.

Chapter 4 presents the results and discussions, in this chapter land cover change in Hunza catchment is explained. Percentage snow cover over the Hunza catchment and with respect to elevation is presented. Hydrological models results after calibration and validation was described and statistical parameter were presented. Climate models results before and after bias correction was presented in graphical form and statistical analysis are shown in table form. Climate change impact on streamflow is also presented in this chapter.

Chapter 5 is composed of summery of the study i.e. conclusions drawn from study and recommendations was proposed.

## **LITERATURE REVIEW**

### **2.1 GENERAL**

Hydrological modeling is essential for better water resources management in the context of flood control, drought and irrigation, under climate change which is rather challenging due to the uncertainty in simulated streamflow. Commonly, the hydrological models are designed on the basis of two algorithms such as rainfall–runoff and snowmelt–runoff, and in most of the cases models are primarily followed by one algorithm which restricts their utilization. Recently, research community has developed several hydrological models with the combination of both algorithms to model the streamflow of a catchment characterized by rainfall– and snowmelt–runoff contribution. Different tools, methods and techniques are briefly discussed below.

### **2.2 DESCRIPTION OF ERDAS IMAGINE TOOL**

ERDAS Imagine is a remote sensing image processing tool used for analyzing, displaying and enhancing of digital image that further used in Geographic Information System (GIS) and other designing software i.e. Computer Aided Drawing (CAD). The reflected light from earth surface is helpful for minerals and vegetation analysis (Hugenholtz et al., 2012).

#### **2.2.1 Methods for Land Cover Classification**

There are two methods available in ERDAS Imagine software for classification of remote sensing satellite data.

- a) Unsupervised classification
- b) Supervised classification

##### **2.2.1.1 Unsupervised classification**

In unsupervised classification method Computer classifies unknown classes. Unsupervised classification involve algorithm in which unidentified pixels of an image are inspected and gathered into classes based on natural grouping. The outcome of unsupervised classification is a spectral class because it depends on clusters present in image value. Initially spectral classes cannot be identified. To identify the spectral class

the analyst must compare classification results with maps or large scale images. In supervised classification information category is define and then their spectral separate-ability is checked and in unsupervised classification first spectral classes are defined and then information utility about them. In the supervised classification classifier has to define the class many of these classes may not be apparent to the classifier initially but in unsupervised classification these classes are found automatically which shows advantage of unsupervised classification (Hugenholtz et al., 2012). The classification algorithms for unsupervised classification are,

- i. K-means
- ii. ISODATA

### **2.2.1.2 Supervised classification**

In supervised classification method user classify unknown classes using samples of some known classes. In supervised classification user must have knowledge of the area for which image classification is done and user must provide some input before applying selected algorithm. The input may be derived from air photo analysis, field work surveying the study area, previous reports and study area topographic map (Hugenholtz et al., 2012). The algorithms used for supervised classification are,

- i. Parallelepiped
- ii. Minimum distance to means
- iii. Maximum likelihood classifiers

## **2.3 DESCRIPTION OF HYDROLOGICAL MODELS**

In this section we mainly focused on the application of Hydrological models and their capabilities to simulate the streamflow. A comparative hydrological modeling study of two different hydrological model (rainfall runoff model; HEC-HMS and snowmelt runoff model; SRM) was carried out for selection of a suitable hydrological model and presented in sections below.

### **2.3.1 Rainfall-Runoff Model (HEC-HMS)**

The HEC-HMS is a rainfall-runoff hydrological modeling system developed by U.S. Army Corps of Engineers, to compute the daily streamflow generated by rainfall as well as snowmelt of dendritic watershed systems. It can be used for both large and small river watersheds. Hydrographs that are produced by the model can be used for water

availability, flow forecasting, urban drainage, floodplain regulation, reservoir spillway design, flood damage reduction, future urbanization impact and systems operation studies.

Principally, HEC–HMS consists of 4 components such as meteorological, basin, time specifications and time series component. A basin model component comprises loss, transfer and baseflow estimations by using various methods of watershed. A meteorological model, which incorporate precipitation gauge weights, evaporation–evapotranspiration and snowmelt methods. A control specification model that handles the time variable data records (Bajwa and Tim, 2002).

Different loss method are available that are selected on the basis of nature of simulation either event based or continuous modeling. Some loss methods (Soil Moisture Accounting Loss Method and Gridded Loss Method) requires a high number of input parameter whereas other method (Deficit and Constant Loss Method) is quite a simple method. There are 7 different rainfall to runoff transformation methods are available in this model. Some of these transformation are SCS unit hydrograph, Snyder unit hydrograph and Clark unit hydrograph.

HEC–HMS has two different snowmelt methods, temperature index and gridded temperature index. The temperature index method measures the melt rate based on past and current atmospheric conditions and incorporates cold content to account the ability of snow cover to freeze the rain water falling on it (HEC–HMS user manual 2013). In HEC–HMS total 17 parameters are available, which are initial deficit, constant rate, lag time, maximum deficit, impervious area, standard lag time, rain rate limit, base temperature, melt rate coefficient,  $P_x$  temperature, cold limit, wet melt rate, lapse rate, DDF, water capacity, cold rate coefficient and ground melt.  $P_x$  temperature distinguish between precipitation as snow fall or rain. In the temperature index method, the lapse rate and DDF are the most main parameters for the proficient assessment of snowmelt impact.

### **2.3.2 Snowmelt Runoff Model (SRM)**

SRM is an energy dependent temperature index (degree–day) model was use to simulate and predict daily streamflow in mountainous catchment where main runoff factor is a snowmelt. It also provide user to conduct climate change on snow and runoff by changing the percentage of SCA and temperature. The SRM has been successfully

applied in Ganges River catchment having elevation up to 8,840 m a.s.l and area of 917,444 km<sup>2</sup> (Martince et al., 2008). The SRM has been successfully used in more than a hundred of catchments located in the different region of the world. Precipitation, Temperature and SCA are the input variables required for the model and some physical features of such as area elevation curve and zone/basin area. Runoff produced from rainfall and snowmelt, overlaid on the calculated recession flow and changed into daily discharge is computed on the basis of following equation 3.6.1.

$$Q_{n+1} = \{C_{Sn} \times a_n(T_n + \Delta T_n)S_n + C_{Rn}P_n\} \frac{A}{8.64} (1 - k_{n+1}) + Q_n k_{n+1} \rightarrow (2.3.1)$$

In above equation Q is the average daily discharge (m<sup>3</sup>/sec), C is the runoff coefficient describing the losses as a ratio of measured runoff and precipitation, C<sub>S</sub> refers to snowmelt runoff coefficient and C<sub>R</sub> to rain runoff coefficient, a is the degree day factor (DDF) (cm °C<sup>-1</sup>d<sup>-1</sup>) represents the depth of snowmelt by one degree–day T (°C d), T is the total number of degree–days (°C d), ΔT is the adjustment by temperature lapse rate when extrapolating the temperature from the station to the average hypsometric elevation of the basin or zone (°C d), S is the ratio of snow to the total area of basin/zone, P is the precipitation contributing to streamflow (cm), A is the basin/zone area, k is the recession coefficient. Recession constants are calculated for each basin/zone to compute accurate value of k.

The detail description of parameters and variables are defined in user manual of SRM (Martinec et al 2008). There are three basic model input variables: precipitation P, temperature T, and snow cover area S and seven other model parameters: DDF, recession constants, critical temperature, temperature lapse rate, rainfall contributing area, lag time, runoff coefficient ( for rain and snow). All variable and parameters were specified on daily time step are described in upcoming chapter.

## 2.4 TERMS USED FOR CLIMATE STUDIES

### 2.4.1 General Circulation Model (GCM)

A mathematical model of the general movement of a terrestrial atmosphere. GCMs are used for weather predicting and forecasting climate change (IPCC, 2014).

## 2.4.2 Coupled Model Inter–Comparison Project (CMIP)

CMIP is a structure and the correspondent of the Atmospheric Model Inter–comparison Project (AMIP) for global coupled ocean–atmosphere general circulation models (GCMs). CMIP5 is the recently phase of the project (IPCC, 2014).

## 2.4.3 Representative Concentration Pathways (RCPs)

The four RCPs are provided in the CMIP5 called RCP 8.5, 6.0, 4.5 and 2.6  $W/m^2$ , and these labels show a rough estimate of the radiative forcing at the end of the 21st century. RCP8.5 scenario describes that the radiative forcing reaches at approximately 8.5  $W/m^2$  by the end of 21<sup>st</sup> century. RCP6.0 and RCP4.5 scenarios depict that the radiative forcing will stabilize at approximately 6  $W/m^2$  and 4.5  $W/m^2$  after 21<sup>st</sup> century. RCP2.6 tells that the radiative forcing would rise to approximately 3  $W/m^2$  before the end of 21<sup>st</sup> century and then declines (IPCC 2014).

## 2.4.4 Climate Data Downscaling

Downscaling is a general technique in which data at large scale are transfer at local scales. Dynamical downscaling and statistical downscaling are the main methods to downscale climate data (Ramirez–Villegas and Jarvis, 2010).

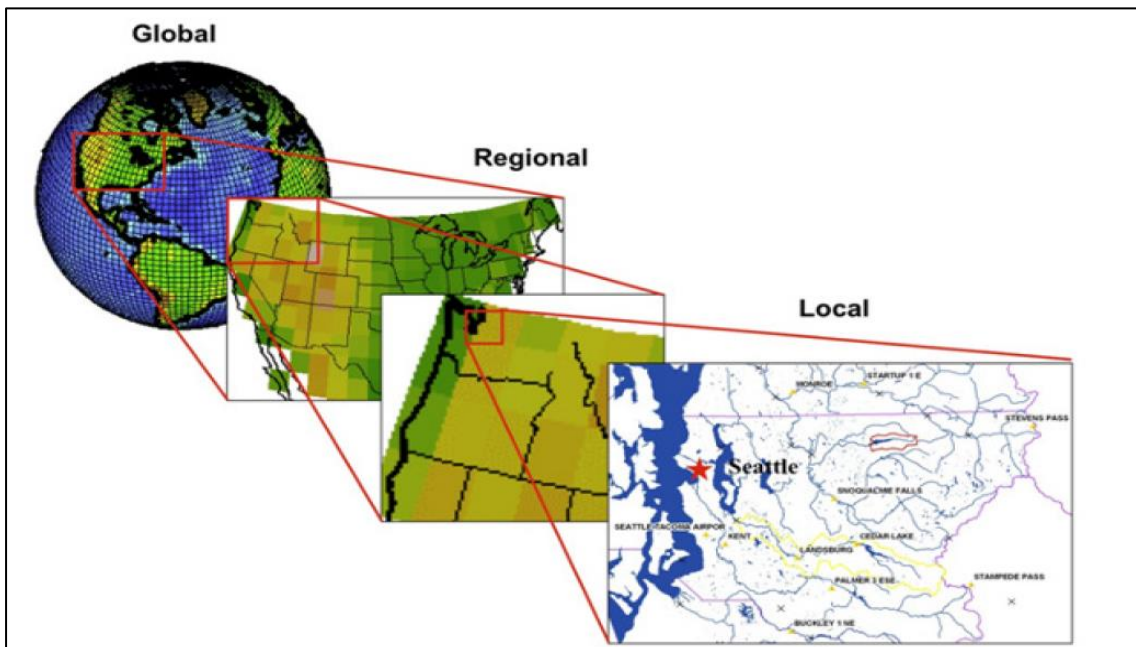


*Figure 2.1: Climate Data Downscaling Scheme*

## 2.4.5 Bias Correction

Output of climate models shows some systematic biases (Climate impact portal, 2016) which are due to:

- Numerical structures
- Inadequate spatial resolution
- Lack of understanding of climate system processes
- Basic physics and thermodynamic processes

Climate model's data should be corrected before using it. Several methods are available to correct climate model's data i.e.

- Multiple linear regression
- Local intensity scaling
- Delta change approach
- Quantile mapping
- Analogue methods

### 2.4.5.1 Delta technique

Delta technique was used to refine precipitation data and temperature data was corrected by adding the difference of observed and baseline data in model's projected data and the data was again plotted to see the accuracy. The equations used in delta method are described below.

$$V_{tuned} = \frac{\overline{V_{obs}}}{\overline{V_{ref}}} \rightarrow (2.2)$$

$$S_{tuned} = \frac{\overline{S_{obs}}}{\overline{S_{ref}}} \rightarrow (2.3)$$

$$E_s = (V_{proj} - \overline{V_{ref}}) \cdot S_{tuned} \rightarrow (2.4)$$

$$E_{proj} = E_s + (\overline{V_{ref}} \cdot V_{tuned}) \rightarrow (2.5)$$

$\overline{V_{obs}}$  is the observed climatology,  $\overline{V_{ref}}$  is the reference climatology for the GCM/RCM baseline,  $V_{tuned}$  is the adjusted factor for mean climate,  $\overline{S_{obs}}$  is the standard deviation of monthly observed data set,  $\overline{S_{ref}}$  is the standard deviation of GCM/RCM,  $S_{tuned}$  is the signal to noise ratio,  $V_{proj}$  is the particular projected month that needs correction,  $E_s$  is the signal enhance or signal dampened for particular projection month and  $E_{proj}$  is the

bias corrected climatic variable for particular month (Maraun, 2016: Burhan et al., 2015 and Hay et al., 2000).

## **2.5 PREVIOUS STUDIES**

### **2.5.1 Land Cover Classification**

Efe et al. (2012) carried out a study for land use change detection in Karınca River catchment Turkey using GIS and remote sensing. Two images of year 1979 and 2007 were analyzed for 1979 Land use data was derived from historical topographic and land use map of the study area after transferring them in digital format and Landsat ETM+ satellite image of 2007 was used. Unsupervised classification method was used and Iterative self-organizing analysis technique (ISODATA) was used for Landsat ETM+ image. The classification of 1979 image showed 43.4 % forest, 26.5% grass land, 18.3 % olive groves, 10 % agriculture and 1.2 % built up area similarly land use data of 2007 Image consisted of 44.2% forest, 20.7 % grass land, 25.4% olive and 7.9 % agriculture areas. Changes occurred from 1979 to 2007 were 2.7 % decrease in cropland, 7.1 % increase in olive groves, 0.8% increase in forest and 0.7 % increase in built-up area.

Coskun et al. (2008) carried out a study for analysis of land use change and urbanization in the Kucukcekmece Water Basin (Istanbul, Turkey) using GIS and remote sensing. The study was carried out for 15 years from 1992 to 2007. Satellite images of year 1992, 1993, 2000 and 2007 from Landsat-5 TM, SPOT-XS and Pan, IRS-IC, IRS-LISS and Landsat-5 TM respectively were analyzed. The spatial resolution for SPOT- Pan, XS, IRS-1C/D, IRS-LISS, and Landsat-5 TM are 10 m, 20 m, 5.8 m, 23.5 m and 30 m respectively and 1:25,000, 1:5,000 scaled maps of the study area and orthophotos of 1:5,000 air photos for ground truth were used. To achieve geometric registration satellite data was converted into UTM zone 35 using 1:5,000 topographic maps. Different classification methods were applied to enhance spectral data in unsupervised classification method ISODATA algorithm was applied for all images the threshold value was .95 and number of iteration was 20 and 50 clusters were obtained. Due to similarity of reflected values of different classes efficiency of unsupervised classification was poor therefore supervised classification method was applied and maximum likelihood algorithm was applied and number of clusters were increased from 50 to 80. The classes of water, forest

evergreen, forest deciduous, forest intermixture, barren land, agriculture, grass land, soil, urban, road were made. The results of classification were evaluated 100 random pixels were chosen and these were compared with results of fieldwork the user accuracy was 84% ,84%, 83.33% and 86% for 1992,1993,2000 and 2006 respectively,

Yüksel et al. (2008) carried out a study for land use/cover classification for an area representing the heterogonous characteristics of eastern Mediterranean regions in Kahramanmaras, Turkey. Supervised classification 80 training signature finally 10 classes. After supervised classification process, classified image was post–processed by using “Expert Classification System”. Supervised classification showed irrigated land 33%, grass land 28%, woodland/shrub 11%, coniferous forest 6%, bare rocks 5%, urban fabric 4%, inland marshes 0%, water courses 2%, non–irrigate arable land 10% and roads/rails networks and associated land 1%.

### **2.5.2 Hydrological Modeling**

Accurate hydrological modeling is essential for better water resources management in the context of flood control, drought and irrigation, under climate change which is rather challenging due to the uncertainty in simulated streamflow. The impacts of the climatic anomalies on streamflow predicted by the utilization of hydrological models are strictly connected with the efficiency of hydrological models (Azmat et al., 2016a). However, the application of an appropriate model in high–altitude cryosphere (snow and ice) catchments is important because of two fold streamflow sources i.e. rainfall–runoff and snow– and glacier–melt runoff (Azmat et al., 2015). Mostly, the efficiency of the hydrological models is questioned in high–altitude regions due to large contribution of snow– and glacier–melt runoff (Martinec et al., 2008). The snow accumulation and melting processes are highly complex due to the involvement of different mass balance relationships such as energy and mass balance; mass and heat transport by sublimation and vaporization (Tarboton and Luce, 1996) and these complexities make the hydrological models less efficient.

Generally, the hydrological models are designed on the basis of two algorithms such as rainfall–runoff and snowmelt–runoff, and in most of the cases models are primarily followed by one algorithm which restricts their utilization. Recently, research community has developed several hydrological models with the combination of both algorithms to model the streamflow of a catchment characterized by rainfall– and snowmelt–runoff contribution (Ohara et al., 2010 and Şensoy, 2005). However, the

rainfall–runoff models also providing snowmelt–runoff contribution; are observed less efficient in high–altitude catchments (Azmat et al., 2016a). Consequently, the modeling of streamflow in high–altitude catchment is always a challenge faced by the hydrologist community. Therefore, the comparison of different hydrological models is essential to compare the accurate streamflow predications.

Choudhari et al. (2014) carried a study on rainfall–runoff simulate using HEC–HMS model in Balijore Nala Watershed of Odisha, India. A total 24 rainstorm events were selected from 2010 to 2013 data. Twelve events were chosen for calibration of and remaining twelve for validation of rainfall runoff model (HEC–HMS). Exponential recession, SCS unit hydrograph, SCS curve number, Muskingum routing methods were selected. The model was calibrated manually and showed the value of Mean Absolute Error (MAE) of 0.25 and 0.20 for peak discharge and runoff depth, respectively. Similarly, the values of Root Mean Square Error (RMSE) were obtained as 0.28 m<sup>3</sup>/s and 2.30 mm for peak discharge and runoff depth, respectively. Then parameters were optimized and error functions reduced to 0.12, 0.10, 0.09 m<sup>3</sup>/sec and 0.75 mm in sequence. Further, same parameters were used for validation of HEC–HMS that showed satisfactory results with low statistical error functions.

Nabi et al. (2011) carried out a study in snow and glacier–melt Astor basin. Snowmelt Runoff Model (SRM) was used to estimate the snow melt runoff in Astor basin during, year 2000. The daily temperature and precipitation and snow cover data was used as input data. Basin was sub–divided in to five elevation zones about 1300 elevation interval using SRTM of 90 m resolution DEM. The basin elevation varied from 1270 m a.s.l to 7713 m a.s.l. Snow cover information were extracted by Landsat TM satellite data on monthly basis. The COE (Coefficient of Efficiency) for simulation was 0.91 and volume difference (Dv) of 9.01 percent was observed.

A few comparative studies have been carried out to simulate daily streamflow of high–altitude glacierized catchment. Rulin et al. (2008) have applied NedbØr–AfstrØmnings Rainfall–Runoff Model (NAM) and Snowmelt Runoff Model (SRM), in a snow–fed arid mountainous Aksu River catchment and stated that the SRM performed better than NAM. Azmat et al. (2016a) compares the two hydrological models, Hydrological Engineering Center – Hydrological Modeling System (HEC–HMS) and SRM for the streamflow simulation in a seasonal snow–fed Jhelum River catchment and indicated that the HEC–HMS performed better than the SRM during the peak flow season (i.e.

summer) due to the capability of capturing the rapid runoff peaks generated by rainfall better than SRM. Tahir et al. (2011b) have applied SRM successfully in high–altitude Hunza River catchment with the integration of MODIS SCA.

### **2.5.3 Climate Change Impact Assessment**

For climate change impact assessment future climate data (i.e. temperature and Precipitation) at different spatial as well as temporal scale is required. Daily observed climate data are available to perform such impact studies for the past decades. However, the lack of daily future climate data at adequately fine spatial resolution is a main issue to execute fine–scale analyses on future climatic studies. The spatial resolutions of General Circulation Models (GCMs) model outputs are too low and cannot be directly used for small–scale impact assessment. Moreover, all GCMs outputs involve large no. of biases that firstly need to be corrected before impact assessments. Therefore, bias correction of GCM outputs are necessary before their use in hydrological modeling. (Terink et al., 2009; Teutschbein and Seibert, 2012; Berg et al., 2012; Burhan et al., 2015 and Immerzeel et al., 2012)

The potential implications of climatic anomalies on the catchment hydrology in the form of water resources availability in streams and hydrological extremes (Ling et al., 2011) which is strictly connected with the efficiency of the hydrological models (Fischer et al., 2014; Azmat et al., 2015). The global climate change is also affecting the hydrologic system by varying timing and amount of snow– and glacier–melt, in mountainous catchments (Meenu et al., 2013). In order to assess the climate change impact, some hydrological models have capability to show their sensitivity to climate variables (Abudu et al., 2012). Previous studies directly analyzed the impact of climate change on streamflow without evaluating suitability and sensitivity of the hydrological models with input parameters and catchment characteristics. In the context of input parameters, the HEC–HMS model mainly sensitive to the precipitation; however, the quality of precipitation data at high–altitude catchments is always been problematic. While, in case of catchment characteristics, the rainfall–runoff models are primarily designed for the simulation of streamflow of a rain–fed catchment but the efficiency of snowmelt–runoff model is often questioned (Rasmussen et al., 2012). Furthermore, the models based on snow cover data such as SRM are sensitive to the temperature and snow data while less sensitive to the precipitation data (Azmat et al., 2016a). Therefore,

appropriate model selection in high–altitude cryosphere catchments is essential for the streamflow predictions under changing climate, globally.

Lutz et al. (2016) developed an advanced envelope–based selection approach for selecting representative climate models for climate change impact studies. This methodology (Figure 2.2) was adopted for a study area covering the Indus, Ganges and Brahmaputra river basins.

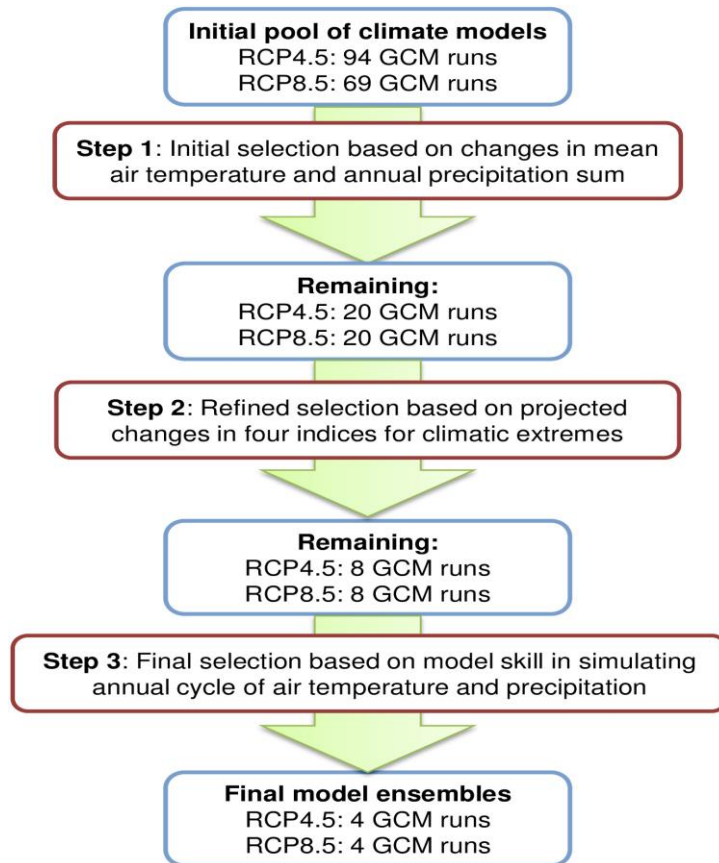


Figure 2.2: Methodology Adopted for Selection of Climate Models by Lutz et al. (2016)

Table 2.1: Selected Climate Models by Lutz et al. (2016).

GCMs	RCP4.5	RCP8.5
BNU–ESM_r1i1p1	×	cold, wet
inmcm4_r1i1p1	×	cold, dry
CMCC–CMS_r1i1p1	×	warm, wet
CSIRO–Mk3–6–0_r4i1p1	×	warm, wet
inmcm4_r1i1p1		×
CMCC–CMS_r1i1p1		×
bcc–csm1–1_r1i1p1		×
CanESM2_r3i1p1		×

Author scrutinized eight (8) GCM runs (Table 2.1) from 163 GCM runs obtained from Coupled Model Intercomparison Project Phase 5 (CMIP5), for the IGB on the basis of extreme projections. The projected precipitation and temperature dataset for aforementioned eight (8) General Circulation Models (GCMs) downscaled at 5×5 km grid size were obtained from HI-AWARE project. Further, detailed description of the aforementioned dataset used in current study is given by Arthur et al. (2016)

In this study, two well-known hydrological models (SRM; snowmelt based runoff model and HEC-HMS; rainfall based runoff model) used to compute daily streamflow in high-altitude cryosphere Hunza River catchment. Subsequently, best efficient hydrological model was used to assess the impact of climate change on streamflow of the Hunza River catchment by using different climate change scenarios.

## 2.6 EFFICIENCY CRITERIA

### 2.6.1 Nash–Sutcliffe Coefficient (NS)

Nash–Sutcliffe Coefficient is used to assess the simulation power of hydrological models (Krause et al., 2005). The governing equation is given below.

$$NS = 1 - \frac{\sum_{t=1}^T (Q_{ot} - Q_{mt})^2}{\sum_{t=1}^T (Q_{ot} - \bar{Q}_o)^2}$$

Where,  $\bar{Q}_o$  is the mean observed discharges,  $Q_m$  is modeled discharge at time t,  $Q_o^t$  is observed discharge at time t.

\*Nash–Sutcliffe efficiency can range from  $-\infty$  to 1.

### 2.6.2 Percent Volume Difference

Difference b/w the total simulated and measured runoff (Tahir et al., 2011b). It is defined as:

$$Dv (\%) = \left( \frac{V - V'}{V} \right) \times 100$$

Where,

V is the simulated runoff volume, V' is the observed runoff volume;

\*Difference volume can range from  $-\infty$  to  $+\infty$

### 2.6.3 Correlation Coefficient

Correlation coefficient represent the linear interdependence or strong relationship of two variables or sets of data (Krause et al., 2005). It is calculated as,

$$R = \frac{n(\sum xy) - (\sum x)(\sum y)}{\sqrt{\{n \sum x^2 - (\sum x)^2\} \{n \sum y^2 - (\sum y)^2\}}}$$

Where,

n is the number of observations, x is the value of first variable, y is the value second variable

\*Coefficient of correlation value range from -1 to 1

### 2.6.4 Coefficient of Determination

This is the Square of correlation coefficient (Krause et al., 2005). It is calculated as,

$$R^2 = \left( \frac{n(\sum xy) - (\sum x)(\sum y)}{\sqrt{\{n \sum x^2 - (\sum x)^2\} \{n \sum y^2 - (\sum y)^2\}}} \right)^2$$

\*Coefficient of determination value range from 0 to 1

### 2.6.5 Mean absolute error (MAE)

The MAE measures the average magnitude of the errors in a set of forecasts (Chai and Draxler, 2014). It is calculated as,

$$MAE = \frac{1}{n} \sum |Observed - Model|$$

### 2.6.6 Root mean squared error (RMSE)

The RMSE is a quadratic scoring rule which measures the average magnitude of the error (Chai and Draxler, 2014). It is calculated as,

$$RMSE = \sqrt{\left( \frac{1}{n} \sum_{i=1}^n (model_i - observed_i)^2 \right)}$$

\*Both the MAE and RMSE can range from 0 to  $\infty$ .

## METHODOLOGY

### 3.1 STUDY AREA

The present study was conducted in Hunza River catchment, a major tributary of Indus River System (IRS), with catchment area of 13,718 km<sup>2</sup> (Figure 3.1), located in high–altitude (ranges from 1395 to 7849 m a.s.l.) central Karakoram mountainous region, northern Pakistan. Approximately, 32.5% (4,460 km<sup>2</sup>) of the total catchment area is located above 5000 m a.s.l. which is considered as glaciated part of the catchment (Akhter et al., 2008). The streamflow in Hunza River is mainly contributed by the seasonal snow– and glacier–melts with slight influence of summer monsoon, while westerlies circulations (winter precipitation pattern) plays a significant role in snow and glaciers advancement and this phenomena is acting more significantly in high–altitude part of the Hunza River catchment (Tahir et al., 2016).

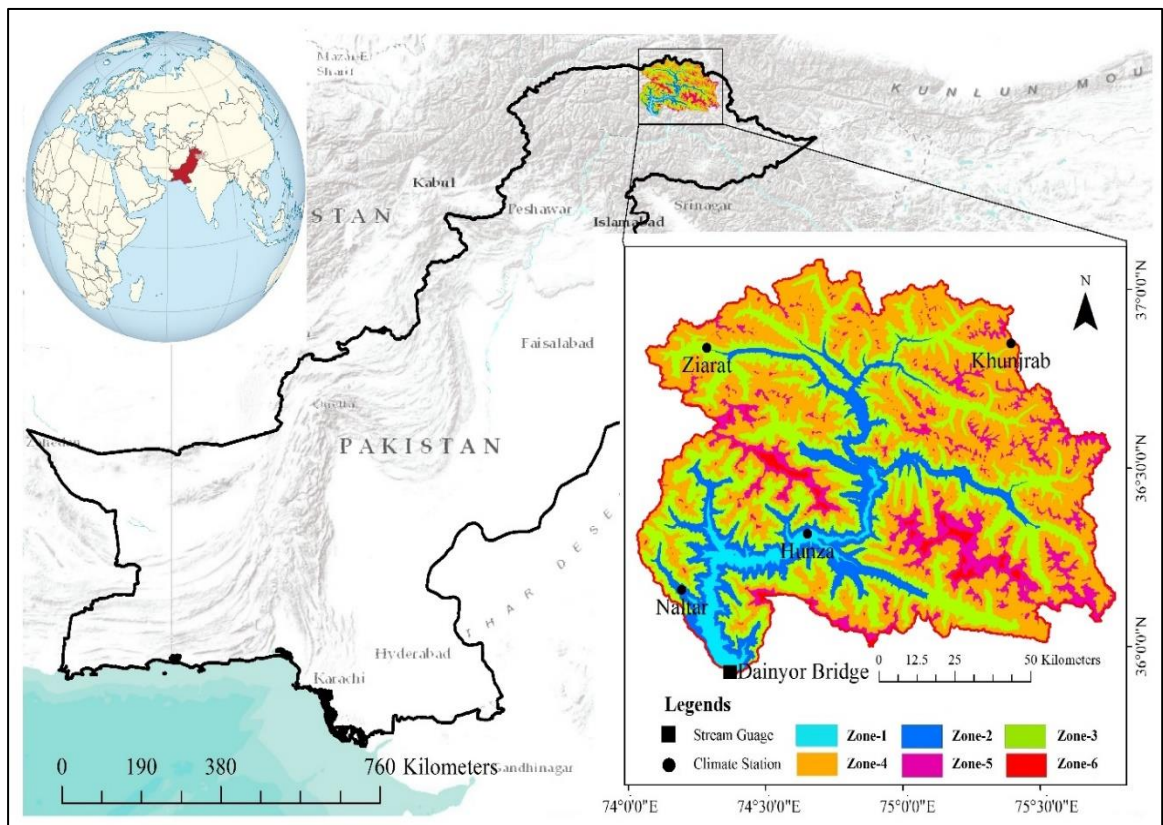


Figure 3.1: Hunza River Catchment along with Climate Stations and Stream Gauge Locations

The basin-wide (BW) SCA (average of 2000–2010) during winter and summer seasons varies approximately 80% and decreases to 34%, respectively, as also confirmed by Tahir et al. (2011a). While, the mean annual precipitation at climate stations, Hunza (2156 m a.s.l.), Naltar (2858 m a.s.l.), Ziarat (3669 m a.s.l.) and Khunjrab (4730 m a.s.l.) are 389, 679, 247 and 187 mm, respectively, while the mean annual streamflow at Dainyor Bridge is 323 m<sup>3</sup>/sec (1966–2010) as also stated by Tahir et al. (2011a, 2011b), other salient feature are given in Table 3.1. The most active hydrological zone of the Hunza River is located above 5000 m a.s.l. (Tahir et al., 2011b), where five– to tenfold precipitation increase as reported by Hewitt (2005, 2007) with a large drop in temperature, resulting snow and glacier accumulation. Almost 90% of total glaciated area lies in the Karakoram Range above 5000 m a.s.l.

*Table 3.1: Salient Feature Hunza River catchment*

Climate Stations	Station Name	Elevation (m a.s.l.)	Mean Annual Precipitation (mm)	Mean Annual Temperature (°C)	Agencies/ Department
1	Hunza	2156	389	11.29	PMD
2	Naltar	2858	679	6.66	WAPDA
3	Ziarat	3669	247	2.75	WAPDA
4	Khunjrab	4730	187	–5.32	WAPDA

## 3.2 DESCRIPTION OF DATASET

### 3.2.1 Hydro–Climatic Data

In Pakistan, the hydro–meteorological database mostly managed by the Water and Power Development Authority (WAPDA) and Pakistan Meteorological Department (PMD). The meteorological data (daily precipitation, minimum and maximum temperature) were made available for three (3) stations (Naltar, Ziarat and Khunjrab) from WAPDA, while, for Hunza station, the data were obtained from PMD, during 2001 to 2010, as shown in Table 3.1. Further, the streamflow data of Hunza River at Dainyor Bridge, were obtained from Surface Water Hydrology Project of the WAPDA (SWHP–WAPDA), during 2001–2010 (excludes 2007 due to unavailability of streamflow records). The observed hydro–climatic data for a base period of 10 years i.e. 2001 to 2010 is used as reference which is hereafter referred to as baseline (observed).

### 3.2.2 RCPs Climate Dataset

Himalayan Adaptation, Water and Resilience (HI-AWARE) project offers reference climate dataset (i.e. daily precipitation and mean air temperature) for the Indus, Ganges and Brahmaputra (IGB) River Basins. Arthur et al. (2016) scrutinized eight (8) GCM runs [inmcm4\_r1i1p1, CMCC-CMS\_r1i1p1, bcc-csm1-1\_r1i1p1, CanESM2\_r3i1p1 (RCP8.5); BNU-ESM\_r1i1p1, inmcm4\_r1i1p1, CMCC-CMS\_r1i1p1, CSIRO-Mk3-6-0\_r4i1p1 (RCP4.5)] from 163 GCM runs obtained from Coupled Model Intercomparison Project Phase 5 (CMIP5), for the IGB on the basis of extreme projections. The datasets downscaled on the basis of Representative Concentration Pathways (RCPs) under HI-AWARE project, were obtained to study the projected changes in hydrological regime of Hunza River catchment. The projected precipitation and temperature dataset for aforementioned General Circulation Models (GCMs) downscaled at 5×5 km grid size were obtained from HI-AWARE project. Further, detailed description of the aforementioned dataset used in current study is given by Arthur et al.(2016).

## 3.3 SATELLITE DATA

### 3.3.1 ASTER GDEM

The Advance Spaceborne Thermal Emission and Reflection Radiometer Global Digital Elevation Model (ASTER GDEM) available at 30×30 m resolution were utilized in this study for the delineation of Hunza catchment and extraction of physical parameters such as elevation, slope and catchment area, etc. The six altitude zones were extracted for the Hunza catchment with the difference of 1000 m by using the ASTER GDEM, for the zone-wise (ZW) snowmelt runoff simulation (see Figure 3.2 and Table 3.2).

*Table 3.2: Zone Wise Characteristics of Hunza River Catchment*

<b>Zone / Sub-basins</b>	<b>Elevation Range (m a.s.l)</b>	<b>Mean Elevation (m a.s.l)</b>	<b>Area (%)</b>	<b>Area (km<sup>2</sup>)</b>	<b>Max SCA (%)</b>	<b>Min SCA (%)</b>	<b>Climate Stations</b>
Zone-1	1395–2500	1965	3.1	431	7	1	Hunza
Zone-2	2501–3500	3000	11.5	1581	54	3	Naltar
Zone-3	3501–4500	4000	29.3	4025	83	13	Ziarat
Zone-4	4501–5500	5000	44.7	6127	96	52	Khunjrab
Zone-5	5501–6500	6000	10.0	1377	98	96	–
Zone-6	6501–7849	7175	1.3	177	98	97	–

Several key features of different hydro–climate stations and elevation zones (for the implementation of SRM), are given in Table 3.2 and shown in Figure 3.2.

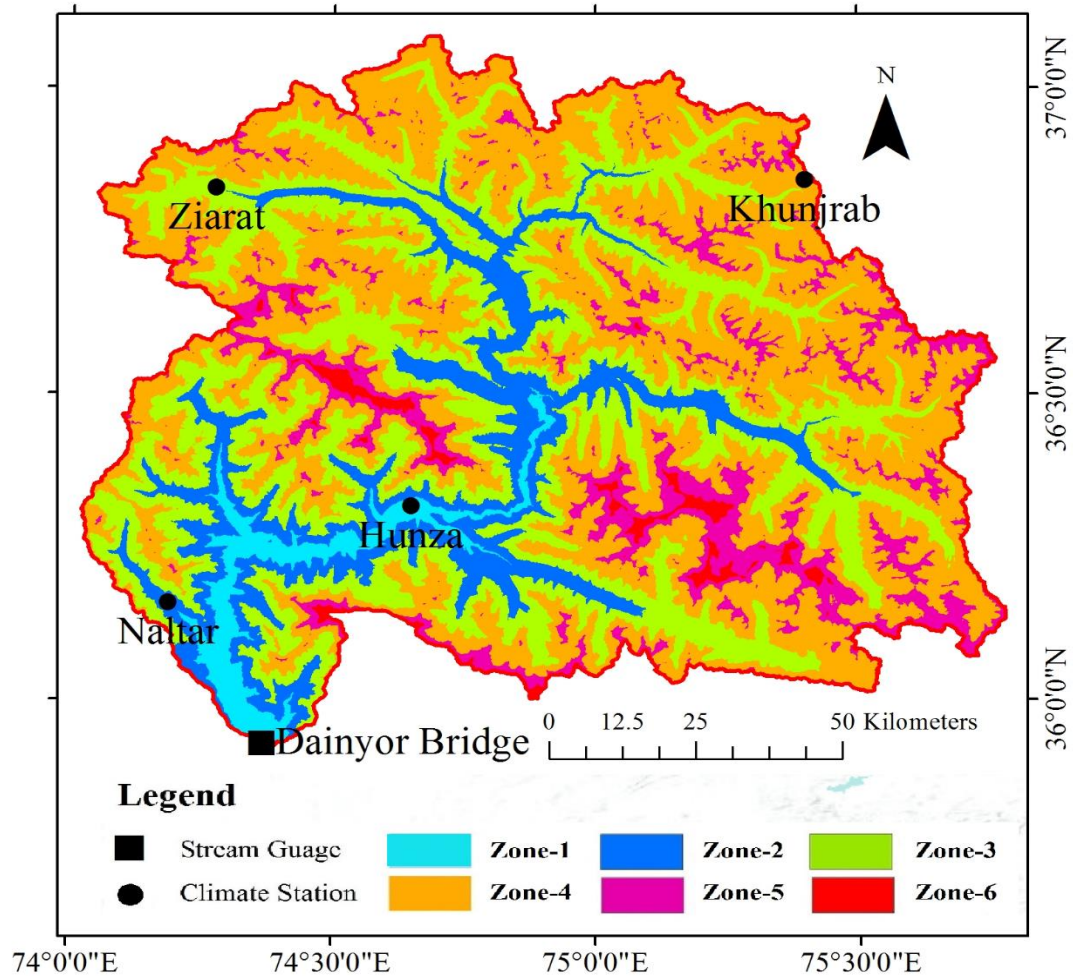
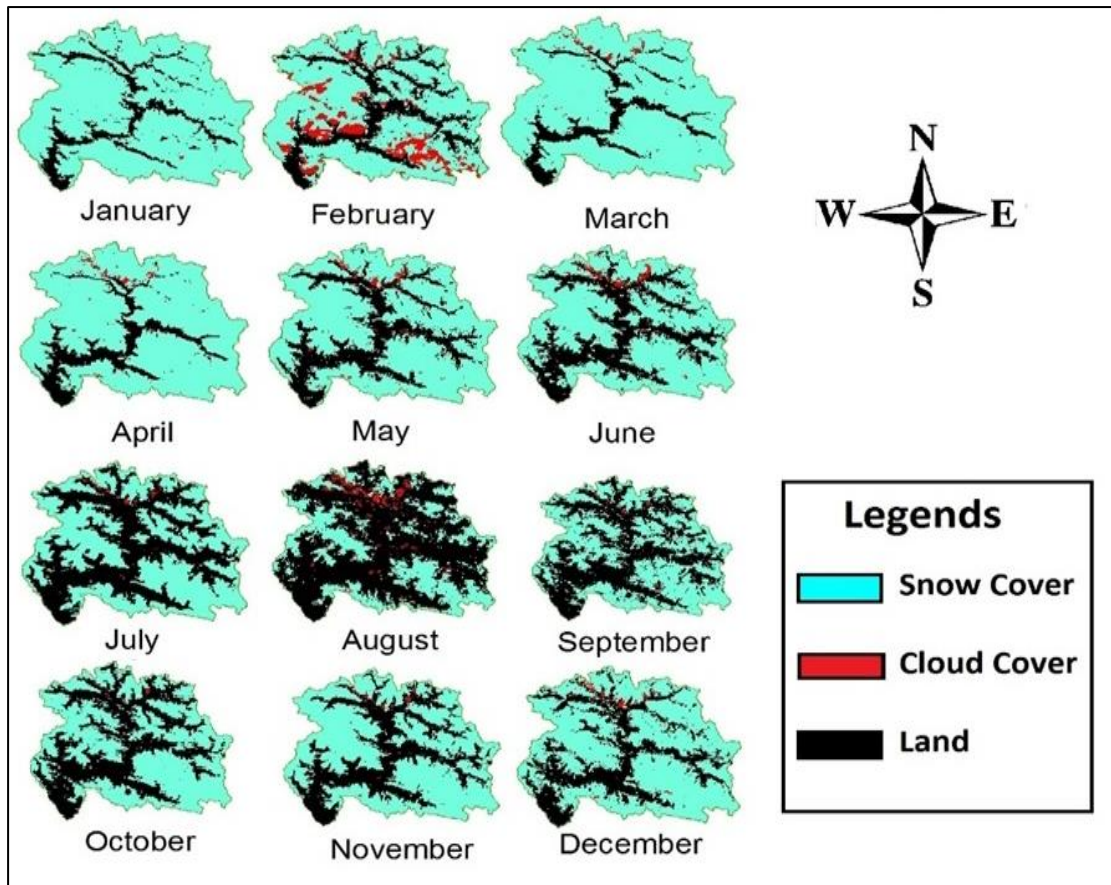


Figure 3.2: Zone Wise Distribution of the Hunza Catchment along with Location of Climate Stations and Streamflow Gauging Station

### 3.3.2 MODIS Snow Cover Data

The Moderate Resolution Imaging Spectroradiometer (MODIS) SCA products MYD10A2 and MOD10A2 at 8–days interval available on Aqua and Terra satellite with approximately 500 m resolution (Figure 3.3), were selected for the determination of percentage of SCA over Hunza River catchment. The dataset of 450 processed images were downloaded from <http://nsidc.org/cgi-bin/snowi/search.pl> during 2001 to 2010.



*Figure 3.3: MODIS Satellite Images Presenting the Mean Monthly SCA in the Hunza River Catchment (2001–2010).*

### 3.3.3 Landsat Data

The Landsat–5&8 surface reflectance data product at sixteen (16) day interval, approximately 30×30 m spatial resolution, was selected for the Hunza River catchment for the determination of land cover features and percentage area of individual land cover. The Landsat –5 data of 1994 and Landsat–8 data of 2014 in month of August was downloaded from <http://earthexplorer.usgs.gov/>. Two different time interval data was selected for identification of land cover change during that period. After downloading Landsat data, the spectral bands were then stacked to make a single composite image (Figure 3.4) by using ERDAS Imagine tool and then projected to WGS1984 UTM 43N ZONE projection system. Furthermore, the image classification was carried out in ERDAS Imagine environment.

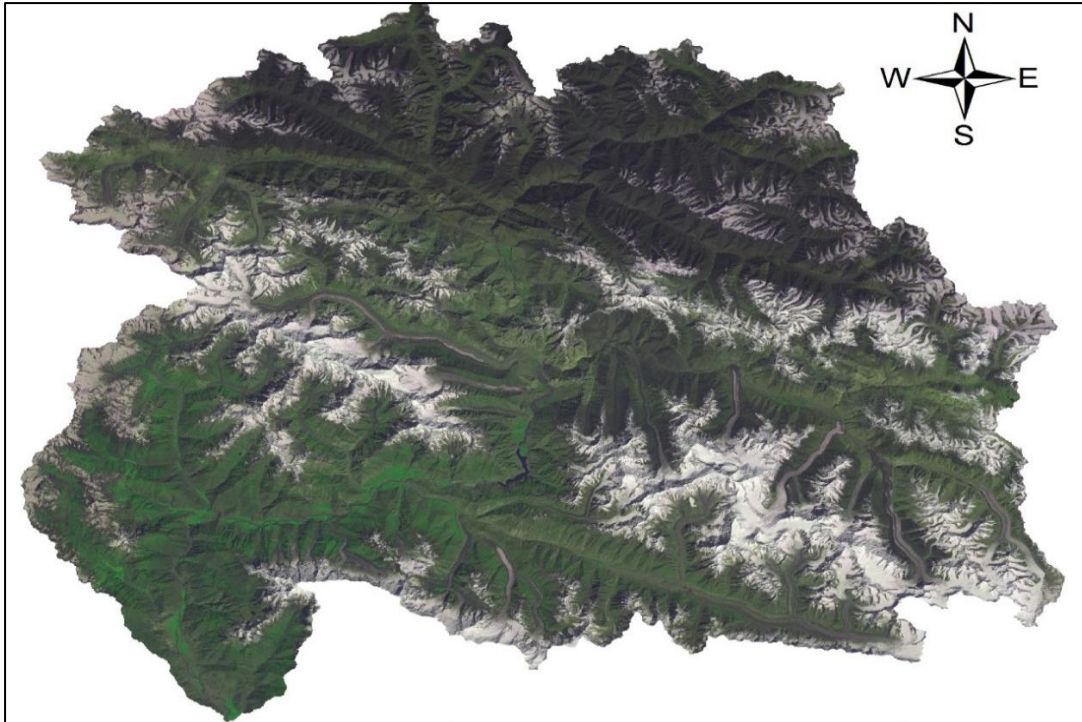


*Figure 3.4: Landsat-8 Image for Hunza River Catchment*

## **3.4 PRELIMINARY DATA ANALYSIS**

### **3.4.1 Time Series Analysis**

Time series analysis was conducted on climate data to analyze the climatic behavior of Hunza catchment.

#### **3.4.1.1 Precipitation analysis**

The analysis on change in precipitation recorded on the climate station present in Hunza River catchment is shown in Figure 3.5. The station is Khunjrab climate station is at highest elevation (4730 m a.s.l). The total annual precipitation is considerable low as compared to the other climate station precipitation. The average annual precipitation of 187 mm was observed which is significant low as compare to Naltar climate station (2858 m a.s.l), that have average annual precipitation of 679 mm, according to the 10-year record form 2001–2010 (Table 3.1). The current precipitation data record is not representing the trend of whole catchment because above 4730 m a.s.l there is no climate station installed which is the main hydrological active zone (Tahir et al. 2011b) of catchment due to snowmelt runoff contribution from zone above 5000 m a.s.l during summer season.

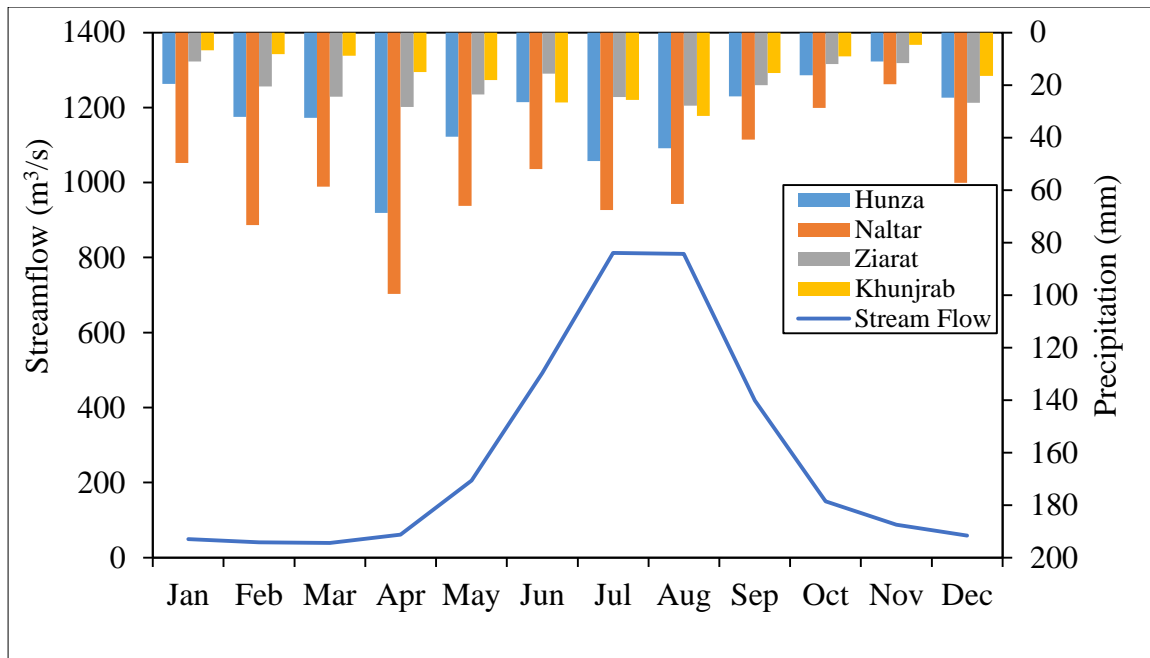


Figure 3.5: Preliminary Time Series Data ( Precipitation, Temperature and Streamflow) Analysis (2001–2010)

### 3.4.1.2 Temperature analysis

The variation in mean annual observed temperature all climate stations present in Hunza catchment is shown in Table 3.1. The maximum mean annual temperature of 11.29 °C was found at Hunza climate station (2156 m a.s.l) and minimum of -5.3 °C was found at Khunjrab (4730 m a.s.l) climate station which clearly shows that with the increase in elevation the temperature goes to decrease according to the 10-year record from 2001–2010.

### 3.4.1.3 Stream flow data analysis

The variation in observed streamflow on mean annual basis at Dainyor Bridge station was analyzed to understand the hydrological behavior of Hunza catchment. The data record is available for 25 years (1986–2010) duration. Maximum mean annual streamflow of 378 m<sup>3</sup>/sec and minimum mean annual streamflow of 200 m<sup>3</sup>/sec was observed in 1994 and 1997, respectively shown in Figure 3.6 and mean annual streamflow of 269 m<sup>3</sup>/sec (Figure 3.5) was observed over 10-year (2001–2010) data record. Mean annual streamflow was also analyzed that shows slightly increasing trend.

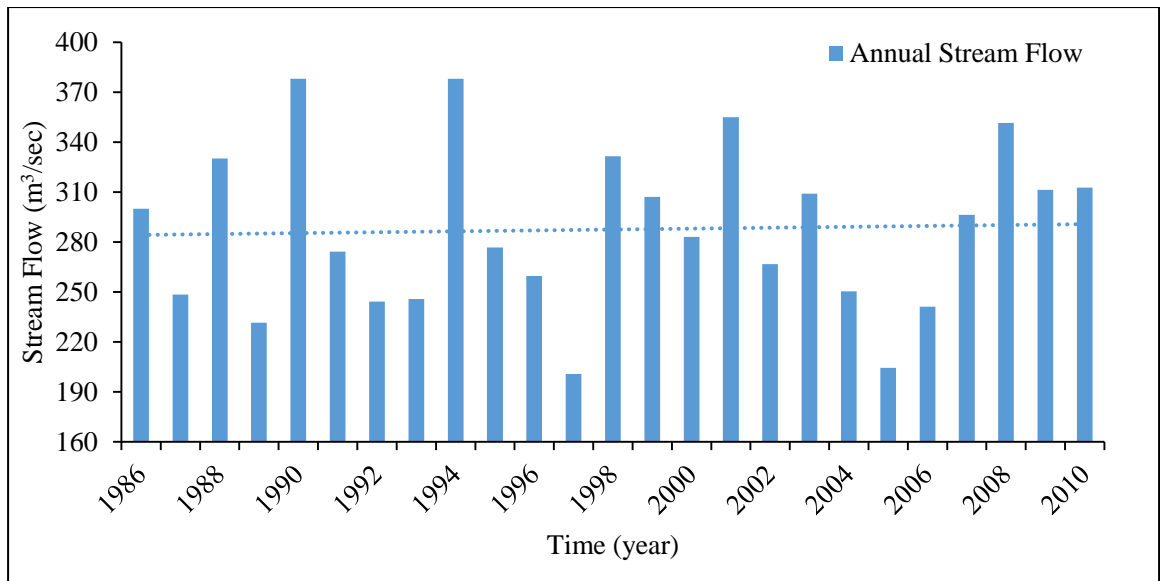


Figure 3.6: Streamflow at Dainyor Bridge Station in Hunza River Catchment

### 3.5 METHODOLOGY

The overall methodology used in this study is presented in Figure 3.7 and will be discussed in subsequent sections.

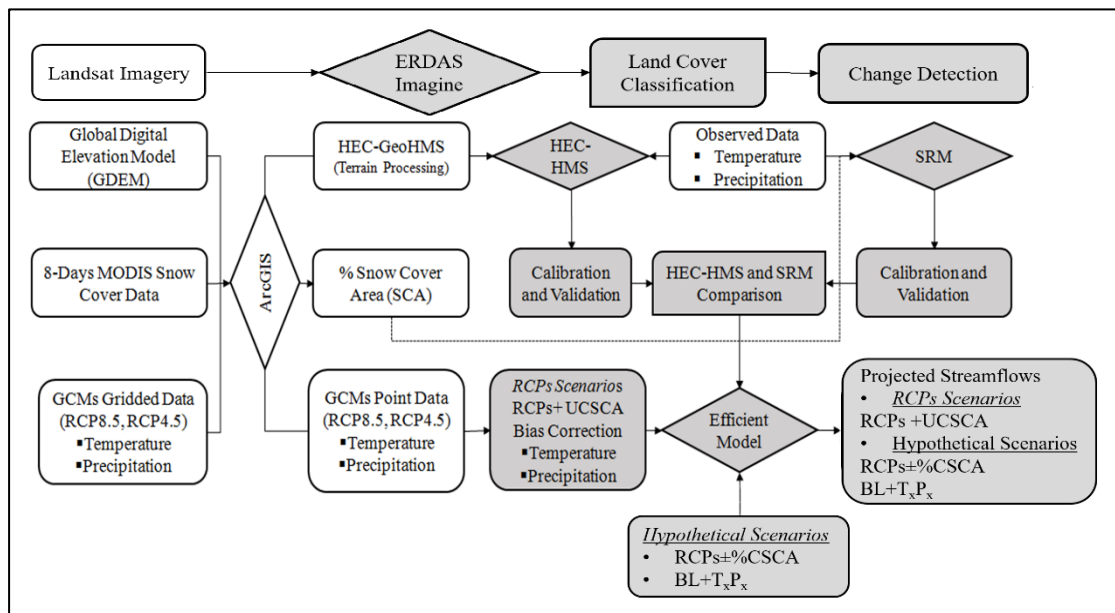


Figure 3.7: Schematic Diagram Showing the Methodology, Hunza River Catchment

#### 3.5.1 Land Cover Classification

In this study the supervised classification was chosen for identification of land cover features present in Hunza catchment using ERDAS Imagine Tool. The maximum likelihood algorithm was used. Total 40 number of training samples were generated as

a signature on which the classification was performed. Maximum 10 number of iteration and convergence threshold value of 0.950 was selected. After performing supervised classification the classes were then recoded into six land cover categories. These land cover classes are Forest, Vegetation, Water bodies, Snow and Glaciers, Exposed Rocks and Barren Land.

### **3.5.2 Snow Cover Variability**

ArcGIS tool was employed to extract and estimate the BW and ZW SCA from the processed MODIS images for the Hunza River catchment. Since, the presence of clouds is always problematic for the accurate extraction of SCA. Therefore, to improve the accuracy by removal of clouds, both SCA products were used for the generation of cloud free composite. The accuracy and functionality of the cloud removal technique adopted in this study has been discussed by Hasson et al. (2014) and Azmat et al. (2016b). Two steps were involved in this technique, first, both Aqua and Terra same day images were merged by considering Terra as a base due to relatively less cloud cover. The cloud free pixels of Aqua image replaced the cloudy pixels of Terra. Second, the current day cloudy pixels replaced by the previous day snow cover pixels. This SCA product has been used successfully by several researchers for the streamflow simulations (Tahir et al., 2011b; Azmat et al., 2016a). Further, the 8–days interval SCA was converted into daily data by using linear interpolation method.

### **3.5.3 Application of Hydrological Models**

The daily streamflows were simulated at Dainyor Bridge by using both Snowmelt Runoff and Rainfall–Runoff models in Hunza River catchment. Both models were calibrated and validated for periods of 6 years (during 2001–2006) and 3 years (during 2008–2010), respectively. The methodology used in this study is described schematically in Figure 3.7.

#### **3.5.3.1 Application of HEC–HMS**

Hunza catchment was divided into five (5) sub–catchments as shown in Figure 3.8 and described in Table 3.3. Observed precipitation and temperature dataset were used as an important input in HEC–HMS. Principally, HEC–HMS consists of four components such as basin, meteorological, time specifications and time series component. HEC–HMS basin component offers various methods to model loss, transfer, channel routing and baseflow (Azmat et al 2015).

In this study various methods to model loss, transfer, channel routing and baseflow with different combination were used for hydrological modeling. A good agreement was found by using Initial and constant (loss), Clark Unit Hydrograph (transfer), Muskingum (channel routing) and Constant Monthly (baseflow) combination of methods (Table 3.4). Previously, Clark unit hydrograph and Muskingum methods are successfully used by Cunderlik and Simonovic (2007) and Banitt (2010).

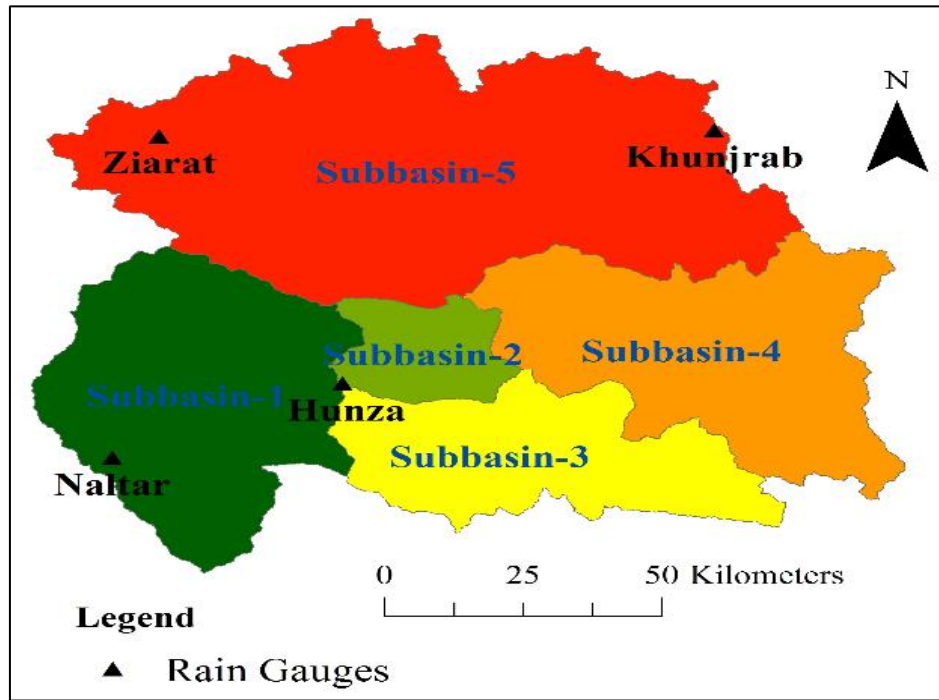


Figure 3.8: Five Subbasins of Hunza River Catchment used for HEC–HMS

Table 3.3: Subbasin Wise Characteristics of Hunza River Catchment

Zone / Sub-basins	Elevation Range (ma.s.l.)	Mean Elevation (ma.s.l.)	Area (%)	Area (km <sup>2</sup> )	Climate Stations
Subbasin-1	1395–7739	4567	20.5	2809	Naltar
Subbasin-2	2047–7558	4803	4.6	631	Hunza
Subbasin-3	2052–7849	4951	13.5	1850	–
Subbasin-4	2423–7847	5135	20.2	2771	–
Subbasin-5	2439–7765	5102	41.2	5658	Khunjra, Ziarat

Table 3.4: Methods used in HEC–HMS

Transform Method	Base Flow Method	Loss Method	Routing Method
Clark Unit Hydrograph	Constant Monthly	Initial & Constant	Muskingum
SCS Unit Hydrograph	Recession Base Flow	Deficit & Constant	Lag
—	Bounded Recession	SCS CN	—

Meteorological data such as precipitation, snowmelt and temperature were incorporated through the meteorological component of the model. Gage weight method was used and weights were measured by Thiessen polygon method over the entire catchment.

*Table 3.5: Gage Weights for Hunza River Catchment*

Sub-basins	Area	Area under Thiessen Polygon (km <sup>2</sup> )	Gauge Weights (%)	Climate Stations
Subbasin-1	5655	2378	42	Khunjrab
		2411	43	Ziarat
		866	15	Hunza
Subbasin-2	2770	2009	73	Khunjrab
		761	27	Hunza
Subbasin-3	631	630	100	Hunza
Subbasin-4	2808	1063	38	Hunza
		1565	56	Naltar
Subbasin-5	1849	180	6	Ziarat
		1849	100	Hunza

*Table 3.6: Range of Parameter Values for Application of HEC-HMS in Hunza River Catchment*

Parameters	Parameters Value Ranges	Initial Values
	<b>for Hunza River Catchment</b>	
Initial loss (mm)	3 to 8	Trial optimization
Constant loss (mm/hr)	0.5 to 2.5	Trial optimization
Impervious area (%)	5 to 30	Trial optimization
Time of concentration (hrs)	4 to 20	Equation developed by US Soil Conservation Service for time of concentration (Wanielista et al., 1997)
Storage time (hrs)	3 to 15	Equation developed by US Soil Conservation Service for time of concentration (Wanielista et al., 1997)
PX temperature (°C)	1.0 to 3.0	Trial optimization
Lapse rate (°C/100 m)	-0.65 to -0.45	By using observed temperature data (WAPDA)
Degree day factor (mm °C <sup>-1</sup> day <sup>-1</sup> )	4 to 5.7 for snow 5.7 to 7.4 for ice	Extract from previous studies conducted on Himalayan range (Immerzeel et al., 2010; Prasad and Roy, 2005).

The temperature index approach was selected in this study to incorporate the snowmelt contribution because of less data intensive. The temperature index method measures the melt rate based on past and current atmospheric conditions and incorporates cold content to account the ability of snow cover to freeze the rain water falling on it. In the temperature index method, the lapse rate and DDF are the most important parameters for the efficient estimation of snowmelt contribution. The lapse rates were calculated by using the measured temperature of four different installed gauges. The lapse rate, DDF and base flow were calculated from the observed hydro–meteorological data. While, initial loss, constant loss, time of concentration, percent of impervious area and storage coefficient were optimized by trial and error approach. Initial values selected for HEC–HMS calibration of different parameter are given in Table 3.6.

### 3.5.3.2 Application of SRM

For the application of SRM on Hunza River catchment the study area was divided into six (6) altitude zones (Figure 3.2), with difference of 1000 m elevation as suggested by Tahir et al. (2011b) and Azmat et al. (2016a) as described in Table 3.2 and shown in Figure 3.9.

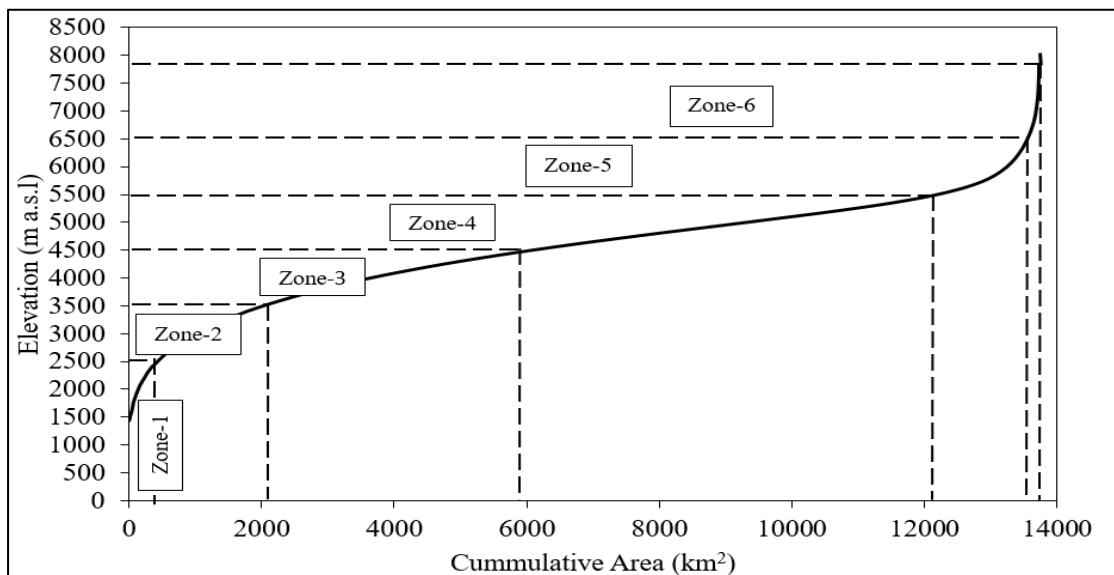


Figure 3.9: Hypsometric Curve of the Hunza River Catchment is Showing the Area Distribution in six Different Elevation Zones (Zones–1, Zone–2, Zones–3, Zone–4, Zone–5 and Zone–6)

The hypsometric analysis shows that the maximum catchment area is located in Zone–4 ranges from 4501–5500 m a.s.l. (44.7%). Since, the Zone–5 and Zone–6 have no meteorological station, therefore, precipitation of both zones was assessed by average

precipitation of Zone-3 and Zone-4. And mean temperature for Zone-5 and Zone-6 were assessed by the extrapolation of observed daily mean temperature using the lapse rate value of 0.7 °C/100 m. The zone-wise daily temperature, observed and estimated by using lapse rate method, distribution is shown in Figure 3.10a.

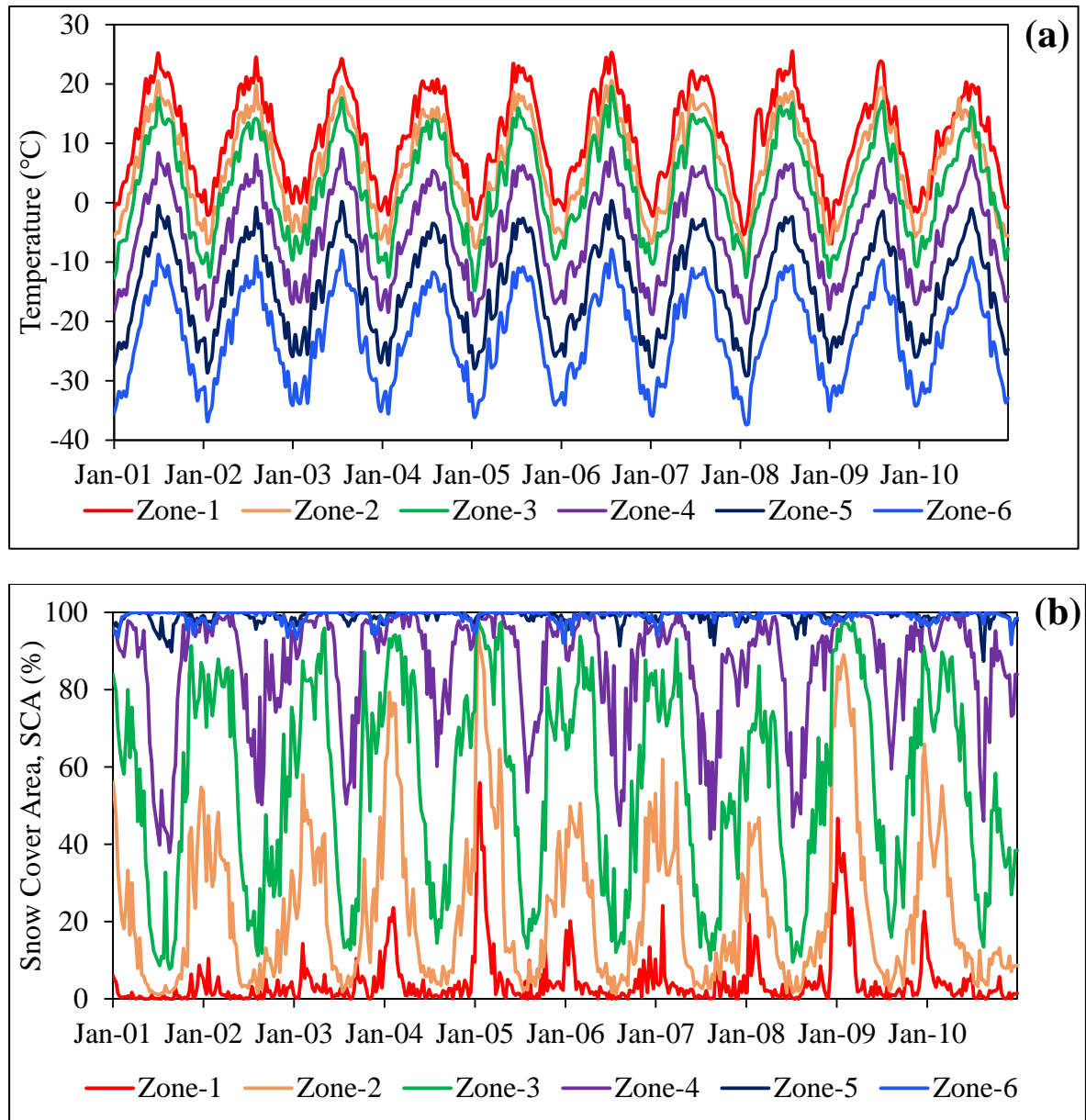


Figure 3.10: Zone Wise Distribution of (a) Temperature (°C), and (b) SCA (%), during 2001–2010, Hunza River Catchment

SRM is a snowmelt runoff model and simulation is mainly dependent on snow cover data. The daily SCA for each zone was produced by the linear interpolation of percent SCA extracted from cloud free composite MODIS images at 8-days interval (Figure 3.10b). The initial DDF value for snow, ice and glaciers were obtained from

the previous studies carried out in Himalayan and Karakorum region (Zhang et al., 2005 and Hock, 2003) and other initial parameters values are given in Table 3.7.

*Table 3.7: Range of Parameter Values for Application of SRM in Hunza River Catchment*

Parameters	Parameters Value Ranges for Hunza catchment
Temperature lapse rate, Lr ( $^{\circ}\text{C}/100\text{ m}$ )	0.75 to 0.4
Critical temperature, $T_{\text{crit}}$ ( $^{\circ}\text{C}$ )	0 to 1
Degree day factor, DDF ( $\text{mm } ^{\circ}\text{C}^{-1}\text{day}^{-1}$ )	4 to 7
Lag time, L (hrs)	4–20
Rainfall contributing area (RCA)	0– 1
Runoff coefficient for rainfall ( $C_r$ )	0 to 0.4
Runoff coefficient for snow ( $C_s$ )	0 to 0.5
Recession coefficient ( $X_c$ ), k	0.9–1.06
Recession coefficient ( $Y_c$ ), k	0.018–0.025

### 3.5.3.3 Comparison of HEC–HMS and SRM

The accuracy of both models during calibration and validation were assessed by using three well-known statistical descriptors i.e. Nash–Sutcliffe coefficient (NS), coefficient of determination ( $R^2$ ), and the percentage volume difference (Dv %), to study the relationship between simulated and observed daily streamflows at Dainyor Bridge. Further, the most efficient model was used for assessing the impact of climate change on streamflows of the Hunza River catchment.

### 3.5.4 Bias Correction of Climatic Dataset

IGB climate dataset, of eight GCMs models downscaled at  $5\text{km} \times 5\text{km}$  grid size for Upper Indus basin was selected for future climate impact study. Detail methodology of selection of eight GCMs is described by Arthur et al. (2016).

For the base period of 10–years (2001–2010), the IGB dataset (i.e. daily precipitation and mean air temperature was extracted for specific point at which climatic stations are actually located within the Hunza River catchment, then the baseline (observed) climatic dataset (climate station data) were compared with the IGB climatic dataset to observe uncertainties. Since, the large uncertainties were found in IGB climatic dataset in comparison with observed, therefore bias correction of IGB gridded climatic dataset

were done on daily basis using the delta technique to derive corrected baseline (GCMs) climatic dataset for future decadal (2030s, 2060s, 2090s) climate. This technique for the bias correction has been applied and discussed with detail by several researchers (Teutschbein and Seibert, 2012 and Burhan et al., 2015). Accuracy of corrected baseline (GCMs) climatic dataset was assessed and found no change between baseline (observed) and IGB corrected dataset as also confirmed by Teutschbein and Seibert (2012). The future decadal climatic dataset were corrected by using correction factor driven from baseline (observed) and baseline (GCMs) dataset during base period. Accuracy of bias corrected data was assessed by some proficiency parameters (MAE, RMSE and  $R^2$ ), described in next the chapter.

### **3.5.5 Climate Change Impact on Streamflows**

Recently, for climate change impact assessment studies, mostly researchers are using the coarse resolution general circulation models (GCMs) dataset of Coupled Model Inter-comparison Project (CMIP3 and CMIP5) developed on the basis of various scenarios like Special Report Emissions Scenarios (SRES) or Representative Concentration Pathways (RCPs), while some others are using the hypothetical based climate change scenarios. However, the downscaled climate variables at fine resolution ( $5 \times 5$  km) for IGB River basins is also available for eight GCMs based on RCP8.5 and RCP4.5 scenarios on HI-AWARE project (Lutz et al., 2016). Previously, Tahir et al. (2011b) has adopted hypothetical scenarios to investigate the impact of climate change on the streamflows of the Hunza River catchment, however, in current study the climate change impact assessment was carried out in two steps; first, the downscaled daily precipitation and temperature data of RCPs were adopted after careful bias corrections of the climate datasets by employing delta bias correction technique, to study the projected changes in hydrological regime of the study area. Second, the change in SCA was adopted with conjunction of RCPs dataset to analyze the impact of SCA change on streamflows. Additionally, the change in temperature and precipitation were also adopted to analyze the impact on streamflows. The observed hydro-climatic and IGB climatic dataset for period of 2001 to 2010 were used as reference hydro-climatic conditions hereafter referred as baseline (observed) and baseline (GCMs) for future decadal climate i.e. 2030s (2030–2039), 2060s (2060–2069) and 2090s (2090–2099).

### **3.5.5.1 Based on RCPs scenarios (RCPs+UCSCA)**

The projected changes in decadal (2030s, 2060s and 2090s) climate variables (temperature and precipitation) both for RCP8.5 and RCP4.5 were assessed in comparison with the baseline (observed) climatic dataset. Subsequently, the corrected decadal climatic dataset were utilized as an input in hydrological model to project the potential daily streamflows in Hunza River catchment, for RCP8.5 and RCP4.5 scenarios (bias corrected climatic RCPs dataset) by keeping SCA constant i.e. unchanged SCA (UCSCA). Further, the projected changes in streamflows of the Hunza River catchment were assessed in comparison with baseline (observed) streamflow, denoted by RCPs+UCSCA scenarios. The aforementioned potential changes in climate and streamflows were assessed by taking average of four GCMs belongs to each of RCP8.5 and RCP4.5.

### **3.5.5.2 Hypothetical scenarios (RCPs±%CSCA)**

Further, the investigations were also carried out to analyze the impact of change in SCA (CSCA) on streamflows under the hypothetical scenarios developed by the combination of percent change in SCA ( $\pm 5\%$ CSCA for 2030s,  $\pm 10\%$ CSCA for 2060s and  $\pm 15\%$ CSCA for 2090s) with the bias corrected RCPs climate dataset denoted as (RCPs±%CSCA). The hypothetical changes in SCA (CSCA) were adopted due to unavailability of change in SCA under future scenarios. Since, the Hunza River catchment is dominantly covered with snow particularly during winter season; therefore, it is essential to investigate the sensitivity of CSCA on streamflows of Hunza River.

### **3.5.5.3 Hypothetical scenarios (BL+T<sub>x</sub>P<sub>x</sub>)**

The investigation of projected streamflows were also carried out by hypothetical change in Temperature and Precipitation (T<sub>x</sub>P<sub>x</sub>). The changes in observed climate data (temperature and precipitation) were considered within the range of IPCC (2014), to estimate streamflows for future decades (2030s, 2060s and 2090s). Therefore total four scenarios were assumed that are described below:

- (i) T<sub>1</sub>P<sub>5</sub> → 1 °C increase in temperature and 5 % increase in precipitation by 2030s.
- (ii) T<sub>2</sub>P<sub>10</sub> → 2 °C increase in temperature and 10 % increase in precipitation by 2060s.

- (iii) T<sub>3</sub>P<sub>15</sub> → A 3 °C increase in temperature and 15 % increase in precipitation by 2090s.
- (iv) T<sub>4</sub>P<sub>20</sub> → A 4 °C increase in temperature and 20 % increase in precipitation by 2090s.

#### **3.5.5.4 Comparison of RCPs and hypothetical scenarios**

Projected streamflows under RCPs and hypothetical scenarios (BL+T<sub>x</sub>P<sub>x</sub>) were also compared to analyze the sensitivity of climate variable (temperature, precipitation and SCA) in Hunza River catchment.

## RESULTS AND DISCUSSIONS

### 4.1 LAND COVER CHANGE IN HUNZA RIVER CATCHMENT

Land cover classification was performed for Hunza catchment for the identification of changes occurred from 1994 to 2014 for 21 years period using landsat-5 and landsat-8 imagery in the month of August. The details land cover is shown in Figure 4.1 and Figure 4.2, for 1994 and 2014, respectively. The land cover type is described in Table 4.1.

#### 4.1.1 Land Cover Change from 1994–2014 in Hunza Catchment

Hunza River catchment was classified into six number of classes as, Bare Land, Exposed Rocks, Forest, Snow & Glaciers, Vegetation and Water Bodies. The land cover maps of Hunza River catchment for 1994 and for 2014 (August) are shown in Figure 4.1 and Figure 4.2 and described in Table 4.1, respectively.

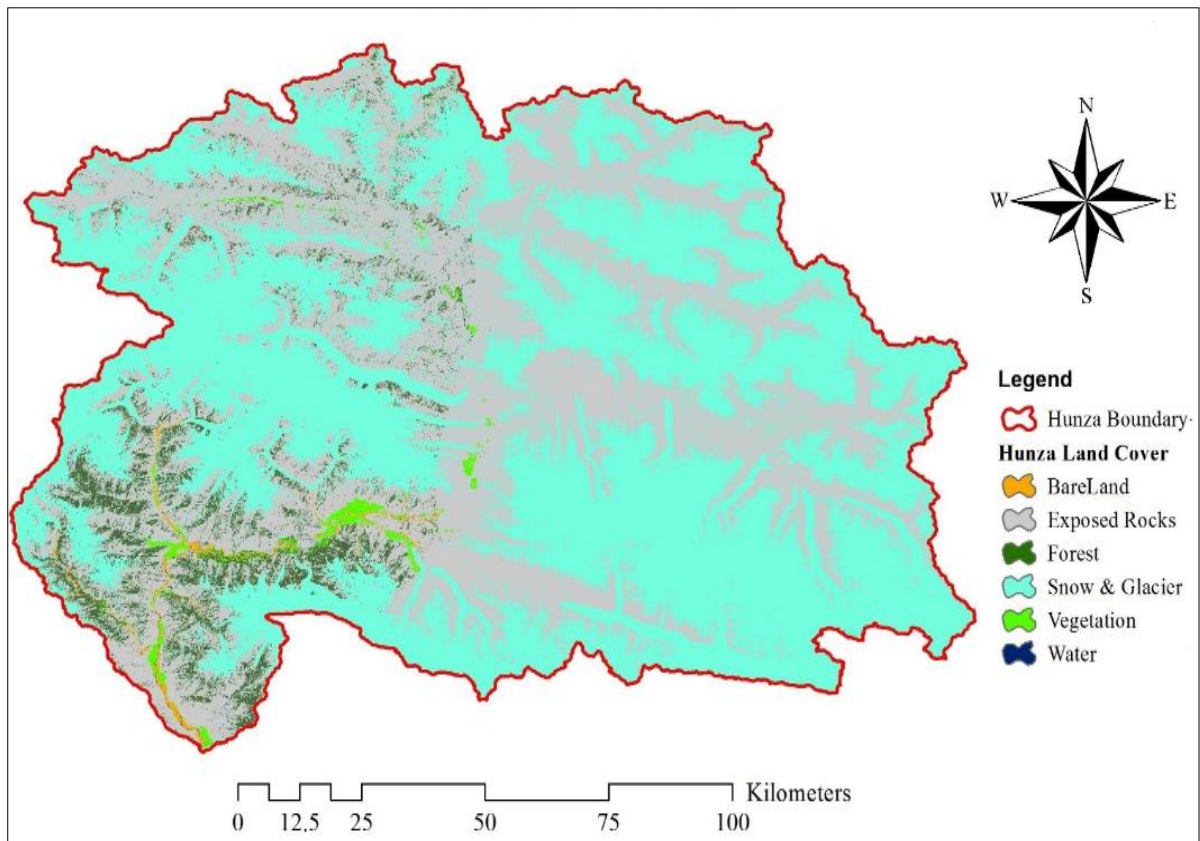
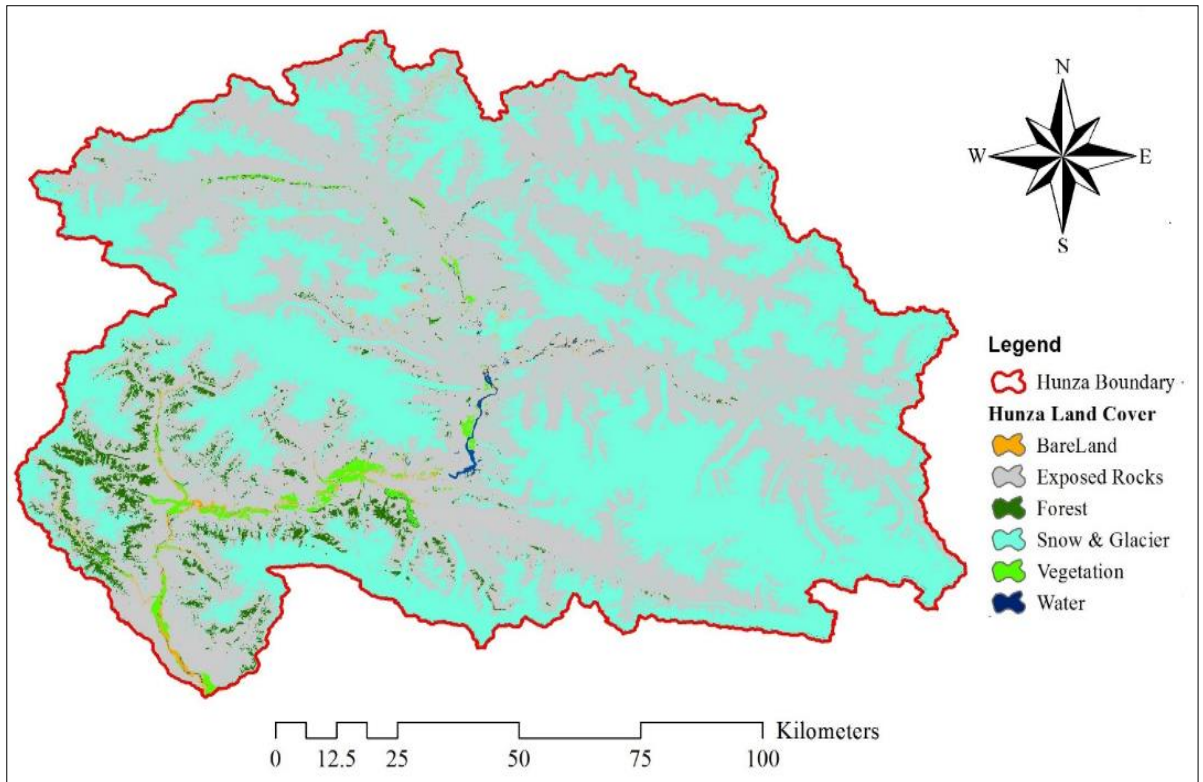


Figure 4.1: Land Cover Map of Hunza River Catchment in August, 1994.



*Figure 4.2: Land Cover Map of Hunza River Catchment in August, 2014.*

According to 1994 Hunza land cover map, maximum of 54.35% (7456.4 km<sup>2</sup>) exposed rocks and minimum of 0.04% (5.6 km<sup>2</sup>) water bodies were present. But in 2014, maximum land cover 48.84% (6700 km<sup>2</sup>) as exposed rocks and minimum of 0.09% (12.4 km<sup>2</sup>) water bodies were present. A lot of change in exposed rocks and snow & glacier cover area from 1994 to 2014 is due to the temperature dependent snow & glaciers cover area. As the temperature increases the snow & glaciers area decreases which result in increase in exposed rocks area. Which means both are anti-proportional to each other. To understand this relationship, we take the sum of both land cover area (exposed rocks and snow & glaciers) for both duration (1994 and 2014) given below,

In 2014;        Exposed Rocks + Snow & Glaciers = 48.84 % + 47.62% = 96.46 %

In 1994;        Exposed Rocks + Snow & Glaciers = 54.35 % + 41.61 % = 95.96 %

A total 0.5 % increase in both land cover area was found from above relationship from 1994 to 2014, which is difficult to describe that which land cover is increased and which is decreased. Forest land cover decreased by 0.52 % (71.5 km<sup>2</sup>) which is a lot of change that happened from 1994 to 2014. This change is clarified by Ali et al. (2012) stated that total population of Hunza valley is dependent on the forest wood to cook their food and warm their living places from wood burning. It is also noted that 0.05 % (6.8 km<sup>2</sup>)

change in water bodies was happened from 1994 to 2014. Which is also described by Ali et al. (2012) that massive land sliding occur in 2010 which result in formation of Atta-bad Lake that causes submergence of several villages and crop area shown in Figure 4.3

*Table 4.1: Percentage Change in Land Cover Area from 1994 to 2014 for Hunza Catchment*

Land Cover	2014		1994		Change (2014–1994)	
	% age	Km <sup>2</sup>	% age	Km <sup>2</sup>	%age	Km <sup>2</sup>
<b>Forest</b>	2.6	351.2	3.08	422.7	-0.52	-71.5
<b>Water Bodies</b>	0.09	12.4	0.04	5.6	0.05	6.8
<b>Snow &amp; Glaciers</b>	47.62	6532.4	41.61	5708.1	6.01	824.4
<b>Exposed Rocks</b>	48.84	6700	54.35	7456.4	-5.51	-756.6
<b>Vegetation</b>	0.62	85.5	0.59	81.4	0.03	4.2
<b>Barren Land</b>	0.26	36.2	0.32	43.9	-0.06	-7.7

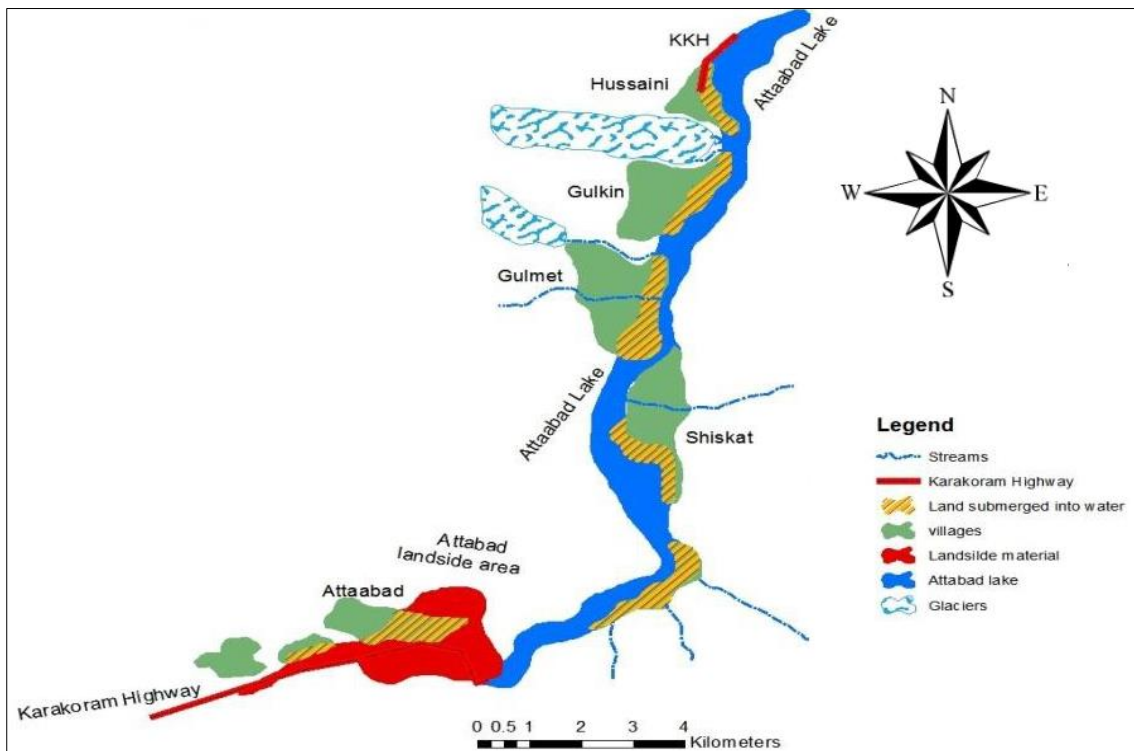


*Figure 4.3: Attabad Lake in Hunza River Catchment (Ali et al., 2015)*

## 4.2 SNOW COVER IN HUNZA RIVER CATCHMENT

Snow cover was extracted for 10–years (2001–2010) for Hunza River catchment is shown in Figure 4.4. Maximum 10–year mean daily average SCA of 85 % and minimum of 38 % was found in the Hunza River catchment.

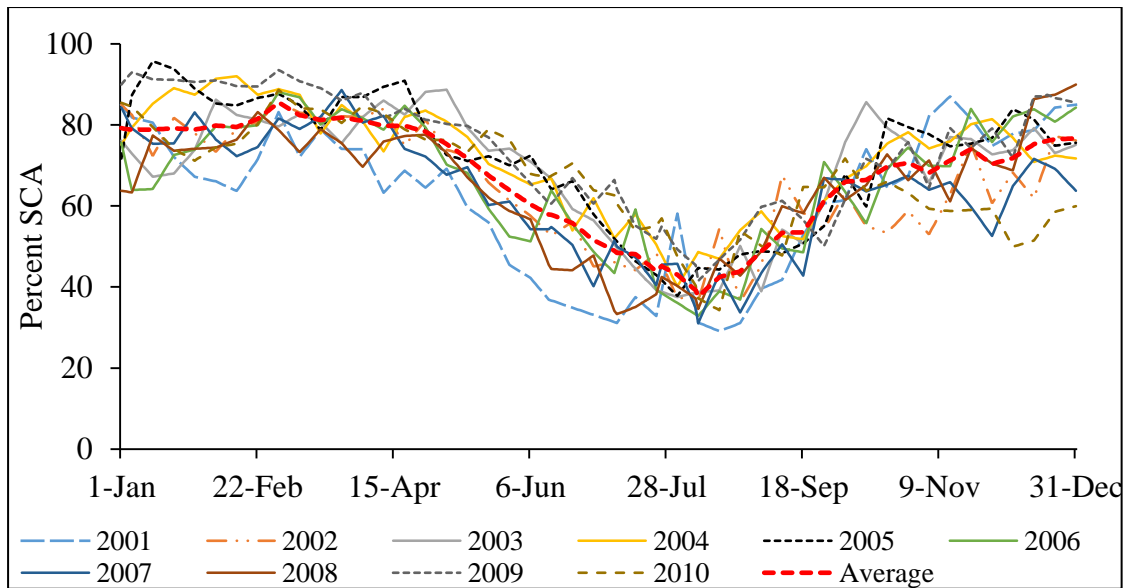


Figure 4.4: Percentage SCA form 2001–2010 in Hunza River Catchment.

Mean annual SCA was also plotted to see the annual variability in snow cover (Figure 4.5). SCA is showing the increasing trend which is also clarified from the time series analysis of precipitation described in the previous chapter that three of the four gauges showing the increasing trend of precipitation from 2001–2010.

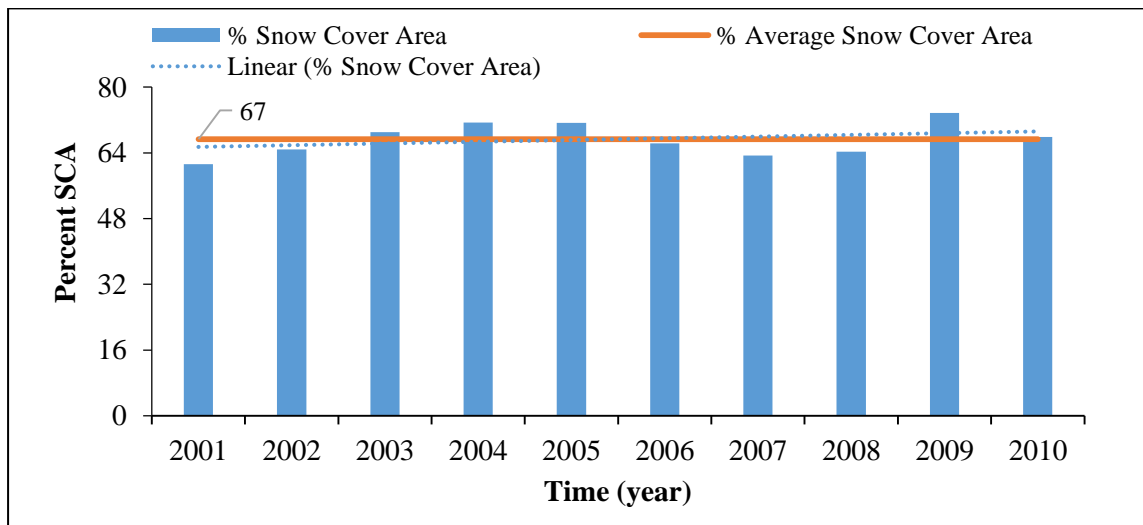


Figure 4.5: Inter Annual Variability in SCA in Hunza River Catchment from 2001–2010.

Elevation zone wise SCA was also extracted to see the behavior of snow cover against the elevation in Hunza River catchment (Figure 3.10b), is showing the SCA for six elevation zones. It is observed that maximum SCA is present in highest elevation zones (Zone–5 and Zone–6) and minimum SCA in the lowest elevation Zone–1. Both zones (Zone–5 and Zone–6) most of the time always remain 100% covered with the snow and

glaciers cover. The reason is also conform from the previous chapter in time series analysis of temperature data that the temperature of highest elevation zones remain less than 0 °C. Which means that very less or zero % of melting of snow and glaciers in that zones. It's also means that precipitation occur in that area is accumulated in form of snow and glaciers.

### **4.3 COMPARISON OF HYDROLOGICAL MODELS**

The accuracy of both models during calibration and validation were assessed by using three well-known statistical descriptors i.e. Nash–Sutcliffe coefficient (NS), coefficient of determination ( $R^2$ ), and the percentage volume difference (Dv %), to study the relationship between simulated and observed daily streamflows at Dainyor Bridge. Further, the most efficient model was used for assessing the impact of climate change on streamflows of the Hunza River catchment.

#### **4.3.1 Calibration and Validation**

The optimized parametric values for the SRM and HEC–HMS during calibration and validation are described in Table 4.2 and Table 4.3, respectively. In case of SRM, parametric values were calibrated and validated, spatially (zone-wise) and temporally (season wise) as given in Table 4.2, however, in HEC–HMS the parametric values can only be calibrated for subbasins (spatial calibrated) direction. In SRM, the parametric values of  $C_S$  and  $C_R$  were found between 0.25–0.5 and 0–0.4, respectively. Similarly, the DDF, lapse rate and lag time were found between 0.4–0.6 cm/°C–day, 0.45–0.7 °C/100 m and 6–18 hrs, respectively. However, the values of parameters used to incorporate rainfall contribution in runoff, for HEC–HMS such as initial loss (mm), constant loss (mm/hr) and impervious area (%) varies between 4–5, 1.0–1.5 and 15–23, respectively (Table 4.3). While, for the snowmelt process, the values for the parameters such as lapse rate (°C/100 m), DDF (cm/°C–day), ATI–meltrate, ATI–coldrate, water capacity (%) and  $P_x$  temperature (°C) varies between 0.45–0.65, 0.5, 0.98, 0.84, 5 and 0–1, respectively. It was observed that the value of the parameters used for rainfall–runoff simulation in HEC–HMS varies very slightly, which may be due to the less rainfall depth occurrence in Hunza River catchment. Moreover, the difference in SRM and HEC–HMS parametric values (DDF and lapse rate) is due to the different computation approach in both hydrological models.

Table 4.2: Calibrated Zone Wise Parametric Values for SRM Model, Hunza River Catchment

Parameters	Zone Wise Parametric Values					
	Zone-1	Zone-2	Zone-3	Zone-4	Zone-5	Zone-6
Lapse Rate (°C/100 m)	0.45	0.5	0.55	0.6	0.7	0.7
Tcrit (°C)	1	1	1	1	1	1
DDF(cm/°C-day)	0.4	0.45	0.5	0.55	0.55	0.6
Lag Time (hrs)	6	6	12	12	18	18
C <sub>s</sub>	0.3	Jun-Aug=0.35 Sep-May=0.3	Jun-Aug=0.35 Sep-May=0.3	Jun-Aug=0.4 Sep-May=0.3	Jun-Aug=0.5 Sep-May=0.3	Jun-Aug=0.4 Sep-May=0.25
C <sub>R</sub>	Jun-Aug=0.4 Sep-May=0.25	Jun-Aug=0.35 Sep-May=0.3	Jun-Aug=0.3 Sep-May=0.25	Jun-Aug=0.25 Sep-May=0.2	Jun-Aug=0 Sep-May=0.15	0
RCA	1	1	1	Jun-Aug=1 Sep-May=0	Jun-Aug=1 Sep-May=0	0
Xc	1.08	1.08	1.08	1.08	1.08	1.08
Yc	0.022	0.022	0.022	0.022	0.022	0.022

Table 4.3: Calibrated Subbasin Wise Parametric Values for HEC-HMS Model, Hunza River Catchment

Sub-basins	Initial loss (mm)	Constant loss (mm/hr)	Impervious Area (%)	Time of Concentration (hrs)	Storage coefficient (hrs)	Lapse Rate (°C/100m)	DDF (cm/°C-day)
1	5	1	18	8	3	0.45	0.5
2	5	1.5	21	6	2	0.5	0.5
3	4	1.5	20	14	2	0.65	0.5
4	4	1	23	10	3	0.6	0.5
5	4	1	15	18	4	0.65	0.5

As SRM is based on single relationship to incorporate both snowmelt-runoff and rainfall-runoff contribution, however, HEC-HMS incorporate rainfall and snowmelt-runoff separately.

### 4.3.2 Comparison of HEC-HMS and SRM

The results for the calibration (2001-2006) and validation (2008-2010) of SRM and HEC-HMS for simulation of daily streamflows of Hunza River are given in Table 4.4 and Figure 4.6. On annual basis, the R<sup>2</sup> and NS coefficient values during calibration period were 0.95 and 0.92 (for SRM); 0.63 and 0.57 (for HEC-HMS), respectively. While, during validation period the R<sup>2</sup> and NS coefficient values for SRM were found

0.97 and 0.89, and for HEC–HMS were 0.61 and 0.54, respectively (Table 4.4). However on seasonal basis, it observed that SRM model performed significantly efficient during winter and monsoon seasons as compare to HEC–HMS descriptors. During winter season, the  $R^2$  and NS coefficient over the calibration and validation period ranges from 0.93 to 0.97 and 0.89 to 0.93, respectively, for SRM and 0.47 to 0.56 and 0.38 to 0.46, respectively, for HEC–HMS. Similarly, during monsoon season, the  $R^2$  and NS coefficient varies between 0.73 to 0.75 and 0.69 to 0.71, respectively, for SRM and 0.50 to 0.52 and 0.26 to 0.29, respectively, for HEC–HMS. On the other hand, both models performed efficiently during pre–monsoon season with least  $R^2$  and NS coefficient values of 0.81 and 0.79 (for SRM) and 0.71 and 0.68 (for HEC–HMS), respectively. Overall results showed that the efficiency of SRM is fairly better than that of HEC–HMS in high–altitude snow and glaciers–fed Hunza River catchment, for the daily streamflows simulation.

*Table 4.4: Statistical Performance of SRM and HEC–HMS Models during Calibration (2001–2006) and Validation (2008–2010) Periods, Hunza River Catchment*

Annual (Jan–Dec)	Calibration (2001–2006)		Validation (2008–2010)	
	SRM	HEC–HMS	SRM	HEC–HMS
$R^2$	0.95	0.63	0.97	0.61
NS Coefficient	0.92	0.57	0.89	0.54
Dv%	2.09	–2.11	1.91	19.42
<b>Winter or Snow Accumulation Season (Oct–March)</b>				
$R^2$	0.97	0.56	0.93	0.47
NS Coefficient	0.93	0.46	0.89	0.38
Dv%	1.41	–0.57	1.31	5.26
<b>Pre–monsoon or Snowmelt Season (April–June)</b>				
$R^2$	0.85	0.71	0.81	0.72
NS Coefficient	0.82	0.69	0.79	0.68
Dv%	–2.08	1.7	–3.79	–16.65
<b>Monsoon or Extreme Rainfall Season (July–Sep)</b>				
$R^2$	0.75	0.50	0.73	0.52
NS Coefficient	0.71	0.29	0.69	0.26
Dv%	3.31	–3.25	3.21	30.63

The comparative analysis of simulated streamflows with observed showed that the HEC–HMS is poor in capturing streamflow peaks (underestimations) during monsoon season in contrast to SRM which is fairly efficient to pick up such peaks (Figure 4.6). On the other hand, even the streamflows during winter season were not substantial, nevertheless, the HEC–HMS producing unnecessarily peaks during January to March (Figure 4.6). While, it is noticed that the SRM reproduce streamflow very efficiently in

during winter, pre-monsoon and monsoon season. In addition, it is observed that the both models performed well during pre-monsoon season which may be associated with the fact that during pre-monsoon season precipitation contribution into streamflows of Hunza River is slightly low as compare to snow- and glacier-melt.

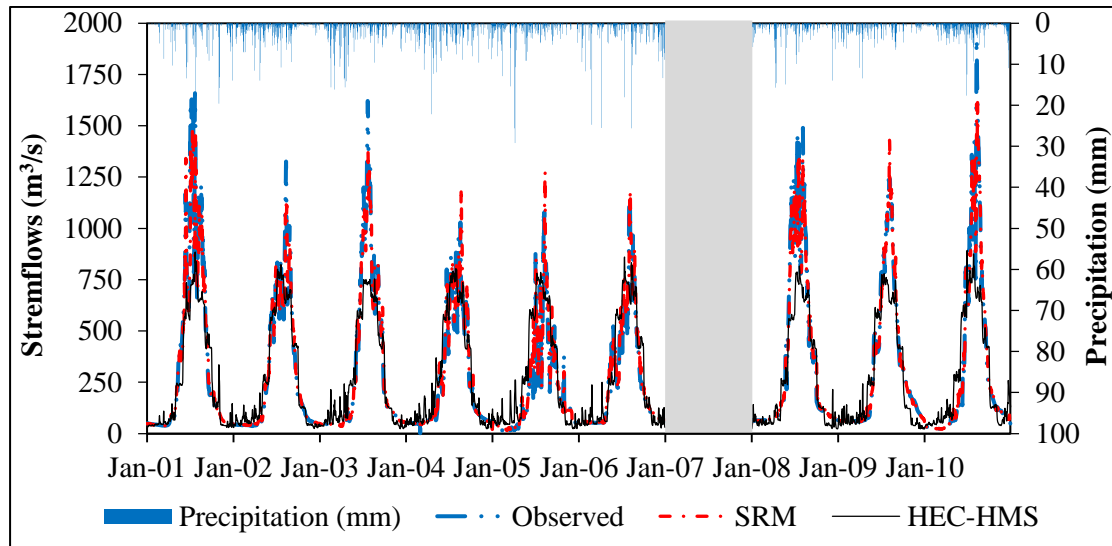


*Figure 4.6: Simulations of Daily Streamflows ( $m^3/s$ ) during Calibration (2001–2006) and Validation (2008–2010) Periods using SRM and HEC-HMS Models, Hunza River Catchment*

Seasonal performance of SRM and HEC-HMS models during 9-year simulation period (calibration 2001–2006 and validation 2008–2010) for Hunza River catchment is shown in Figure 4.7. Over 9-year's simulation, the  $R^2$  (NS) coefficient values was 0.96 (0.91) for SRM and 0.62 (0.56) for HEC-HMS. Overall the simulation performance of SRM is much better than HEC-HMS.

A slight discrepancy between results obtained by several studies were found which may be due to the difference in hypothesis, methods and most important study area characteristics. For example, Azmat et al. (2015 and 2016a) applied both models in Jhelum River catchment and stated that the HEC-HMS is slightly better than that of SRM. This discrepancy is may be due to the difference in snow and glacier extent and precipitation pattern in both catchments i.e. Jhelum River basin is influenced by monsoon during summer and Hunza River catchment with westerlies circulation during winter season.

In addition, the change in altitude could largely affects the climate variables (precipitation and temperature) which are the key inputs for both models and each model is based on its specialized algorithm to entertain rainfall and cryosphere (snow

and ice). While, the results produced by SRM are in line with the results generated by Tahir et al. (2011b) in Hunza River catchment. By considering the better efficiency, the SRM is being utilized for further assessing the climate change impacts on streamflows in Hunza River catchment.

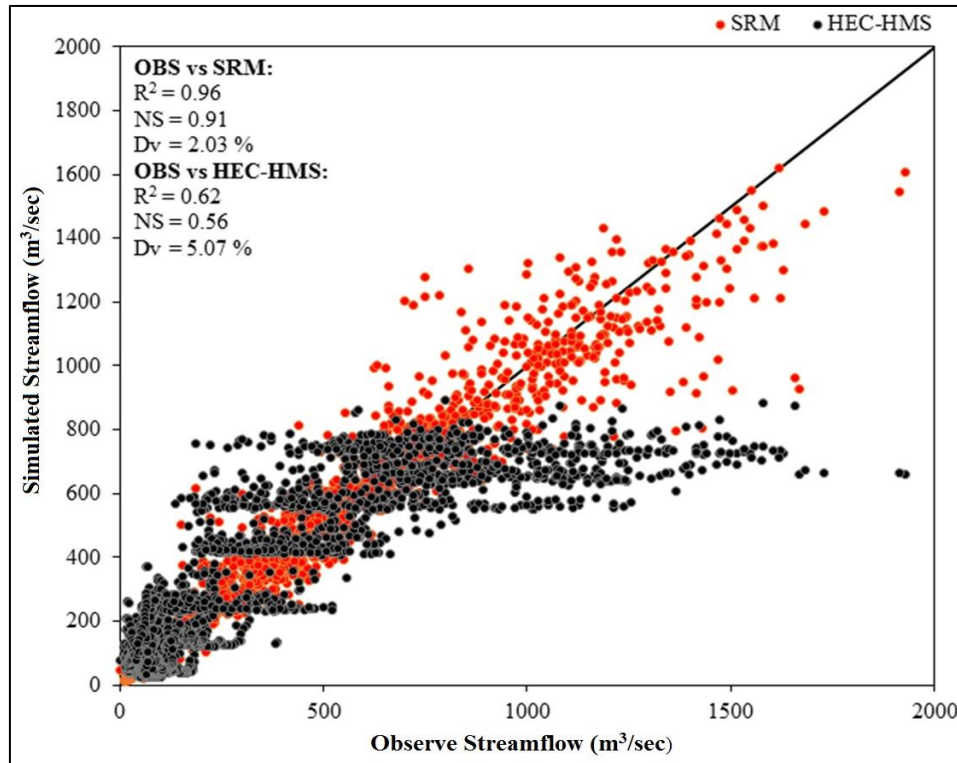


Figure 4.7: Scattered plot Showing the Performance of SRM and HEC–HMS Models during 9–year simulation Period (Calibration 2001–2006 and Validation 2008–2010), of Hunza River Catchment.

#### 4.4 CLIMATE CHANGE IMPACT ASSESSMENT

Future climate dataset was acquire by two different ways. One is to use Hi–AWARE dataset and other is to develop hypothetical climate change scenarios.

##### 4.4.1 Climate Dataset

The projection of climatic dataset (i.e. temperature and precipitation) for 2030s, 2060s and 2090s showed an increasing tendency in both climate variables (precipitation and temperature) on annual and seasonal basis at all the four stations (Hunza, Naltar, Ziarat and Khunjrab) within the Hunza River catchment for both RCP8.5 and RCP4.5 scenarios as shown in Table 4.6.

##### 4.4.1.1 Monthly dataset

IGB climatic dataset i.e. temperature and precipitation before and after bias correction for 2030s, 2060s and 2090s were plotted on monthly basis for eight (8) climate models

(RCP4.5 and RCP8.5) for four climate stations (Hunza, Naltar, Ziarat and Khunjrab) within the Hunza River catchment shown in Figure 4.8 to Figure 4.15. Lot of uncertainties were found in IGB climatic dataset in comparison with observed climate data (2001–2010), therefore bias correction of IGB gridded climatic dataset were done on daily basis to derive corrected climatic dataset for future decadal (2030s, 2060s, 2090s) climate.

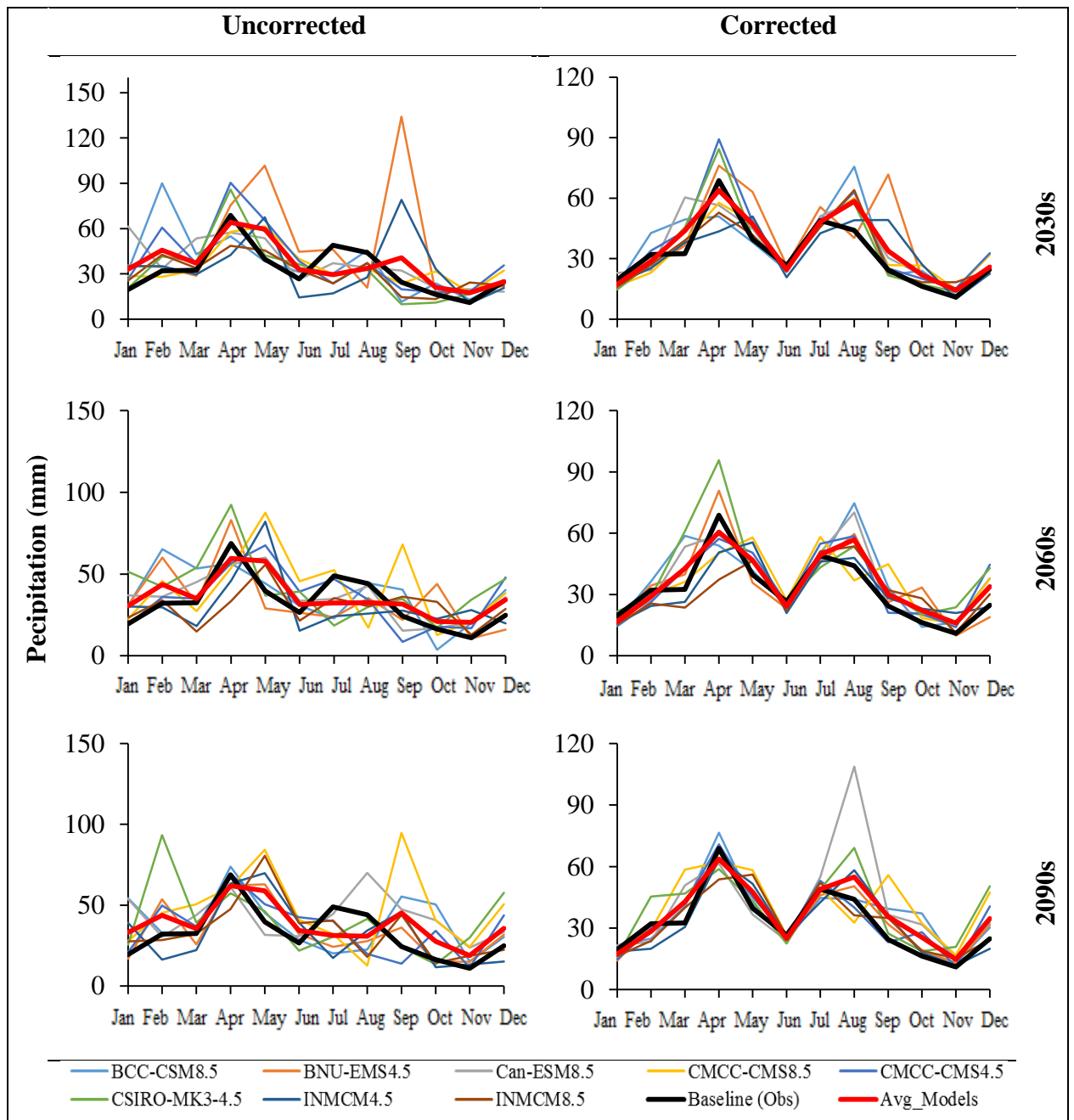


Figure 4.8: IGB Precipitation Data before and after Bias Correction for Hunza Climate Station

At Hunza climate station slightly uncertainties were found in uncorrected projected precipitation data (see Figure 4.8). After bias correction the efficiency parameter value of MAE and RMSE (see Table 4.5) for Hunza climate station for RCP4.5 (RCP8.5) ranges from 6.3–7.8 (7.0–9.5) and 8.1–11.2 (9.7–13.4), respectively for bias corrected projected precipitation.

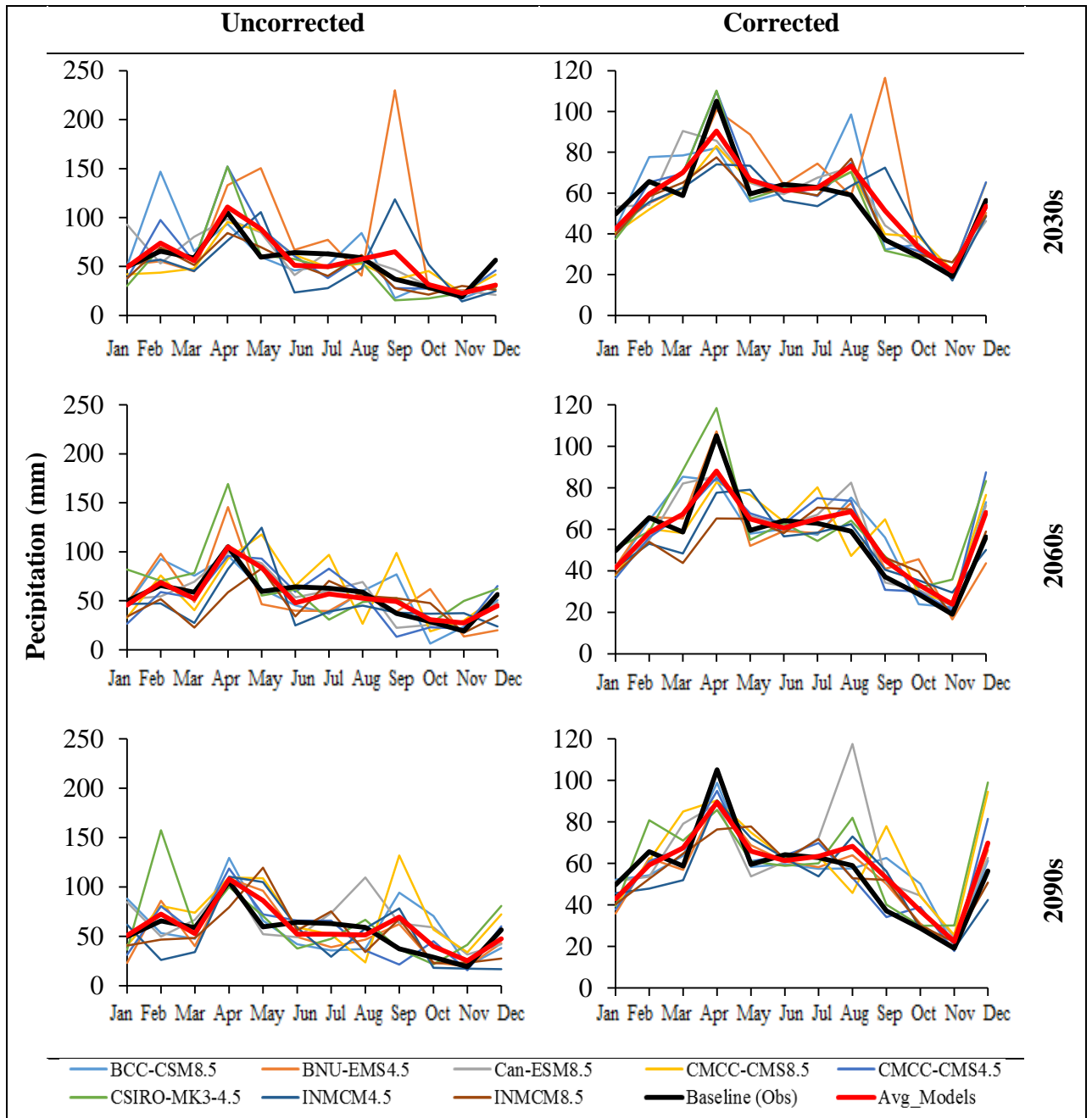


Figure 4.9: IGB Precipitation Data before and after Bias Correction for Naltar Climate Station

At Naltar climate station similar trend was observed as at Hunza climate station (see Figure 4.9), little uncertainties were found in uncorrected projected precipitation data.

After applying bias correction the efficiency parameter value of MAE and RMSE (see Table 4.5) for Naltar climate station for RCP4.5 (RCP8.5) ranges from 9.0–9.6 (8.9–11.7) and 11.6–13.7 (12.1–15.8), respectively for bias corrected projected precipitation.

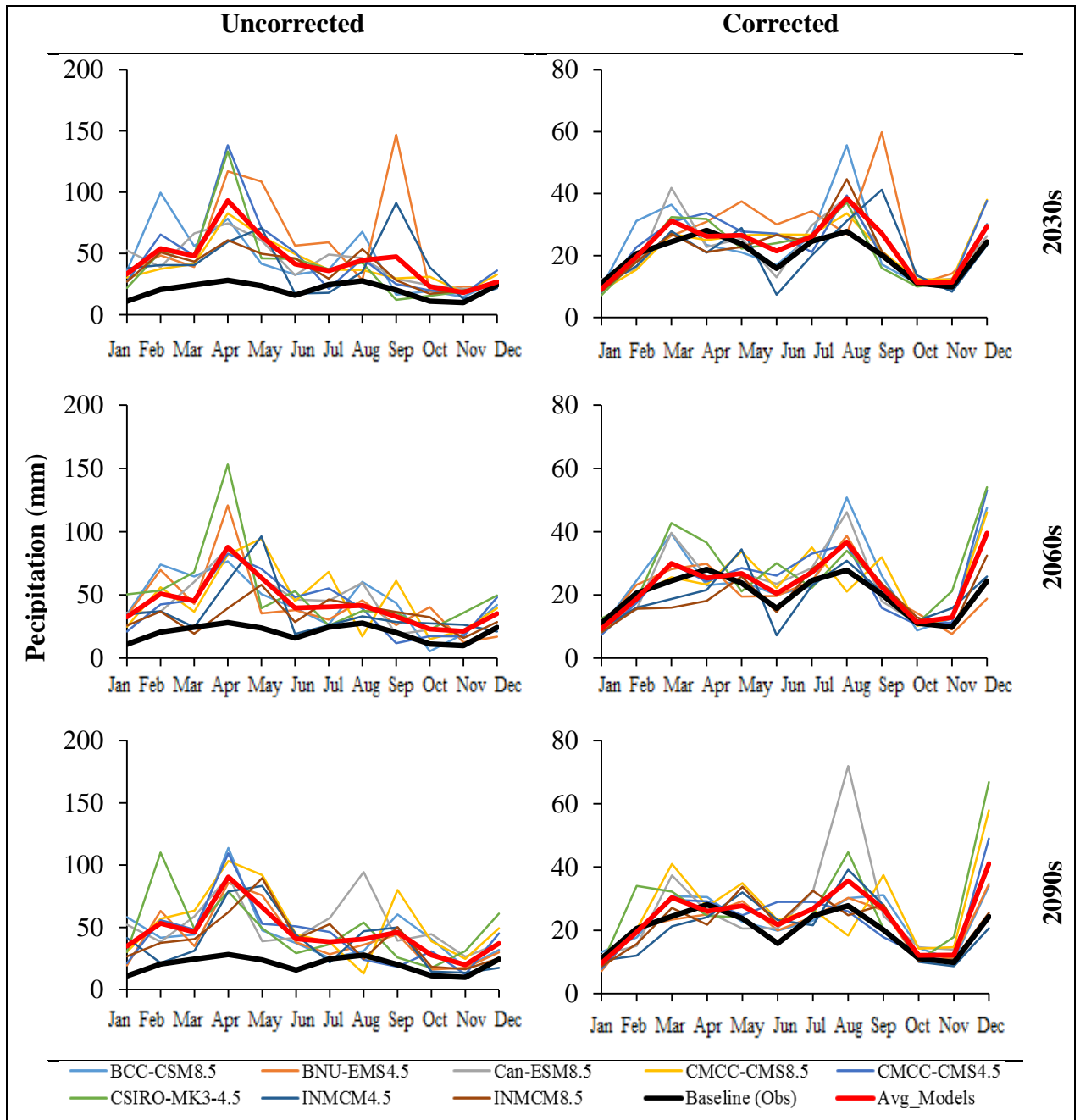


Figure 4.10: IGB Precipitation Data before and after Bias Correction for Ziarat Climate Station

At Ziarat climate station similar trend was observed as in Hunza climate station (see Figure 4.10), lot of uncertainties were found in uncorrected projected precipitation data as compare with Hunza and Naltar climate stations that might be due to its slightly high elevation (3669 m a.s.l) range. After applying bias correction the efficiency parameter

value of MAE and RMSE (see Table 4.5) for Ziarat climate station for RCP4.5 (RCP8.5) ranges from 5.3–5.7 (4.8–6.6) and 7.8–8.3 (7.1–9.5), respectively for bias corrected projected precipitation.

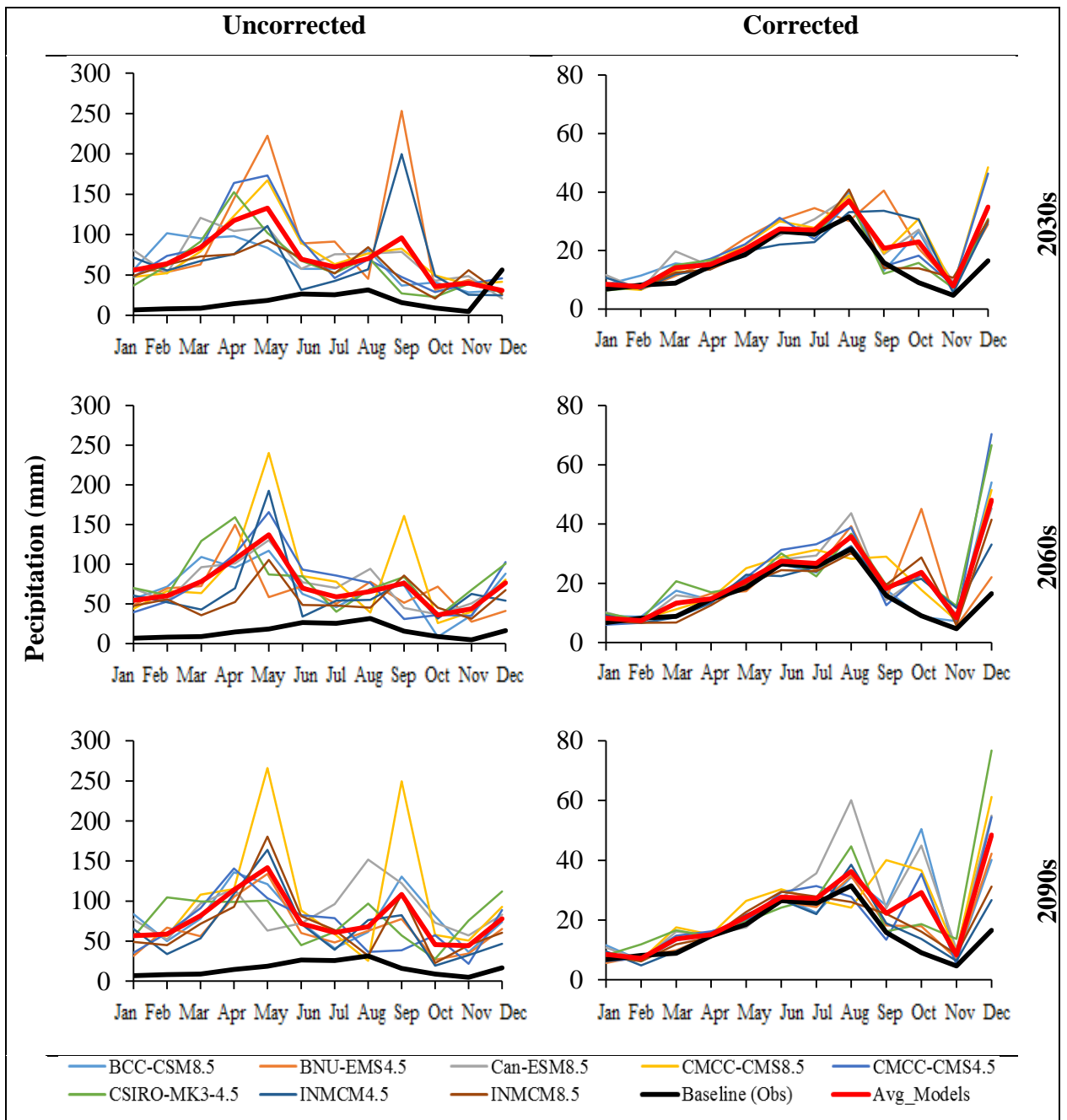


Figure 4.11: IGB Precipitation Data before and after Bias Correction for Khunjrab Climate Station

At Khunjrab similar trend was found as observed at Ziarat climate station more uncertainties were found in uncorrected projected precipitation data (see Figure 4.11) as compare with other climate station that might be due to its higher elevation (4730 m a.s.l) range. The efficiency parameter value of MAE and RMSE (see Table 4.5) for

Khunjrab climate station for RCP4.5 (RCP8.5) ranges from 5.5–6.7 (5.4–8.9) and 8.4–12.4 (8.3–13.8), respectively for bias corrected projected precipitation

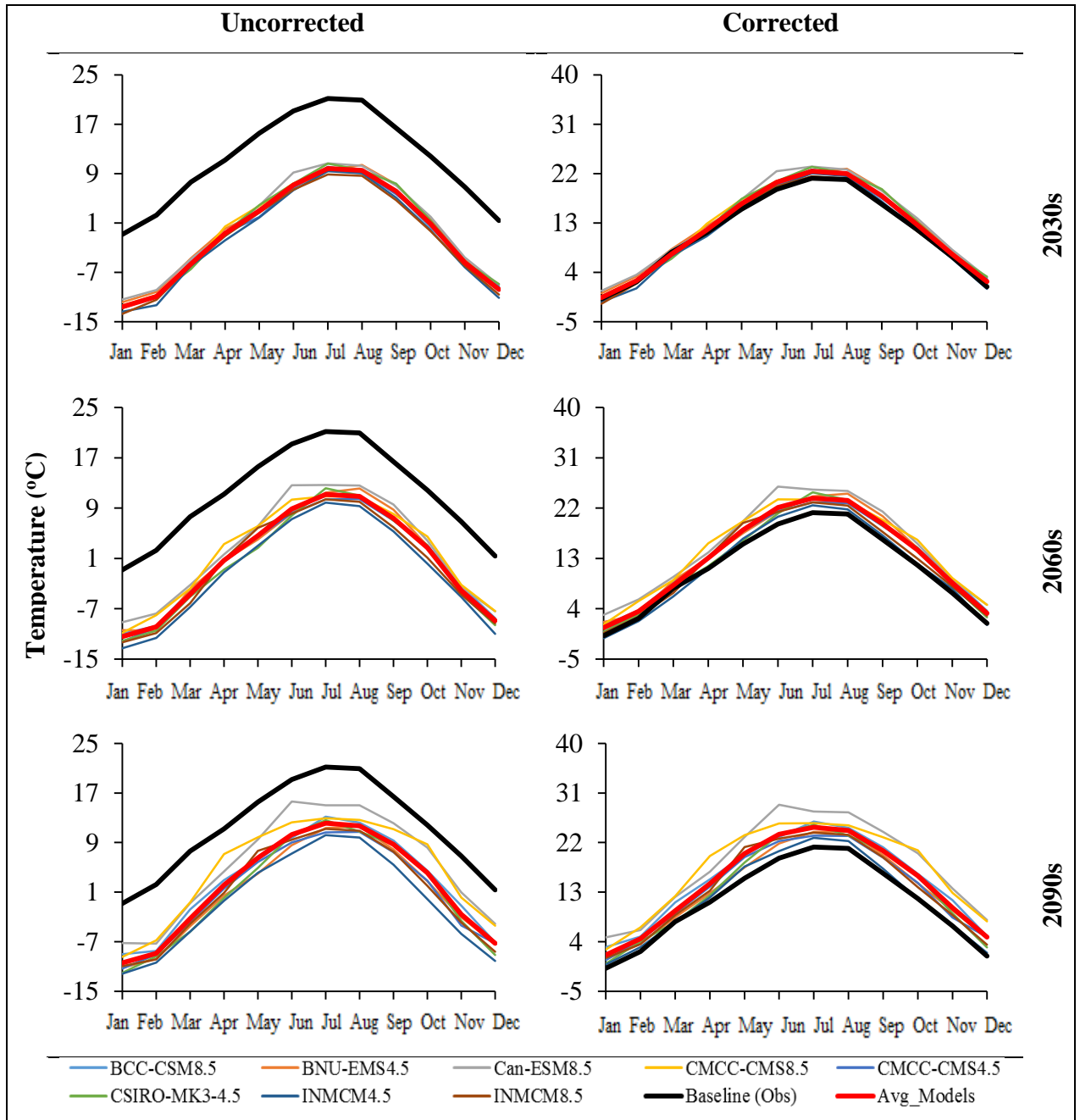


Figure 4.12: IGB Temperature Data before and after Bias Correction for Hunza Climate Station

At Hunza climate station a lot of uncertainties were found in uncorrected projected temperature data (see Figure 4.12) as compare with observed dataset that is may be due to the difference in grid mean elevation and climate station elevation because of temperature sensitivity with elevation lapse rate with the elevation as discussed with Lutz et al. (2016). Around 10–11 °C difference is noticed in uncorrected and observed

temperature data. After applying bias correction the efficiency parameter value of MAE and RMSE (see Table 4.5) for Hunza climate station for RCP4.5 (RCP8.5) ranges from 0.9–2.0 (0.9–4.8) and 1.1–2.2 (1.1–4.9), respectively for bias corrected temperature dataset.

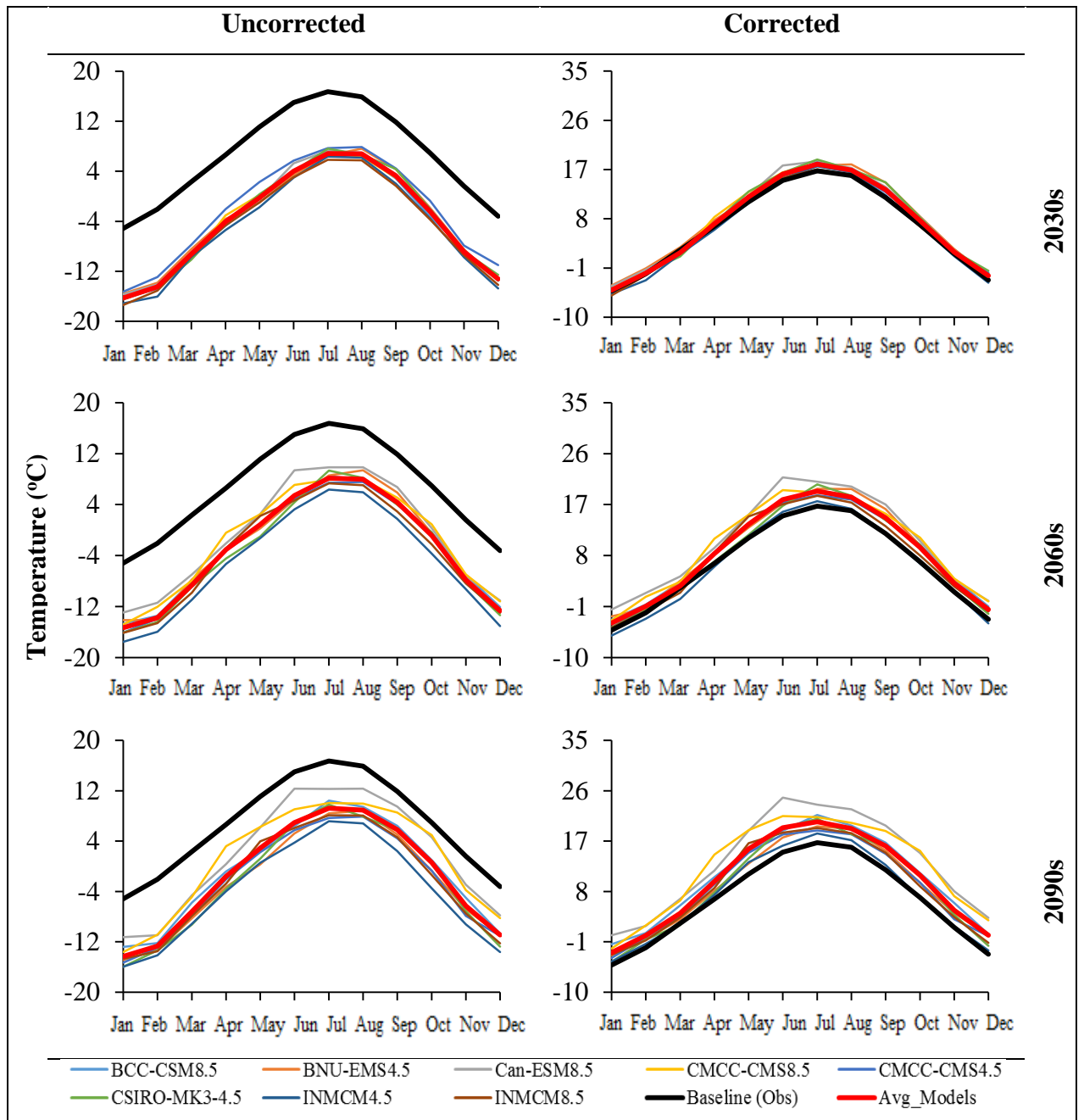


Figure 4.13: IGB Temperature Data before and after Bias Correction for Naltar Climate Station

Similar trend was found at Naltar climate station as at Hunza climate station a lot of uncertainties were found in uncorrected projected temperature data (see Figure 4.13) that is also may be due to the difference in grid mean elevation and climate station

elevation because of temperature sensitivity with elevation (Lutz et al., 2016). Around 9–10 °C difference was noticed in uncorrected and observed temperature data. After applying bias correction the efficiency parameter value of MAE and RMSE (see Table 4.5) for Naltar climate station for RCP4.5 (RCP8.5) ranges from 0.9–2.0 (0.8–4.7) and 1.1–2.2 (0.9–4.9), respectively for bias corrected temperature dataset.

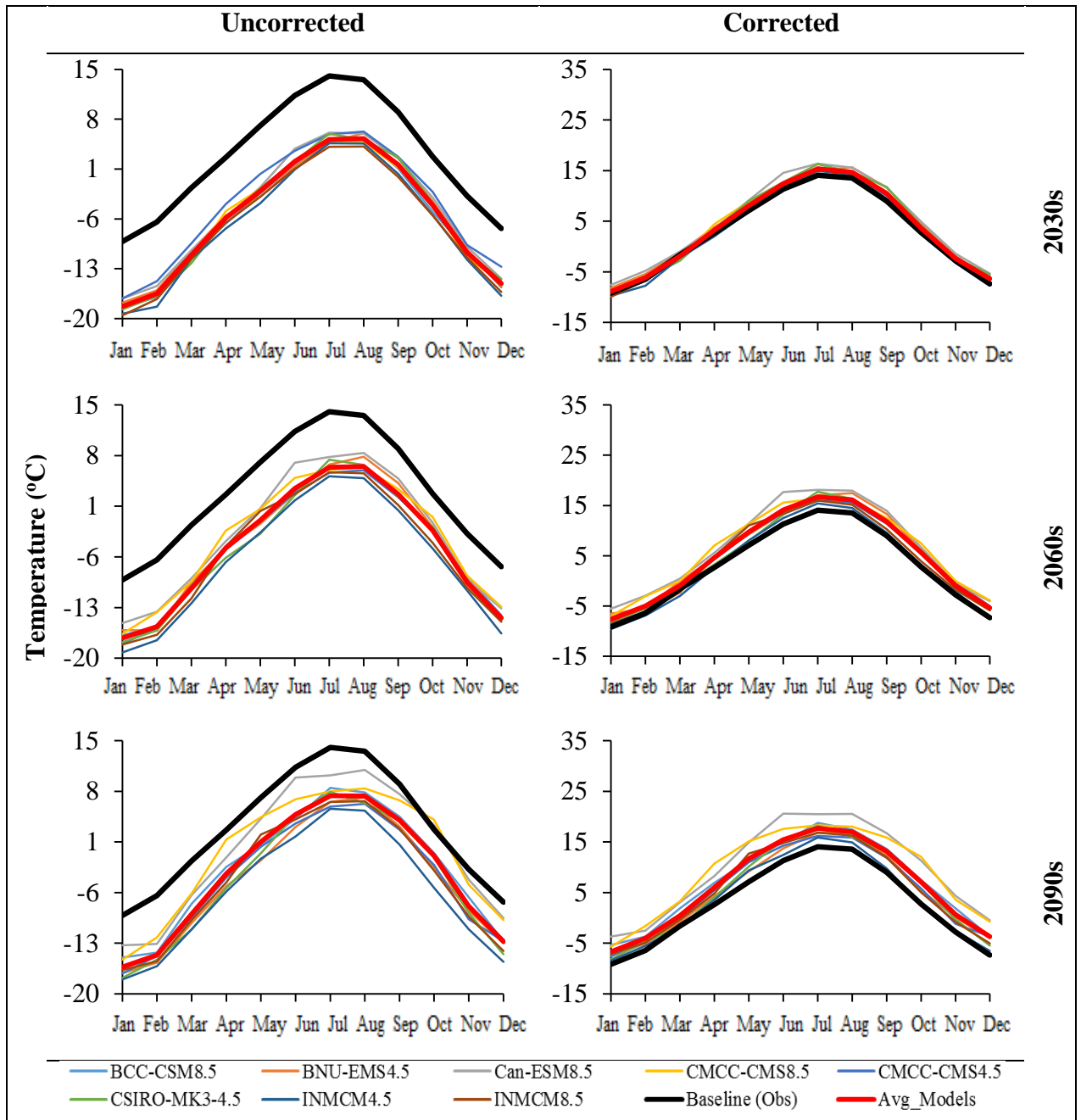


Figure 4.14: IGB Temperature Data before and after Bias Correction for Ziarat Climate Station

Interestingly, similar trend was found at Ziarat climate station as at Hunza and Naltar climate station lot of uncertainties were found in uncorrected projected temperature data

(see Figure 4.13) that is also associated with difference in grid mean elevation and climate station elevation (Lutz et al., 2016). Around 8–9 °C difference was noticed in uncorrected and observed temperature data. After applying bias correction the efficiency parameter value of MAE and RMSE (see Table 4.5) for Ziarat climate station for RCP4.5 (RCP8.5) ranges from 0.9–2.1 (1.0–4.9) and 1.1–2.3 (1.1–5.0), respectively for bias corrected temperature dataset.

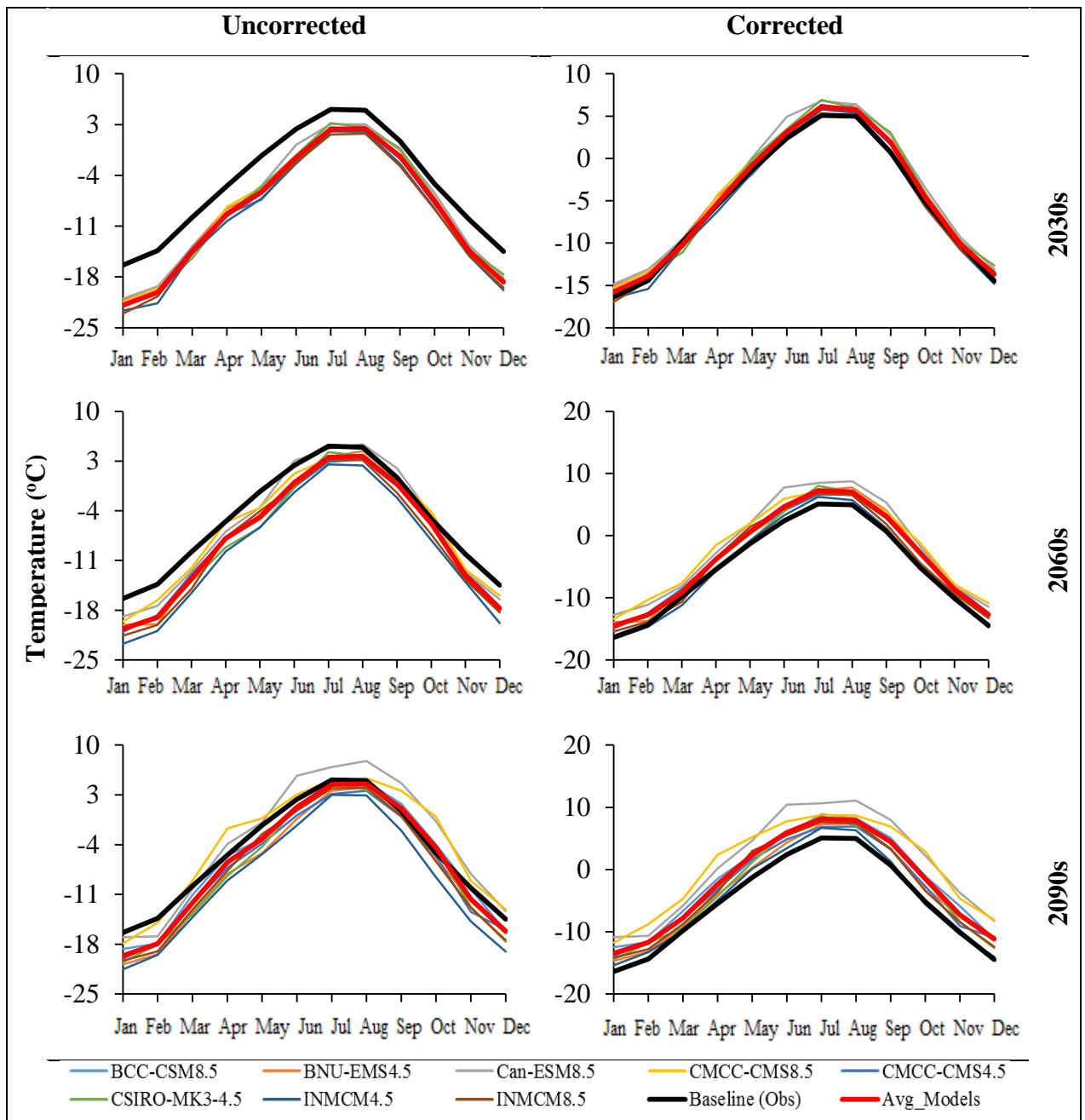


Figure 4.15: IGB Temperature Data before and after Bias Correction for Khunjrab Climate Station

At Khunjrab climate station opposite trend was found as compared to other climate station (Hunza, Naltar and Ziarat) small uncertainties were observed in uncorrected

projected temperature data (see Figure 4.15) that is also may be associated with difference in grid mean elevation and climate station elevation the less uncertainty is due to its higher elevation (4730 m a.s.l) as described by Lutz et al. (2016). Around 3–4 °C difference was noticed in uncorrected and observed temperature data. After applying bias correction the efficiency parameter value of MAE and RMSE (see Table 4.5) for Ziarat climate station for RCP4.5 (RCP8.5) ranges from 6.3–7.6 (7.0–9.5) and 8.1–11.2 (9.7–13.4), respectively for bias corrected projected temperature.

*Table 4.5: Efficiency Parameters after Bias Correction for Climate Station (Hunza Naltar, Ziarat and Khunjrab)*

Climate Stations	Efficiency Parameter	RCP8.5	RCP4.5	RCP8.5	RCP4.5	RCP8.5	RCP4.5
		2030s	2060s	2060s	2090s	2090s	2090s
<b>Precipitation</b>							
<b>Hunza</b>	<b>MAE</b>	7.0	7.6	8.6	7.8	9.5	6.3
	<b>RMSE</b>	9.7	11.2	11.7	10.0	13.4	8.1
	<b>R<sup>2</sup></b>	0.7	0.7	0.6	0.7	0.6	0.8
<b>Khunjrab</b>	<b>MAE</b>	5.4	5.5	5.9	6.7	8.9	6.0
	<b>RMSE</b>	8.3	8.4	10.6	12.4	13.8	11.1
	<b>R<sup>2</sup></b>	0.6	0.6	0.4	0.4	0.3	0.5
<b>Naltar</b>	<b>MAE</b>	8.9	9.1	10.9	9.6	11.7	9.0
	<b>RMSE</b>	12.1	13.7	13.9	12.0	15.8	11.6
	<b>R<sup>2</sup></b>	0.7	0.6	0.6	0.7	0.5	0.7
<b>Ziarat</b>	<b>MAE</b>	4.8	5.6	6.3	5.7	6.6	5.3
	<b>RMSE</b>	7.1	8.1	8.5	7.8	9.5	8.3
	<b>R<sup>2</sup></b>	0.6	0.6	0.6	0.6	0.5	0.6
<b>Temperature</b>							
<b>Hunza</b>	<b>MAE</b>	0.9	0.9	2.7	1.6	4.8	2.0
	<b>RMSE</b>	1.1	1.1	2.8	1.8	4.9	2.2
	<b>R<sup>2</sup></b>	1.0	1.0	1.0	1.0	1.0	1.0
<b>Khunjrab</b>	<b>MAE</b>	0.8	0.8	2.4	1.4	4.4	1.9
	<b>RMSE</b>	0.9	0.9	2.5	1.5	4.5	2.0
	<b>R<sup>2</sup></b>	1.0	1.0	1.0	1.0	1.0	1.0
<b>Naltar</b>	<b>MAE</b>	0.8	0.9	2.6	1.5	4.7	2.0
	<b>RMSE</b>	0.9	1.1	2.8	1.8	4.9	2.2
	<b>R<sup>2</sup></b>	1.0	1.0	1.0	1.0	1.0	1.0
<b>Ziarat</b>	<b>MAE</b>	1.0	0.9	2.9	1.7	4.9	2.1
	<b>RMSE</b>	1.1	1.1	3.0	1.9	5.0	2.3
	<b>R<sup>2</sup></b>	1.0	1.0	1.0	1.0	1.0	1.0

#### 4.4.1.2 Seasonal dataset

The projection of climatic dataset (i.e. temperature and precipitation) for 2030s, 2060s and 2090s showed an increasing tendency in both climate variables (precipitation and temperature) at all the four stations (Hunza, Naltar, Ziarat and Khunjrab) within the Hunza River catchment for both RCP8.5 and RCP4.5 scenarios as shown in Table 4.6.

The station-wise maximum increase in temperature (°C) was found during monsoon season of 2030s, with values range of 1.0–1.3 (for RCP8.5) and 1.2–1.6 (for RCP4.5), while minimum increasing tendency was observed during winter season with similar (0.1–0.4) values range for RCP8.5 and RCP4.5. On the other hand, during 2060s and 2090s, the behavior of both RCPs is slightly different in comparison of 2030s with maximum increase in temperature during pre-monsoon for RCP8.5 [2.7–3.5 (2060s) and 4.9–5.8 (2090s)] and monsoon for RCP4.5 [2.0–2.4 (2060s) and 2.2–2.6 (2090s)]. Interestingly, the behavior of minimum temperature increasing tendency in winter season was found similar for both RCPs during all the decades (2030s, 2060s and 2090s). On annual basis, the maximum increase in temperature was found at Ziarat station with values of 0.8, 2.6 and 4.9 °C (for RCP8.5) and 0.7, 1.5 and 2.0 °C (for RCP4.5), during 2030s, 2060s and 2090s, respectively. Similarly, the basin-wide annual increase in temperature is expected with values of 0.7, 2.4 and 4.6 °C (for RCP8.5) and 0.6, 1.3 and 1.9 °C (for RCP4.5), during 2030s, 2060s and 2090s, respectively. Further, it noticed that the increasing response of RCP8.5 is significantly higher than that of RCP4.5, as also confirmed by Arthur et al. (2016) and IPCC (2014).

In case of precipitation, an increasing trend was found at all four stations in Hunza River catchment, for both RCPs. However, maximum precipitation rise was found during 2090s as given in Table 4.6. On seasonal basis, a mixed behavior of increasing precipitation trend was observed at all the stations for both RCPs with maximum increase during winter and monsoon seasons and minimum rise during pre-monsoon season. The maximum increasing tendency was noticed at Khunjrab station (4730 m a.s.l.) during winter season with range of deviation 46.1–69.6 mm for RCP8.5; 37.1–53.9 mm for RCP4.5, on decadal basis (2030s to 2090s). However, on annual basis the decadal minimum increasing tendency was found at Naltar station with range of deviation 5.3–40.7 mm for RCP 8.5 and 3.0–19.2 mm for RCP 4.5, from base precipitation (679 mm), while maximum was observed at Khunjrab station with deviation range 58.4–94.4 mm

Table 4.6: Station-wise and Basin-wide Projected Temperature (°C) and Precipitation (mm) Deviations from Baseline (Observed) Temperature and Precipitation for RCP8.5 and RCP4.5 during 2030s, 2060s and 2090s, Hunza River Catchment

Decade	Season	Station-wise										Basin-wide					
		Hunza			Naltar			Ziarat			Khunjrab			RCP8.5	RCP4.5	RCP4.5	
		RCP8.5	RCP4.5	RCP8.5	RCP4.5	RCP8.5	RCP4.5	RCP8.5	RCP4.5	RCP8.5	RCP4.5	RCP8.5	RCP4.5				
Temperature (°C)																	
<b>2030s</b>	Pre-Monsoon	1.1	0.6	0.7	0.2	1.3	0.6	0.6	0.4	0.9	0.5	0.5	0.5	0.5	0.5	0.5	0.5
	Monsoon	<b>1.3</b>	<b>1.4</b>	<b>1.0</b>	<b>1.6</b>	1.1	<b>1.5</b>	<b>1.0</b>	<b>1.2</b>	<b>1.1</b>	<b>1.4</b>	<b>1.1</b>	<b>1.4</b>	<b>1.1</b>	<b>1.4</b>	<b>1.1</b>	<b>1.4</b>
	Winter	<b>0.2</b>	<b>0.1</b>	<b>0.1</b>	<b>0.1</b>	<b>0.4</b>	<b>0.4</b>	<b>0.4</b>	<b>0.3</b>	<b>0.3</b>	<b>0.2</b>	<b>0.2</b>	<b>0.2</b>	<b>0.3</b>	<b>0.3</b>	<b>0.2</b>	<b>0.2</b>
	Annual	<i>0.7</i>	<i>0.5</i>	<i>0.5</i>	<i>0.5</i>	<i>0.8</i>	<i>0.7</i>	<i>0.6</i>	<i>0.5</i>	<i>0.5</i>	<i>0.6</i>	<i>0.6</i>	<i>0.7</i>	<i>0.5</i>	<i>0.7</i>	<i>0.6</i>	<i>0.6</i>
<b>2060s</b>	Pre-Monsoon	<b>3.5</b>	1.5	<b>3.2</b>	0.9	<b>3.5</b>	1.6	<b>2.7</b>	1.0	<b>3.2</b>	1.2	<b>2.7</b>	1.0	<b>3.2</b>	1.2	<b>2.7</b>	1.2
	Monsoon	2.8	<b>2.4</b>	2.8	<b>2.4</b>	2.8	<b>2.3</b>	2.4	<b>2.0</b>	2.7	<b>2.3</b>	2.4	<b>2.0</b>	2.7	<b>2.3</b>	2.4	<b>2.3</b>
	Winter	<b>1.9</b>	<b>0.7</b>	<b>1.8</b>	<b>0.6</b>	<b>2.1</b>	<b>1.1</b>	<b>1.9</b>	<b>0.7</b>	<b>1.9</b>	<b>0.8</b>	<b>1.9</b>	<b>0.7</b>	<b>1.9</b>	<b>0.8</b>	<b>1.9</b>	<b>0.8</b>
	Annual	<i>2.5</i>	<i>1.3</i>	<i>2.4</i>	<i>1.1</i>	<i>2.6</i>	<i>1.5</i>	<i>2.2</i>	<i>1.1</i>	<i>2.4</i>	<i>1.3</i>	<i>2.5</i>	<i>1.1</i>	<i>2.4</i>	<i>1.3</i>	<i>2.5</i>	<i>1.3</i>
<b>2090s</b>	Pre-Monsoon	<b>5.7</b>	2.3	<b>5.5</b>	1.9	<b>5.8</b>	2.2	<b>4.9</b>	1.9	<b>5.5</b>	2.1	<b>4.9</b>	1.9	<b>5.5</b>	2.1	<b>4.9</b>	2.1
	Monsoon	4.8	<b>2.4</b>	5.0	<b>2.6</b>	4.9	<b>2.6</b>	4.3	<b>2.2</b>	4.7	<b>2.4</b>	4.3	<b>2.2</b>	4.7	<b>2.4</b>	4.3	<b>2.4</b>
	Winter	<b>4.0</b>	<b>1.4</b>	<b>3.8</b>	<b>1.3</b>	<b>4.4</b>	<b>1.6</b>	<b>4.1</b>	<b>1.6</b>	<b>4.1</b>	<b>1.5</b>	<b>4.1</b>	<b>1.6</b>	<b>4.1</b>	<b>1.5</b>	<b>4.1</b>	<b>1.5</b>
	Annual	<i>4.6</i>	<i>1.9</i>	<i>4.5</i>	<i>1.8</i>	<i>4.9</i>	<i>2.0</i>	<i>4.3</i>	<i>1.8</i>	<i>4.6</i>	<i>1.9</i>	<i>4.6</i>	<i>1.8</i>	<i>4.6</i>	<i>1.9</i>	<i>4.6</i>	<i>1.9</i>
Precipitation (mm)																	
<b>2030s</b>	Pre-Monsoon	<b>12.7</b>	13.8	<b>13.4</b>	<b>13.9</b>	0.4	12.9	1.7	<b>4.9</b>	7.0	<b>11.4</b>	1.7	<b>4.9</b>	7.0	<b>11.4</b>	1.7	<b>4.9</b>
	Monsoon	21.1	<b>25.3</b>	7.7	<b>19.7</b>	<b>18.1</b>	<b>20.6</b>	10.6	13.1	14.4	16.1	10.6	13.1	14.4	16.1	10.6	13.1
	Winter	<b>21.6</b>	<b>10.8</b>	<b>0.4</b>	14.3	8.4	<b>2.2</b>	<b>46.1</b>	<b>37.1</b>	<b>19.1</b>	<b>19.4</b>	<b>46.1</b>	<b>37.1</b>	<b>19.1</b>	<b>19.4</b>	<b>46.1</b>	<b>37.1</b>
	Annual	<i>29.9</i>	<i>49.9</i>	<i>5.3</i>	<i>19.2</i>	<i>26.9</i>	<i>35.6</i>	<i>58.4</i>	<i>55.2</i>	<i>30.1</i>	<i>40.1</i>	<i>58.4</i>	<i>55.2</i>	<i>30.1</i>	<i>40.1</i>	<i>58.4</i>	<i>55.2</i>
<b>2060s</b>	Pre-Monsoon	<b>12.0</b>	<b>5.3</b>	10.6	<b>3.4</b>	<b>2.7</b>	<b>6.9</b>	2.7	<b>3.7</b>	<b>4.8</b>	2.7	<b>3.7</b>	<b>4.8</b>	2.7	<b>3.7</b>	<b>4.8</b>	2.7
	Monsoon	<b>26.3</b>	11.6	<b>13.4</b>	4.3	<b>19.6</b>	8.1	9.1	6.9	17.1	7.7	9.1	6.9	17.1	7.7	9.1	6.9
	Winter	23.1	<b>26.1</b>	1.7	<b>8.7</b>	15.2	<b>15.9</b>	<b>49.9</b>	<b>60.6</b>	<b>22.4</b>	<b>27.8</b>	<b>49.9</b>	<b>60.6</b>	<b>22.4</b>	<b>27.8</b>	<b>49.9</b>	<b>60.6</b>
	Annual	<i>37.4</i>	<i>42.9</i>	<i>4.5</i>	<i>7.7</i>	<i>37.4</i>	<i>30.9</i>	<i>61.7</i>	<i>71.2</i>	<i>35.2</i>	<i>38.2</i>	<i>61.7</i>	<i>71.2</i>	<i>35.2</i>	<i>38.2</i>	<i>61.7</i>	<i>71.2</i>
<b>2090s</b>	Pre-Monsoon	<b>14.5</b>	<b>0.8</b>	<b>15.6</b>	<b>0.1</b>	<b>8.7</b>	7.7	<b>5.7</b>	<b>2.2</b>	<b>11.1</b>	7.7	<b>5.7</b>	<b>2.2</b>	<b>11.1</b>	7.7	<b>5.7</b>	<b>2.2</b>
	Monsoon	25.1	14.1	<b>22.2</b>	0.3	<b>22.6</b>	10.6	19.1	6.4	23.5	7.8	19.1	6.4	23.5	7.8	19.1	6.4
	Winter	<b>34.1</b>	<b>20.3</b>	19.9	<b>3.2</b>	21.2	<b>15.7</b>	<b>69.6</b>	<b>53.9</b>	<b>36.2</b>	<b>23.2</b>	<b>69.6</b>	<b>53.9</b>	<b>36.2</b>	<b>23.2</b>	<b>69.6</b>	<b>53.9</b>
	Annual	<i>60.7</i>	<i>35.2</i>	<i>40.7</i>	<i>3.0</i>	<i>52.4</i>	<i>33.9</i>	<i>94.4</i>	<i>62.4</i>	<i>63.3</i>	<i>33.6</i>	<i>94.4</i>	<i>62.4</i>	<i>63.3</i>	<i>33.6</i>	<i>94.4</i>	<i>63.3</i>

Bold (seasonal) and Italic (annual) values show minimum and maximum increase, gray shaded are annual values

for RCP8.5 and 55.2–71.2 mm for RCP4.5, from base precipitation (187 mm). The basin-wide analysis depicted that the maximum increasing precipitation trend was found during winter season with range 19.1–36.2 mm for RCP8.5 and 19.4–27.8 for RCP4.5, on decadal basis. Annually, the basin-wide precipitation is expected to increase by 63.3 (RCP8.5) and 33.6 (RCP4.5) during 2090s.

Overall, the maximum increase in precipitation station-wise and basin-wide during winter season in Hunza River catchment, may be associated with the large and strong influence of westerlies circulation pattern in future. While, it observed that the Khunjrab station is expected to receive maximum precipitation in future with comparison of other three stations (Hunza, Naltar and Ziarat), this increasing tendency at Khunjrab station is also confirmed by several researchers and stated that the high-altitude part of the Karakorum region is most active hydrological zone and the elevation greater than 3500 m a.s.l. receives maximum rainfall (Butz and Hewitt, 1986 and Hewitt, 2007).

#### **4.4.2 Projected Streamflows**

The effect of climate change on the Hunza River catchment streamflows were premeditated by means of the SRM (most suitable hydrological model) under different climate change scenarios i.e. RCPs scenarios (RCPs with unchanged SCA denoted as RCPs+UCSCA) and combination of RCPs climate data with percent (%) change in SCA (CSCA) which hereafter referred to as hypothetical scenarios (i.e. RCPs±%CSCA). The observed streamflow data obtained by considering average of 9 years (2001–2006, 2008–2010) as the baseline (observed) streamflow.

##### **4.4.2.1 RCPs scenarios (RCPs+UCSCA)**

The potential changes in daily streamflows of Hunza River catchment were investigated by using optimized parameters during calibration of SRM, while, input climate dataset such as precipitation and temperature were replaced with bias corrected RCPs climate dataset by keeping SCA constant i.e. unchanged SCA (UCSCA). On seasonal basis, it was observed that the streamflows are expected to increase in future by using both RCPs climate dataset (Table 4.7). During 2030s for RCP8.5, the maximum increase in streamflows was found during pre-monsoon and monsoon seasons by 21% (54 m<sup>3</sup>/s) and 20% (137 m<sup>3</sup>/s) in comparison with baseline (observed) streamflows of 253 m<sup>3</sup>/s and 681

$\text{m}^3/\text{s}$ , respectively, with minimum increase of 7% ( $5 \text{ m}^3/\text{s}$ ) during winter season in comparison with baseline (observed) streamflow of  $71 \text{ m}^3/\text{s}$ . While, a significant increase was found over 2060s with values of 92% ( $233 \text{ m}^3/\text{s}$ ), 53% ( $358 \text{ m}^3/\text{s}$ ) and 12% ( $9 \text{ m}^3/\text{s}$ ) during pre-monsoon, monsoon and winter seasons, respectively. Moreover, the seasonal streamflows during 2090s are expected to double than 2060s with percent (%) increase of 193 ( $489 \text{ m}^3/\text{s}$ ), 90 ( $614 \text{ m}^3/\text{s}$ ) and 79 ( $56 \text{ m}^3/\text{s}$ ) during pre-monsoon, monsoon and winter seasons, respectively. Although, the streamflows were found increasing under RCP4.5, however, the tendency was not high as RCP8.5. Overall, a significant increase was found during pre-monsoon and monsoon seasons of 2060s with values of 28 ( $72 \text{ m}^3/\text{s}$ ) and 39% ( $266 \text{ m}^3/\text{s}$ ), respectively, while, the maximum increase of 66% ( $166 \text{ m}^3/\text{s}$ ) and 73% ( $296 \text{ m}^3/\text{s}$ ) were observed during pre-monsoon and monsoon seasons of 2090s. These increasing trends of streamflows were found in consistent with the change in climate variables (Tables 4.6 and Table 4.7). In case of RCP8.5, during pre-monsoon season the streamflow increment was found in consistent with the basin-wide maximum increase in temperature and minimum precipitation increase, this may be due to the high sensitivity of the SRM model with temperature and SCA, while, slight sensitive with precipitation. Therefore, the slight change in temperature could largely affect the streamflows. Interestingly, it observed that the significant basin-wide increase in precipitation was found during winter season of 2030s, 2060s and 2090s, however, the percent (%) of streamflows increment is not substantial as during pre-monsoon and monsoon seasons. This fact may be associated with the temperature changes which is also found increasing but may be still below the critical temperature ( $T_{\text{crit}}$ ) which is responsible to differentiate the precipitation form (solid or liquid), therefore, the SRM incorporates precipitation in the form of solid snow. The similar results were found for RCP4.5 with exception of significant increase in streamflow during monsoon season. Overall, the mean annual streamflows are expected to increase by 16–113% ( $42\text{--}304 \text{ m}^3/\text{s}$ ) and 13–43% ( $35\text{--}115 \text{ m}^3/\text{s}$ ) in comparison with baseline (observed) streamflow of  $269 \text{ m}^3/\text{s}$  for RCP8.5 and RCP4.5, respectively. Further on decadal basis, the maximum streamflow is anticipated for the month of July by  $1006\text{--}1622 \text{ m}^3/\text{s}$  and  $1000\text{--}1259 \text{ m}^3/\text{s}$  for RCP8.5 and RCP4.5, respectively (see Figure 4.16). Moreover streamflow for RCP8.5 is higher due to the extreme nature of the pathway and SRM

sensitivity to temperature for the highly–elevated cryosphere catchments (Dou et al., 2011 and Azmat et al., 2016a).

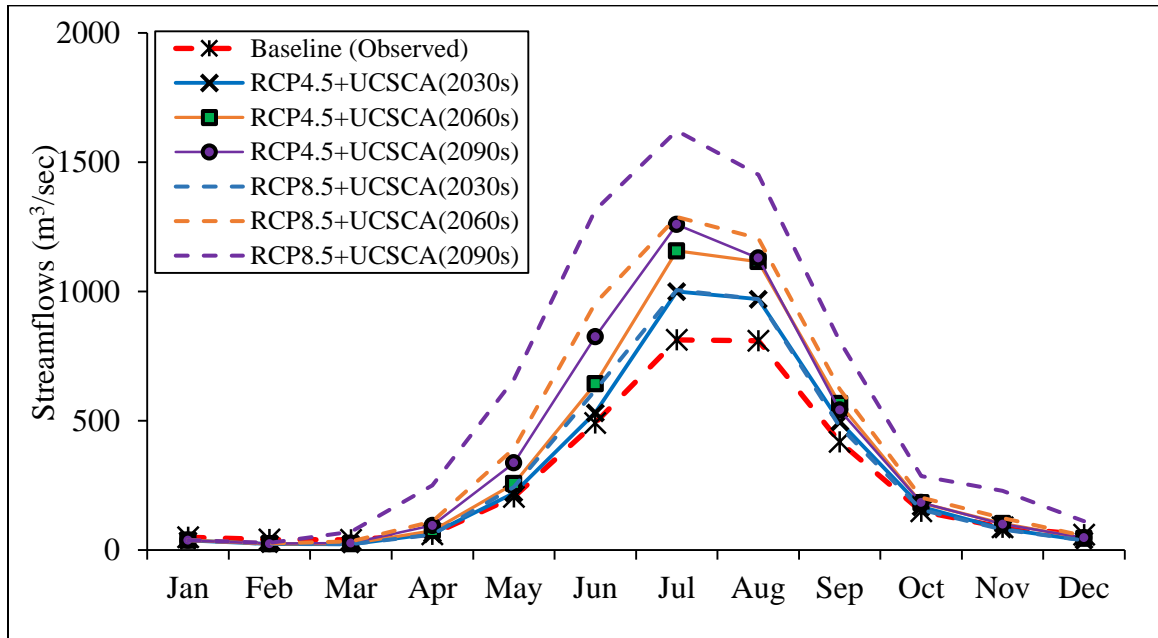


Figure 4.16: Projected Monthly Streamflow ( $m^3/s$ ) for RCP4.5, RCP8.5, under RCPs Scenarios (RCPs+UCSCA) during 2030s, 2060s, and 2090s, Hunza River Catchment.

#### 4.4.2.2 Hypothetical scenarios (RCPs±%CSCA)

Further, the investigations were carried out to analyze the impact of change in SCA (CSCA) on streamflows under the hypothetical scenarios developed by the combination of percent change in SCA ( $\pm 5\%$  CSCA for 2030s,  $\pm 10\%$  CSCA for 2060s and  $\pm 15\%$  CSCA for 2090s) with the bias corrected RCPs climate datasets denoted as (RCPs±%CSCA) (Table 4.7). Since, the Hunza River catchment is dominantly covered with snow particularly during winter season; therefore, it is essential to investigate the sensitivity of change in SCA on Hunza River catchment streamflows. A similar behavior of streamflow was found under both scenarios (CSCA and UCSCA) in comparison with baseline (observed) streamflow. The changes in streamflows by considering the hypothetical scenarios are as given below:

- (i) For RCPs±5% CSCA scenarios, the SCA assumed to increase and decrease by 5% during 2030s for both RCP8.5 and RCP4.5. A SCA increase by 5% resulting 33% ( $87 m^3/s$ ) and 29% ( $79 m^3/s$ ) increase in mean annual streamflow in comparison

with baseline (observed) streamflow for RCP8.5 and RCP4.5, respectively, while by decreasing 5% SCA resulting decrease by 2% (5 m<sup>3</sup>/s) and 4% (12 m<sup>3</sup>/s), for RCP8.5 and RCP4.5, respectively.

- (ii) For RCPs±10% CSCA scenarios, with SCA assumed to increase 10% by 2060s while considering both RCP8.5 and RCP4.5, resulting an increase by approximately 97% (262 m<sup>3</sup>/s) and 68% (184 m<sup>3</sup>/s) of streamflow from baseline (observed) for RCP8.5 and RCP4.5, respectively, while, a 10% decrease in SCA resulting increase (decrease) by 18% (2%) for RCP8.5 (RCP4.5).
- (iii) For RCPs±15% CSCA scenarios, with SCA assumed to increase 15% by 2090s while considering both RCP8.5 and RCP4.5, resulting an increase nearly by 186% (501 m<sup>3</sup>/s) and 103% (276 m<sup>3</sup>/s) of streamflow from baseline (observed) for RCP8.5 and RCP4.5, respectively, while 15% decrease in SCA resulting the mean annual streamflow to increase (decrease) by 42% (7%), for RCP8.5 (RCP4.5).

Overall with increase in SCA by 5% (2030s), 10% (2060s) and 15% (2090s), the mean annual stream flows are expected to increase by 33–186% (87–501 m<sup>3</sup>/s) and 29–103% (79–276 m<sup>3</sup>/s) in comparison with baseline (observed) streamflow of 269 m<sup>3</sup>/s for RCP8.5 and RCP4.5, respectively. Further with increase in SCA on decadal basis, the maximum streamflow is anticipated for the month of July by 1161–2251 m<sup>3</sup>/s and 1154–1793 m<sup>3</sup>/s for RCP8.5 and RCP4.5, respectively. On the other hand, with decrease in SCA by 5% (2030s), 10% (2060s) and 15% (2090s), the mean annual streamflows are expected to increase (decrease) by 42% (7%), for RCP8.5 (RCP4.5) during 2090s. Figure 4.17 (a & b) showed the change in monthly streamflows under the climate change scenarios of RCP8.5 and RCP4.5 (denoted as RCPs+UCSCA) with combination of hypothetical scenarios of change in SCA (RCPs±%CSCA). Figure 4.17a depicted that streamflows significantly increased under RCP8.5+UCSCA (during 2030s, 2060s and 2090s) scenarios which is associated with the temperature and precipitation change (see Table 4.6 for RCP8.5). However, streamflows produced under RCP8.5±5%CSCA (2030s), RCP8.5±10%CSCA (2060s) and RCP8.5±15%CSCA (2090s) scenarios showed a tremendous importance of SCA presence in the study area. It is clear from Figure 3.10a, that streamflow increment was significantly high under the scenario of RCP8.5+5%CSCA (2030s) in the comparison

of RCP8.5+UCSCA (2030s), in contrast to the RCP8.5–5% CSCA (2030s) which showed a decrease in streamflow almost equal to baseline (observed) streamflow.

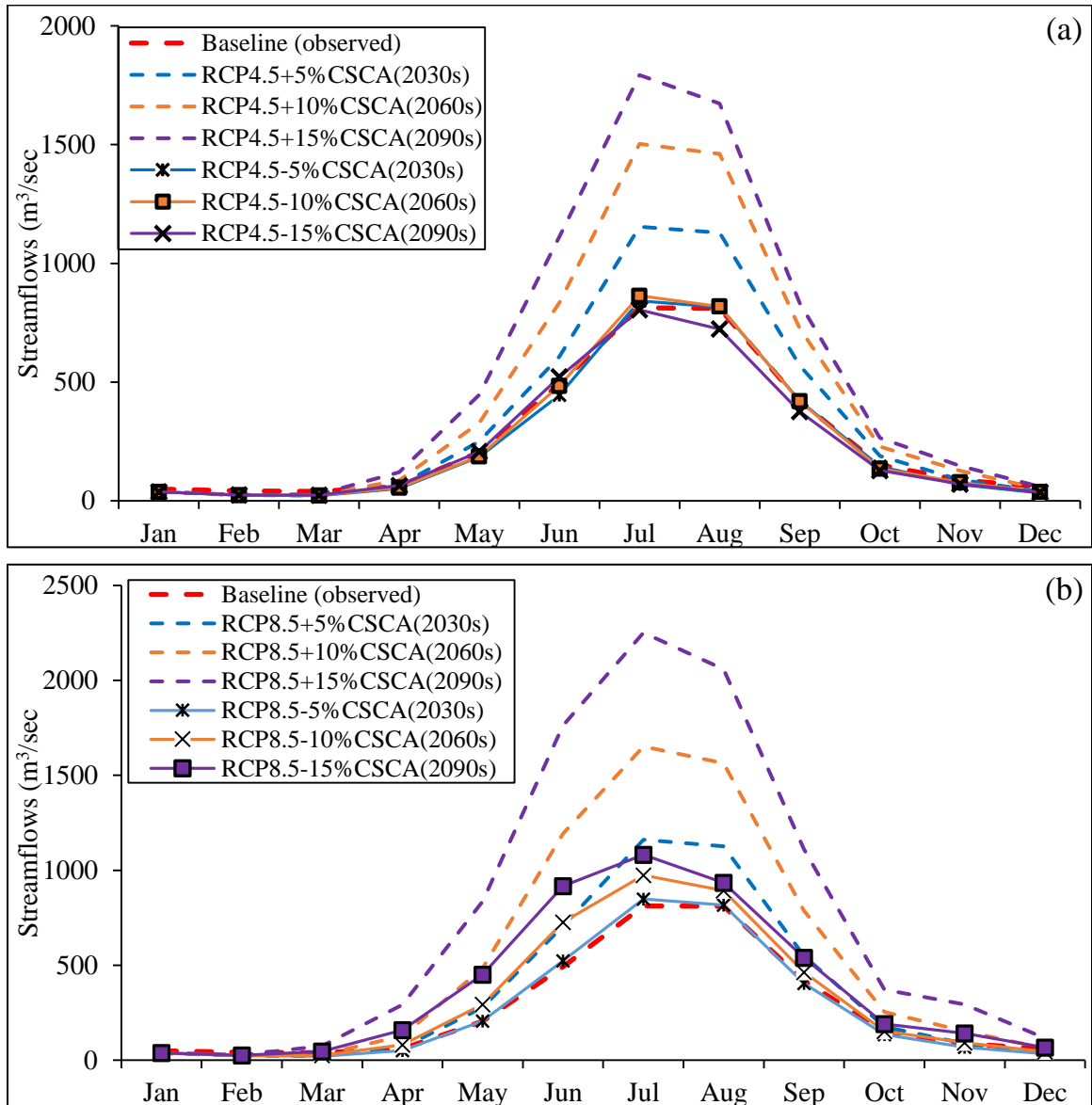


Figure 4.17: Projected Monthly Streamflow ( $m^3/s$ ) for (a) RCP4.5, and (b) RCP8.5, under Hypothetical Scenarios ( $RCPs \pm \%CSCA$ ) during 2030s, 2060s and 2090s, Hunza River Catchment.

Moreover, the similar pattern of streamflow change was found for RCP8.5±10% CSCA (2060s) in comparison of RCP8.5+UCSCA (2060s), interestingly, streamflows produced under both RCP8.5+10% CSCA (2060s) and RCP8.5–10% CSCA (2060s) scenarios approaching to the RCP8.5+UCSCA (2090s) and RCP8.5+UCSCA (2030s), respectively.

A huge impact of change in SCA on streamflows under scenario of RCP8.5±15% CSCA (2090s) was observed in comparison of all the scenarios, particularly, for RCP8.5+UCSCA (2090s). It noticed that the decreases in streamflows for decrease in SCA are still greater than that of baseline (observed) for RCP8.5–10% CSCA (2060s) and RCP8.5–15% CSCA (2090s) with exception of RCP8.5–5% CSCA (2030s). This fact is associated with the significant rise in temperature during 2060s and 2090s as compared to 2030s (see Table 4.6 for RCP8.5). On the other hand, for RCP4.5, the RCP4.5+UCSCA scenarios of 2030s, 2060s and 2090s reflecting similar behavior for the change in streamflows as that of RCP8.5, however, the amount of streamflows are not significantly high as in case of RCP8.5. It should be noted that the streamflows produced under RCP4.5–5% CSCA (2030s), RCP4.5–10% CSCA (2060s) and RCP4.5–15% CSCA (2090s) scenarios are almost equal to the baseline (observed) streamflow, however, significantly decreased in comparison with RCP4.5+UCSCA (during 2030s, 2060s and 2090s) scenarios. With reduction in SCA scenarios under RCP4.5, the streamflows are expected to approach baseline (observed) associated with the aforementioned fact of temperature increase. Moreover, for both RCP8.5 and RCP4.5 scenarios (RCPs+UCSCA and RCPs+% CSCA), a shift in hydrological regime was observed from the April to March as confirmed by Tahir et al. (2011b). It may be associated with the significant rise in temperature during end of winter month or pre–monsoon season which caused early snowmelt and this fact is justified by the significant rise in streamflow generation during pre–monsoon (see Tables 4.6 and Table 4.7). Moreover, an increase in streamflow by 22% ( $101.33 \text{ m}^3/\text{s}$ ) during summer season (average of pre–monsoon and monsoon seasons of 2030s, 2060s and 2090s for RCP8.5) by the rise of  $1 \text{ }^\circ\text{C}$  mean temperature is different from previous studies conducted in Hunza River catchment such as Tahir et al. (2011b), Akhter et al. (2008) and Archer, (2003). Tahir et al. (2011b) stated an increase of 33% ( $164 \text{ m}^3/\text{s}$ ) streamflow while, Archer, (2003) and Akhter et al. (2008) stated 16% increase in streamflow in Hunza River catchment by with increase of  $1 \text{ }^\circ\text{C}$  mean temperature. This discrepancy may be due the difference in data, methodologies, hypothesis and limitations under which current study conducted in comparison with previous studies e.g. Archer (2003) used statistical analysis, Akhter et al. (2008) used a different hydrological model (HBV) with integration of hypothetical scenarios, while, Tahir et al. (2011b) used SRM model (similar to current

study), however, the difference in results could be attributed to the hypothetical climate change scenarios (i.e. change in SCA and temperature). In addition, an increase in temperature and SCA hypothetical scenarios were adopted linearly for data series without considering more detail and reliable information as stated by Tahir et al. (2011b). While, in this study, more detailed and downscaled data series of precipitation and temperature for RCPs provided by HI-AWARE project for the Indus, Ganga and Brahmaputra (IGB) River basins, were used. Additionally, the SCA extracted from cloud free images were utilized to run SRM for calibration and climate change analysis, in contrast to Tahir et al. (2011b).

*Table 4.7: Projected Streamflow Deviations(%) from Baseline (Observed) Streamflow for RCP8.5 and RCP4.5 under RCPs Scenarios(RCPs+UCSCA) and Hypothetical Scenarios (RCPs±%CSCA) during 2030s, 2060s and 2090s, Hunza River Catchment*

Decade	Season	RCPs Scenarios		Hypothetical Scenarios(RCPs±%CSCA)			
		RCP8.5	RCP4.5	RCP8.5	RCP4.5	RCP8.5	RCP4.5
		<b>UCSCA</b>		<b>+5%CSCA</b>		<b>-5%CSCA</b>	
2030s	Pre-Monsoon	21	7	38	21	3	-10
	Monsoon	20	18	39	35	1	2
	Winter	7	1	6	3	-25	-23
	Annual	16	13	33	29	-2	-4
		<b>UCSCA</b>		<b>+10%CSCA</b>		<b>-10%CSCA</b>	
2060s	Pre-Monsoon	92	28	138	65	45	-4
	Monsoon	53	39	96	81	14	3
	Winter	12	3	32	15	-12	-22
	Annual	57	31	97	68	18	-2
		<b>UCSCA</b>		<b>+15%CSCA</b>		<b>-15%CSCA</b>	
2090s	Pre-Monsoon	193	66	281	121	101	4
	Monsoon	90	43	165	111	25	-7
	Winter	79	5	117	32	19	-25
	Annual	113	43	186	103	42	-7

*UCSCA (Unchanged SCA), CSCA (Changed SCA), RCPs (RCP8.5 / RCP4.5), Annual values shaded in gray.*

Overall, the temperature variations could be more influential for the Hunza River catchment because it is largely responsible for streamflow generation through snow- and glacier-melt., as confirmed by Archer (2003) and Tahir et al. (2011b). Therefore, the large storage reservoirs are essentially required to manage and cater the flood conditions resulting from potential increase in water resources under the climate change in Hunza River catchment.

#### 4.4.2.3 Hypothetical Scenarios (BL+T<sub>x</sub>P<sub>x</sub>)

The effect of climate change on the Hunza River catchment was premeditated by means of the SRM under the different climate scenarios. The simulated runoff obtained by averaging of 9 years (2001–2006, 2008–2010) meteorological variables were considered as the base line of the present/ current climate. SCA was assumed to be constant for all scenarios.

- i.** The streamflow was estimated by considering 1 °C increase in temperature and 5% increase precipitation (BL+T<sub>1</sub>P<sub>5</sub>) by 2030s is shown in Figure 4.18 and described in Table 4.8. The outcomes reveal that the river runoff is expected to be increase with increase in both temperature and precipitation. Approximately 29% (~77 m<sup>3</sup>/s) increase in mean annual streamflow (~269 m<sup>3</sup>/s) was observed for 2030s. Maximum streamflow of 1082 m<sup>3</sup>/sec in the month of July was observed that is 33% more than the present streamflow of that month (~812 m<sup>3</sup>/s). More streamflow was observed in summer season (April–September) than winter season (October–March). Summer season streamflow is more dominant by heavily monsoon precipitation as well as temperature in snow and glaciated fed catchment.
- ii.** The mean temperature of the Hunza basin was supposed to rise by 2 °C and 10 % increase in precipitation (BL+T<sub>2</sub>P<sub>10</sub>) by 2060s (see Figure 4.18 and Table 4.8). The results indicate that streamflow will be increased nearly 60% (~278m<sup>3</sup>/s) in the summer season and around 57 % (~153m<sup>3</sup>/s) will increase in mean annual streamflow was found. These result are considerably comparable from that estimated by Tahir et al. (2011b), who described that 2 °C rise in mean temperature causes 64 % increase in summer streamflow in Hunza River. The slightly difference among the results obtained by two different studies and same method maybe due to the consideration of year 2000 as present climate.
- iii.** The streamflow by considering, increase in precipitation by 15% and mean temperature rises by 3°C (BL+T<sub>3</sub>P<sub>15</sub>) causes 89% (415m<sup>3</sup>/s) increase in the summer (April–September) streamflow in 2090s and 72% (51m<sup>3</sup>/s) increase in winter season (October–March) (see Table 4.8). Maximum streamflow of 1510 m<sup>3</sup>/s in the month of July was also observed. The streamflow by

considering, increase in precipitation by 20% and mean temperature rises by 4°C (BL+T<sub>4</sub>P<sub>20</sub>) causes 118% (~317 m<sup>3</sup>/s) increase in the future annual streamflow in 2090s and 120 % (~558 m<sup>3</sup>/s) increase in winter season (October–March).

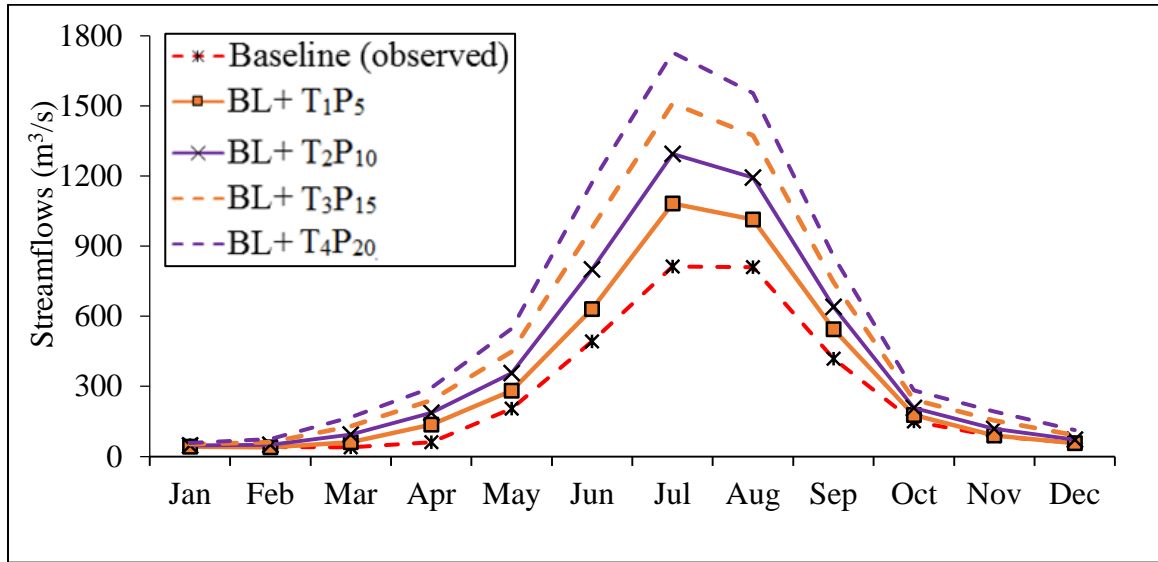


Figure 4.18: Projected Streamflows under Hypothetical Scenarios(BL+T<sub>x</sub>P<sub>x</sub>) in Hunza River Catchment.

Table 4.8: Percent Increase in Projected Streamflows under Hypothetical Scenarios((BL+T<sub>x</sub>P<sub>x</sub>) in Hunza River Catchment.

Decade	2030s		2060s		2090s	
	BL+T <sub>1</sub> P <sub>5</sub>	BL+T <sub>2</sub> P <sub>10</sub>	BL+T <sub>3</sub> P <sub>15</sub>	BL+T <sub>4</sub> P <sub>20</sub>	BL+T <sub>3</sub> P <sub>15</sub>	BL+T <sub>4</sub> P <sub>20</sub>
<b>Per-monsoon</b>	38	77	120	165		
<b>Monsoon</b>	29	53	78	103		
<b>Winter</b>	10	38	72	109		
<b>Annual</b>	29	57	87	118		

#### 4.4.3 Comparison of GCMs and Hypothetical Results

Projected streamflows under both scenarios (IGB dataset i.e. RCPs+UCSCA and hypothetical scenarios i.e BL+T<sub>x</sub>P<sub>x</sub>) shows increasing trend. Overall mean decadal streamflows are expected to increase by 16–113% (42–304 m<sup>3</sup>/s) for RCP8.5 in comparison with 13–43% (35–115 m<sup>3</sup>/s) for RCP4.5 and for hypothetical scenarios (BL+T<sub>x</sub>P<sub>x</sub>) increase

in streamflows are expected to be increase by 29-118% (78-318 m<sup>3</sup>/s). Streamflows under hypothetical scenarios (BL+T<sub>x</sub>P<sub>x</sub>) is showing more streamflows (Figure 4.19).

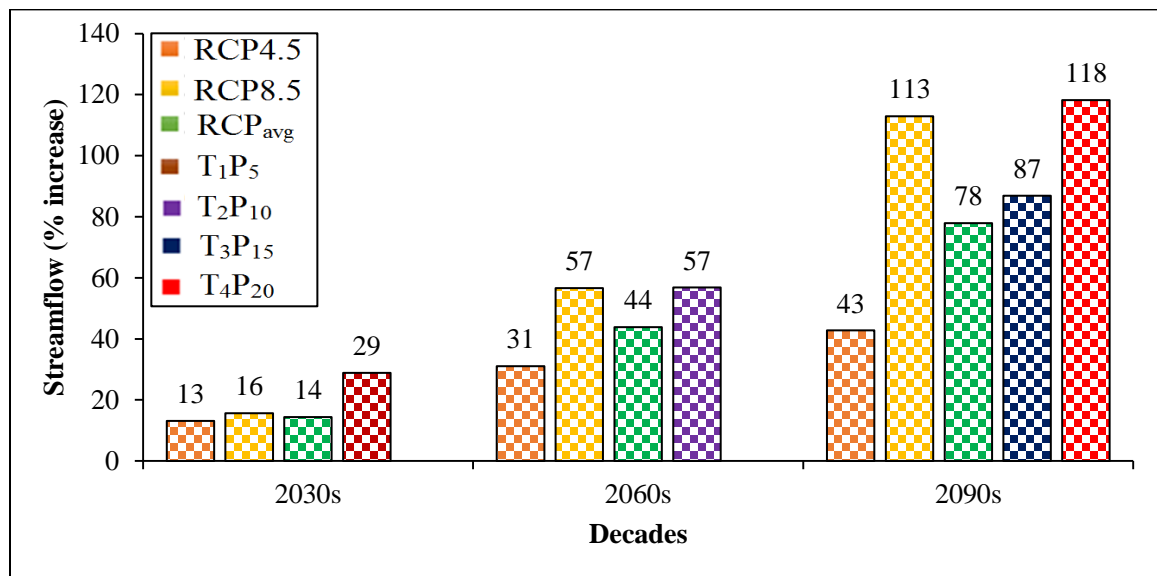


*Figure 4.19: Comparison of Projected Water Availability under RCPs(UCSCA) and Hypothetical Scenarios(BL+T<sub>x</sub>P<sub>x</sub>) for Hunza River Catchment*

Hypothetical scenarios are just an assumption and they does not include any calculation or climate affecting parameters. Hypothetical approach assumed the linear increase in climate variables (temperature & precipitation) which doesn't happen in actual climate. But in the case of climate models, all projected climate variable were derived on the basis of calculation (topography, parameter affecting climate etc.) and doesn't exhibit the linear increase or decrease trend. Climate models are based on the long term previous record are projected data also again refined for the area of study.

## **CONCLUSIONS AND RECOMMENDATIONS**

### **5.1 CONCLUSIONS**

As a part of this study, identification of land cover was carried out using Landsat-5 & 8 imagery with the help of ERDAS Imagine tool, which showed that major changes happened in forest cover that was reduced by 0.52% (71.5 Km<sup>2</sup>) and water bodies were increased by 0.05% (6.8 Km<sup>2</sup>) of total Hunza River catchment area (13718 km<sup>2</sup>) from 1994 to 2014. The MODIS SCA products (i.e. MYD10A2 and MOD10A2 available on Aqua and Terra) were used to generate cloud free composite image by removing the clouds to find percentage SCA. Basin wide maximum SCA of 85% and minimum of 38% was found in the month of February and August, respectively over 10 year duration (2001–2010).

This study used to examine the efficiency of two widely used hydrological models, a standard rainfall–runoff model (HEC–HMS) and a snowmelt–runoff model (SRM) from most suitable SRM model was adopted for the climate change impact on streamflows of Hunza River catchment.

The daily streamflows were simulated using both the models for a period of 9 years (2001–2006 for calibration and 2008–2010 for validation). The performance of SRM was significantly better in comparison with HEC–HMS, as described by performance indicators R<sup>2</sup> and NS coefficient were 0.95 and 0.92 (0.97 and 0.89) for SRM, compared with values of 0.63 and 0.57 (0.61 and 0.54) for HEC–HMS, during calibration (validation) period on annual basis. HEC–HMS poorly captured the streamflow peaks during monsoon and also produced unnecessary peaks during winter season, while SRM reproduce streamflows efficiently during both seasons. Overall, the simulated streamflow results showed that the efficiency of SRM is better than HEC–HMS in high–altitude snow and glacier–fed Hunza River catchment.

Further, considering the better efficiency SRM was used to assess the potential impact of climate change on streamflows of the Hunza River catchment by using different climate change scenarios i.e. RCPs scenarios (RCPs+UCSCA) and Hypothetical scenarios

(RCPs±%CSCA) during decades of 2030s, 2060s and 2090s. Firstly, for all the decades the bias corrected climatic dataset (i.e. temperature and precipitation) was derived which showed an increasing tendency on annual and seasonal basis on all the four stations lies within the study area for both RCP8.5 and RCP4.5. The expected basin-wide mean annual temperature increases are 0.7, 2.4 and 4.6 °C (for RCP8.5), which are significantly higher than that of 0.6, 1.3 and 1.9 °C (for RCP4.5), during 2030s, 2060s and 2090s, respectively. Moreover in case of precipitation, the maximum increase in basin-wide precipitation was found during winter season 19.1–36.2 mm for RCP8.5 in comparison with 19.4–27.8 mm for RCP4.5, on decadal basis, which may be associated with the strengthening of westerlies circulation pattern in future. Secondly, the potential impact of changing climate on streamflows was investigated using RCPs scenarios (RCPs+UCSCA) and hypothetical scenarios (RCPs±%CSCA) during 2030s, 2060s and 2090s. An increasing trends of streamflows were found which were in consistent with the projected climatic dataset and overall mean annual streamflows are expected to increase by 16–113% (42–304 m<sup>3</sup>/s) for RCP8.5 in comparison with 13–43% (35–115 m<sup>3</sup>/s) for RCP4.5 on decadal basis, that fact is associated with the extreme nature of RCP8.5 and sensitivity of SRM to temperature high-altitude cryosphere catchment. Further, for hypothetical scenarios (RCPs+%CSCA) i.e. with increase of SCA by 5% (2030s), 10% (2060s) and 15% (2090s), the potential increase in mean annual streamflows are expected to be 33–186% (87–501 m<sup>3</sup>/s) and 29–103% (79–276 m<sup>3</sup>/s) for RCP8.5 and RCP4.5, respectively, while with decrease in SCA by 5% (2030s), 10% (2060s) and 15% (2090s), the mean annual streamflows are expected to increase (decrease) by 42% (7%) for RCP8.5 (RCP4.5) during 2090s. Additionally, for hypothetical scenarios (BL+T<sub>x</sub>P<sub>x</sub>) i.e. temperature (precipitation) increased by 1 °C (5%) by (2030s), 2 °C (10%) by (2060s), 3 °C (15%) and 4 °C (20%) by (2090s), the potential increase in mean annual streamflows are expected to be 29% (78 m<sup>3</sup>/s) , 57% (153 m<sup>3</sup>/s), 87% (234 m<sup>3</sup>/s) and 118% (318 m<sup>3</sup>/s), respectively.

Overall both RCPs scenarios (RCPs+UCSCA) and hypothetical scenarios (RCPs+%CSCA and BL+T<sub>x</sub>P<sub>x</sub>) indicate the potential increase in streamflows that could considerably lead to augment the water resources of the catchment under the changing climate, therefore, large storage reservoirs are essentially required to manage and cater the flood conditions in Hunza River catchment.

## 5.2 RECOMMENDATIONS

- MODIS snow cover product should be used for other snow and glacier fed catchments located in Upper Indus basin to determine the spatial and temporal behavior toward the snow and glaciers extent. In this study snow cover change analysis performed was short term (10 years), longer term study should be necessary to draw robust conclusions on snow cover changes.
- SRM should be used for higher elevation catchment in conjunction with MODIS snow data for other catchment located in Upper Indus basin for current and future simulation of streamflows.
- Distributed hydrological models (i.e. on the basis of water and energy budget) should be used, to take into account the spatial variability of climate variables.
- IGB climate dataset is available on fine resolution that need a lot of correction and should be used for other adjacent catchment for future climatic studies.
- For policy makers and stakeholders, a study should be conducted for adaptation strategies to changing climate.

## REFERENCES

- Abid I. Effects of Indian Mal–Operations on Jhelum and Chenab Rivers and Suggested Remedial Measures. MS Thesis, NICE–SCEE, National University of Sciences and Technology, Sector H–12, Islamabad, Pakistan (2012).
- Abudu, S., Cui, C., Saydi, M., and King, J. P.: Application of snowmelt runoff model (SRM) in mountainous watersheds: A review, *Water Science and Engineering*, 5, 123–136, 2012.
- Akhtar, M., Ahmad, N., and Booij, M. J.: The impact of climate change on the water resources of Hindukush–Karakorum–Himalaya region under different glacier coverage scenarios, *Journal of Hydrology*, 355, 148–163, 10.1016/j.jhydrol.2008.03.015, 2008.
- Ali, K., Begum, F., Abbas, Q., Karim, R., Ali, S., Ali, H., Akbar, M., Ali, S., and Ishaq, S.: Impact of attaabad landslide induce lake on livelihood of upstream population of upper Hunza, District Hunza–Nagar, 2012.
- Archer, D.: Contrasting hydrological regimes in the upper Indus Basin, *Journal of Hydrology*, 274, 198–210, 10.1016/s0022–1694(02)00414–6, 2003.
- Azmat, M., Laio, F., and Poggi, D.: Estimation of Water Resources Availability and Mini–Hydro Productivity in High–Altitude Scarcely–Gauged Watershed, *Water Resources Management*, 29, 5037–5054, 10.1007/s11269–015–1102–z, 2015.
- Azmat, M., Choi, M., Kim, T.–W., and Liaqat, U. W.: Hydrological modeling to simulate streamflow under changing climate in a scarcely gauged cryosphere catchment, *Environmental Earth Sciences*, 75, 10.1007/s12665–015–5059–2, 2016a.
- Azmat, M., Liaqat, U. W., Qamar, M. U., and Awan, U. K.: Impacts of changing climate and snow cover on the flow regime of Jhelum River, Western Himalayas, *Regional Environmental Change*, 1–13, 2016b.
- Bajwa, H., and Tim, U.: Toward immersive virtual environments for GIS–based Floodplain modeling and Visualization, *Proceedings of 22nd ESRI User Conference*, 2002.
- Banitt, A.: Simulating a century of hydrographs e Mark Twain reservoir, 2nd Joint Federal Interagency Conference, Las Vegas, USA, 2010.

Berg, P., Feldmann, H., and Panitz, H. J.: Bias correction of high resolution regional climate model data, *Journal of Hydrology*, 448–449, 80–92, 10.1016/j.jhydrol.2012.04.026, 2012.

Burhan A, W. I., Syed AAB, Rasul G, Shreshtha AB and Shea JM.: Generation of High–Resolution Gridded Climate Fields for the Upper Indus River Basin by Downscaling Cmp5 Outputs, *Journal of Earth Science & Climatic Change*, 06, 10.4172/2157–7617.1000254, 2015.

Butz, D., and Hewitt, K.: A note in the Upper Indus Basin Weather Stations, Snow and ice hydrology project: annual report, 64–76, 1986.

Chai, T., and Draxler, R.: Root mean square error (RMSE) or mean absolute error (MAE)?, *Geoscientific Model Development Discussions*, 7, 1525–1534, 2014.

Choudhari, K., Panigrahi, B., and Paul, J. C.: Simulation of rainfall–runoff process using HEC–HMS model for Balijore Nala watershed, Odisha, India, *International Journal of Geomatics and Geosciences*, 5, 253, 2014.

Climate impact portal.: Exploring climate model data | For exploration, visualization and analysis of climate model data, URL: [https://climate4impact.eu/impactportal/help/faq.jsp?q=bias\\_correction](https://climate4impact.eu/impactportal/help/faq.jsp?q=bias_correction)

Date Accessed: January 15, 2017.

Coskun, H. G., Alganci, U., and Usta, G.: Analysis of land use change and urbanization in the Kucukcekmece water basin (Istanbul, Turkey) with temporal satellite data using remote sensing and GIS, *Sensors*, 8, 7213–7223, 2008.

Cunderlik, J. M., and Simonovic, S. P.: Hydrologic models for inverse climate change impact modeling, *Proceedings of the 18th Canadian Hydrotechnical Conference, Challenges for Water Resources Engineering in a Changing World Winnipeg*, 2007.

Dou, Y., Chen, X., Bao, A., and Li, L.: The simulation of snowmelt runoff in the ungauged Kaidu River Basin of TianShan Mountains, China, *Environmental Earth Sciences*, 62, 1039–1045, 2011.

- Efe, R., Soykan, A., Curebal, I., and Sonmez, S.: Land use and land cover change detection in Karınca river catchment (NW Turkey) using GIS and RS techniques, 2012.
- Fischer, S., Pluntke, T., Pavlik, D., and Bernhofer, C.: Hydrologic effects of climate change in a sub-basin of the Western Bug River, Western Ukraine, *Environmental Earth Sciences*, 72, 4727–4744, 2014.
- Hasson, S., Lucarini, V., Khan, M. R., Petitta, M., Bolch, T., and Gioli, G.: Early 21st century snow cover state over the western river basins of the Indus River system, arXiv preprint arXiv:1211.7324, 2014.
- Hay, L. E., Wilby, R. L., and Leavesley, G. H.: A comparison of delta change and downscaled GCM scenarios for three mountainous basins in THE UNITED STATES<sup>1</sup>, in, Wiley Online Library, 2000.
- Hydrological Modeling System HEC–HMS User’s Manual, William A. and Scharffenberg, U.S Army Corps of Engineers, Hydrologic Engineering Center, HEC, 609 Second st. Davis CA 95616, 2013.
- Hewitt, K.: The Karakoram anomaly? Glacier expansion and the elevation effect, *Karakoram Himalaya, Mountain Research and Development*, 25, 332–340, 2005.
- Hewitt, K.: Tributary glacier surges: an exceptional concentration at Panmah Glacier, Karakoram Himalaya, *Journal of Glaciology*, 53, 181–188, 2007.
- Hock, R.: Temperature index melt modelling in mountain areas, *Journal of Hydrology*, 282, 104–115, 2003.
- Hugenholtz, C. H., Levin, N., Barchyn, T. E., and Baddock, M. C.: Remote sensing and spatial analysis of aeolian sand dunes: A review and outlook, *Earth–Science Reviews*, 111, 319–334, 2012.
- Immerzeel, W. W., Van Beek, L. P., and Bierkens, M. F.: Climate change will affect the Asian water towers, *Science*, 328, 1382–1385, 2010.

Immerzeel, W. W., van Beek, L. P., Konz, M., Shrestha, A. B., and Bierkens, M. F.: Hydrological response to climate change in a glacierized catchment in the Himalayas, *Climatic change*, 110, 721–736, 10.1007/s10584-011-0143-4, 2012.

IPCC Core Writing Team, Pachauri RK, Meyer LA (2014) Contribution of working groups I, II and III to the fifth assessment report of the intergovernmental panel on climate change. *Climate Change 2014: Synthesis Report*. IPCC, Geneva

Krause, P., Boyle, D., and Bäse, F.: Comparison of different efficiency criteria for hydrological model assessment, *Advances in Geosciences*, 5, 89–97, 2005.

Ling, H., Xu, H., Shi, W., and Zhang, Q.: Regional climate change and its effects on the runoff of Manas River, Xinjiang, China, *Environmental Earth Sciences*, 64, 2203–2213, 2011.

Lutz, A. F., ter Maat, H. W., Biemans, H., Shrestha, A. B., Wester, P., and Immerzeel, W. W.: Selecting representative climate models for climate change impact studies: an advanced envelope-based selection approach, *International Journal of Climatology*, 36, 3988–4005, 10.1002/joc.4608, 2016.

Maraun, D.: Bias Correcting Climate Change Simulations—a Critical Review, *Current Climate Change Reports*, 2, 211–220, 2016.

Martinec, J., Rango, A., and Roberts, R.: *Snowmelt runoff model (SRM) user's manual*, New Mexico State University, Las Cruces, New Mexico, 175, 2008.

Meenu, R., Rehana, S., and Mujumdar, P.: Assessment of hydrologic impacts of climate change in Tunga–Bhadra river basin, India with HEC-HMS and SDSM, *Hydrological Processes*, 27, 1572–1589, 2013.

Nabi, G., Latif, M., and Azhar, A. H.: The role of environmental parameter (degree day) of snowmelt runoff simulation, *Soil & Environment*, 30, 2011.

Null, S. E., Viers, J. H., and Mount, J. F.: Hydrologic response and watershed sensitivity to climate warming in California's Sierra Nevada, *PLoS One*, 5, e9932, 2010.

Ohara, N., Kavvas, M., Easton, D., Dogrul, E., Yoon, J., and Chen, Z.: Role of snow in runoff processes in a subalpine hillslope: field study in the Ward Creek Watershed, Lake

Tahoe, California, during 2000 and 2001 water years, *Journal of Hydrologic Engineering*, 16, 521–533, 2010.

Pakistan Institute of Development Economics, Khan, F. J., and Javed, Y.: Delivering access to safe drinking water and adequate sanitation in Pakistan, 2007.

Pakistan economic survey 2012–13, Farooq, O.: Agriculture, Economic Advisory Wing, Ministry Finance, Government of Pakistan, Islamabad, 2014.

Prasad, V. H., and Roy, P. S.: Estimation of snowmelt runoff in Beas Basin, India, *Geocarto International*, 20, 41–47, 2005.

Ramirez–Villegas, J., and Jarvis, A.: Downscaling global circulation model outputs: the delta method decision and policy analysis Working Paper No. 1, *Policy Analysis*, 1, 1–18, 2010.

Rasmussen, R., Baker, B., Kochendorfer, J., Meyers, T., Landolt, S., Fischer, A. P., Black, J., Thériault, J. M., Kucera, P., and Gochis, D.: How well are we measuring snow: The NOAA/FAA/NCAR winter precipitation test bed, *Bulletin of the American Meteorological Society*, 93, 811–829, 2012.

Rulin, O., Liliang, R., Weiming, C., and Zhongbo, Y.: Application of hydrological models in a snowmelt region of Aksu River Basin, *Water Science and Engineering*, 1, 1–13, 2008.

Şensoy, A.: Physically based point snowmelt modeling and its distribution in Upper Euphrates Basin, Citeseer, 2005.

SIHP.: Snow and ice hydrology project, Upper Indus River Basin, WAPDA-IDRC-Wilfrid Laurier University, 179, 1990.

Tahir, A. A., Chevallier, P., Arnaud, Y., and Ahmad, B.: Snow cover dynamics and hydrological regime of the Hunza River basin, Karakoram Range, Northern Pakistan, *Hydrology and Earth System Sciences*, 15, 2259–2274, 2011a.

Tahir, A. A., Chevallier, P., Arnaud, Y., Neppel, L., and Ahmad, B.: Modeling snowmelt–runoff under climate scenarios in the Hunza River basin, Karakoram Range, Northern Pakistan, *Journal of Hydrology*, 409, 104–117, 2011b.

Tahir, A. A., Adamowski, J. F., Chevallier, P., Haq, A. U., and Terzago, S.: Comparative assessment of spatiotemporal snow cover changes and hydrological behavior of the Gilgit, Astore and Hunza River basins (Hindukush–Karakoram–Himalaya region, Pakistan), *Meteorology and Atmospheric Physics*, 1–19, 2016.

Tarboton, D. G., and Luce, C. H.: Utah energy balance snow accumulation and melt model (UEB), Citeseer, 1996.

Terink, W., Hurkmans, R., Torfs, P., and Uijlenhoet, R.: Bias correction of temperature and precipitation data for regional climate model application to the Rhine basin, *Hydrology and Earth System Sciences Discussions*, 6, 5377–5413, 2009.

Teutschbein, C., and Seibert, J.: Bias correction of regional climate model simulations for hydrological climate–change impact studies: Review and evaluation of different methods, *Journal of Hydrology*, 456–457, 12–29, 10.1016/j.jhydrol.2012.05.052, 2012.

Wanielista, M., Kersten, R., and Eaglin, R.: *Hydrology: Water quantity and quality control*, John Wiley and Sons, 1997.

WAPDA Annual Report. : Pakistan Water and Power Development Authority, Lahore, 2013.

Yang, Y.–C. E., Brown, C., Yu, W., Wescoat, J., and Ringler, C.: Water governance and adaptation to climate change in the Indus River Basin, *Journal of Hydrology*, 519, 2527–2537, 2014.

Young, C. A., Escobar-Arias, M. I., Fernandes, M., Joyce, B., Kiparsky, M., Mount, J. F., Mehta, V. K., Purkey, D., Viers, J. H., and Yates, D.: Modeling the hydrology of climate change in California’s Sierra Nevada for subwatershed scale adaptation<sup>1</sup>, in, Wiley Online Library, 2009.

Yu, W., Yang, Y.–C., Savitsky, A., Brown, C., and Alford, D.: The Indus basin of Pakistan: The impacts of climate risks on water and agriculture, World Bank Publications, 2013.

Yüksel, A., Akay, A. E., and Gundogan, R.: Using ASTER imagery in land use/cover classification of eastern Mediterranean landscapes according to CORINE land cover project, *Sensors*, 8, 1237–1251, 2008.

Zhang, X., Aguilar, E., Sensoy, S., Melkonyan, H., Tagiyeva, U., Ahmed, N., Kotaladze, N., Rahimzadeh, F., Taghipour, A., Hantosh, T. H., Albert, P., Semawi, M., Karam Ali, M., Said Al-Shabibi, M. H., Al-Oulan, Z., Zadari, T., Al Dean Khelet, I., Hamoud, S., Sagir, R., Demircan, M., Eken, M., Adiguzel, M., Alexander, L., Peterson, T. C., and Wallis, T.: Trends in Middle East climate extreme indices from 1950 to 2003, *Journal of Geophysical Research*, 110, 10.1029/2005jd006181, 2005.